

# REPORT DOCUMENTATION PAGE

Form Approved  
OMB No. 0704-0188

Public reporting burden for this collection of information is estimated to average 1 hour per response, including the time for reviewing instructions, searching existing data sources, gathering and maintaining the data needed, and completing and reviewing the collection of information. Send comments regarding this burden estimate or any other aspect of this collection of information, including suggestions for reducing this burden, to Washington Headquarters Services, Directorate for Information Operations and Reports, 1215 Jefferson Davis Highway, Suite 1204, Arlington, VA 22202-4302, and to the Office of Management and Budget, Paperwork Reduction Project (0704-0188), Washington, DC 20503.

1. AGENCY USE ONLY (Leave blank)		2. REPORT DATE 10-30-96	3. REPORT TYPE AND DATES COVERED	
4. TITLE AND SUBTITLE Toughening of Brittle Materials			5. FL - 3 REVISIONS <b>FF9620-</b> 93-1-0449	
6. AUTHOR(S) A. Chudnovsky, D. Baron and Y. Shulkin				
7. PERFORMING ORGANIZATION NAME(S) AND ADDRESS(ES) Department of Civil and Materials Engineering 2095 ERF, 842 W. Taylor Street The University of Illinois at Chicago Chicago, IL 60607			8. PERFORMING ORGANIZATION AFOSR-TR-96 97 0018	
9. SPONSORING / MONITORING AGENCY NAME(S) AND ADDRESS(ES) Air Force Office for Scientific Research Aerospace and Engineering Sciences Building 410, Bolling AFB Washington D.C. 20332			10. SPONSORING / MONITORING AGENCY REPORT NUMBER <b>FF9620-</b> <b>93-1-0449</b>	
11. SUPPLEMENTARY NOTES N/A				
12a. DISTRIBUTION / AVAILABILITY STATEMENT Approved for public release; Distribution unlimited			12b. DISTRIBUTION CODE N/A	
13. ABSTRACT (Maximum 200 words)  This report is dedicated to numerical simulations of subcritical crack growth which are based on the Crack Layer Kinetic Model. Various types of loadings are considered, i.e., simple and eccentric tension, three and four point bending, dipole on the crack boundaries, constant and time varying loads. As a result, lifetime-load relations are established, a new approach to brittle material toughness assessment is proposed, and a method of reliability prediction for structural components is developed.			19970110 042	
14. SUBJECT TERMS subcritical crack growth, numerical simulations, lifetime-load relations, toughness, reliability			15. NUMBER OF PAGES 117	
17. SECURITY CLASSIFICATION OF REPORT UNCLASSIFIED			16. PRICE CODE	
18. SECURITY CLASSIFICATION OF THIS PAGE UNCLASSIFIED		19. SECURITY CLASSIFICATION OF ABSTRACT UNCLASSIFIED		20. LIMITATION OF ABSTRACT

DTIC QUALITY INSPECTED 4

## Abstract

This report<sup>\*</sup> summarizes the 3 year experimental and theoretical research program conducted by the Fracture Research Laboratory under AFOSR support and devoted to some aspects of brittle fracture<sup>\*\*</sup>.

The behavior of materials subjected to brittle fracture is studied using numerical simulations of subcritical crack growth. Various types of loadings are considered, i.e., simple and eccentric tension, three and four point bending, dipole on the crack boundaries, constant and time varying loads. As a result, lifetime-load relations are established, a new approach to brittle material toughness assessment is proposed, and a method of reliability prediction for structural components is developed.

---

\* This report is the Ph.D. thesis of Daniel Baron, which was defended in August 1996.

\*\* The other works in the framework of this program were previously reported:

1. Toughening of Brittle Materials, 1994.
2. The Time Dependency of the Necking Process in PC, 1995.

## TABLE OF CONTENTS

<u>CHAPTER</u>	<u>PAGE</u>
INTRODUCTION .....	1
1. THE CRACK LAYER MODEL FOR SLOW CRACK GROWTH IN ENGINEERING PLASTICS	
1.1 Introduction .....	8
1.2 Energy balance for crack layer growth. Thermodynamic forces .....	9
1.3 Degradation of the process zone material .....	16
1.4 Kinetic equations .....	20
1.5 Conclusions .....	21
2. NUMERICAL ALGORITHMS FOR SOLUTIONS OF CRACK LAYER MODEL EQUATIONS	
2.1 Introduction .....	23
2.2 Algorithm for SEN specimen subjected to creep loading .....	24
2.2.1 Program arrays .....	25
2.2.2 Determination of the remote load function .....	25
2.2.3 Initial time increment .....	26
2.2.4 Calculation loop for time evolution of crack and crack layer .....	26
2.2.4.1 Increment of time step counter .....	26
2.2.4.2 Determination of the surface energy .....	27
2.2.4.3 Calculation of the SIFs and CODs .....	29
2.2.4.4 Calculation of the energy release rate .....	30
2.2.4.5 Calculation of the driving forces .....	30
2.2.4.6 Calculation of the growth increments and new values for the crack and crack layer lengths .....	31
2.2.4.7 Update of program arrays .....	31
2.2.5 Calculation of equilibrium crack layer length .....	31
2.2.6 Enforcement of constraints on the crack and crack layer lengths .....	35
2.2.7 Prevention of crack extension into undegraded material .....	36
2.2.8 Time jumps to decrease required computer time .....	38
2.2.9 Determination of specimen failure .....	41
2.3 Algorithm for SEN specimen subjected to load control .....	42
2.4 Assumption of simplified crack layer model for discontinuous growth .....	44

TABLE OF CONTENTS (continued)	
<u>CHAPTER</u>	<u>PAGE</u>

ii

## TABLE OF CONTENTS (continued)

<u>CHAPTER</u>	<u>PAGE</u>
2.9 Conclusions .....	67
3. ANALYSIS OF COMPUTER SIMULATIONS FOR SEN SPECIMENS SUBJECTED TO CONSTANT LOADS	
3.1 Introduction .....	69
3.2 Forcing and resisting forces .....	69
3.3 Dimensionless representation of simulation input parameters .....	73
3.4 Discontinuous and continuous growth modes .....	76
3.5 Simplified model for discontinuous growth .....	81
3.6 Lifetimes for tension simulations .....	83
3.7 Lifetimes for eccentric tension and pure bending .....	87
3.8 Conclusions .....	88
4. RELIABILITY CALCULATIONS FOR PLASTIC STRUCTURAL COMPONENTS	
4.1 Introduction .....	90
4.2 Method assumptions .....	90
4.3 Analysis of defects .....	91
4.4 Kinetics of crack layer evolution .....	92
4.5 Lifetime - initial defect size relationship .....	94
4.6 Lifetime probability density function .....	95
4.7 Reliability of structural component .....	96
4.8 Conclusions .....	98
5. COMPUTER SIMULATION OF PLASTIC TOUGHNESS TEST	
5.1 Introduction .....	100

## TABLE OF CONTENTS (continued)

<u>CHAPTER</u>	<u>PAGE</u>
5.2 The crack layer model .....	100
5.3 Simulation of displacement control test .....	103
5.4 ASTM procedure .....	104
5.5 Conclusions .....	107
CONCLUSIONS AND FUTURE RESEARCH .....	109
CITED LITERATURE .....	111
APPENDIX.....	114

## TABLE OF CONTENTS (continued)

<u>CHAPTER</u>	<u>PAGE</u>
5.2 The crack layer model .....	100
5.3 Simulation of displacement control test .....	103
5.4 ASTM procedure .....	104
5.5 Conclusions .....	107
CONCLUSIONS AND FUTURE RESEARCH .....	109
CITED LITERATURE .....	111
APPENDIX .....	114
VITA .....	118

## LIST OF FIGURES

<u>FIGURE</u>	<u>PAGE</u>
1. One dimensional approximation of crack layer .....	11
2. Process zone formation stress-strain diagram .....	13
3. Process zone fiber strain-time relation .....	18
4. Surface energy as a function of time .....	29
5. Crack layer configuration .....	32
6. Equilibrium crack layer lengths .....	34
7. Time increment adjustment .....	36
8. Penetration of crack into undegraded material .....	38
9. Time jump under constant load .....	40
10. Simplified model of discontinuous crack growth .....	47
11. Determination of lifetime .....	51
12. Time jump under increasing load .....	53
13. Calculation of edge displacement .....	56
14. Remote stress - crack layer length relationship .....	60
15. Procedures of solution for two equation system .....	62
16. Forcing forces as functions of: (a) crack length; (b) crack layer length .....	73
17. Crack layer growth .....	77
18. Experimental stress-lifetime relationship .....	80
19. Discontinuous growth using simplified CLM .....	81
20. Lifetime versus kinetic coefficients .....	82
21. Failure crack length versus specimen width .....	83
22. Tension simulations lifetime-stress relations .....	84
23. Log(lifetime) - Log(applied stress) best fit line coefficients .....	86
24. Applied stress distributions .....	87
25. Lifetime-stress relations for tension, eccentric tension and pure bending .....	88
26. Modeling probability density function for maximum defect size .....	92
27. Discontinuous growth of crack and process zone .....	94
28. Lifetime versus logarithm of initial crack length for five stress levels .....	95

## LIST OF FIGURES (continued)

<u>FIGURE</u>		<u>PAGE</u>
29.	Lifetime probability density functions for five stress levels .....	96
30.	Lifetime versus stress level for four values of reliability .....	97
31.	Mean lifetimes for five stress levels .....	98
32.	Crack and process zone .....	101
33.	Remote stress, crack length and crack layer length vs. displacement .....	104
34.	Remote stress vs. displacement for three values of displacement rate .....	106
35.	Energy release rates for three values of displacement rate .....	107
36.	Crack layer diagram .....	117

## LIST OF NOMENCLATURE

ASTM	American Society for Testing and Materials.
CDF	Cumulative distribution function.
CLC	Crack layer centerline.
CL	Crack layer.
CLM	Crack Layer Model.
COD	Crack opening displacement. $\delta(x)$ .
CLOD	Crack layer opening displacement. Displacement of PZ material during PZ formation.
CTOD	Crack tip opening displacement. $\delta(l)$ .
NTOD	Notch tip opening displacement. $\delta(N)$ .
PDF	Probability density function.
PZ	Process zone.
SEN	Single edge notched.
SIF	Stress intensity factor.
( )	A symbol immediately followed by parentheses, indicates that the symbol is a function.
[ ]	A symbol immediately followed by square braces, indicates that the symbol is an array.
$B$	Thickness of a plane specimen.
$D_l$	Forcing part of $X_l$ .
$D_L$	Forcing part of $X_L$ .
$\delta(x)$	Has context specific meaning. Either $\delta_\infty(x)$ , $\delta_{dr}(x)$ , or $\delta_\infty(x) + \delta_{dr}(x)$ .

## LIST OF NOMENCLATURE (continued)

$\delta_{dr}(x)$	COD at $x$ due to influence of $\sigma_{dr}$ . Is measured normal to CLC. For $x$ between 0 and $l$ , is equal to the distance between crack faces at location $x$ . For $x$ between $l$ and $L$ , is equal to the distance between crack imaginary faces (between edges of process zone) at location $x$ .
$\delta_{\infty}(x)$	COD at $x$ due to influence of $\sigma_{\infty}$ . Is measured normal to CLC. For $x$ between 0 and $l$ , is equal to the distance between crack faces at location $x$ . For $x$ between $l$ and $L$ , is equal to the distance between crack imaginary faces (between edges of process zone) at location $x$ .
$\Delta$	Relative displacement between the two grips which are holding a specimen.
$\dot{\Delta}$	Time rate of change of $\Delta$ during a displacement control test.
$\epsilon_c$	PZ fiber axial failure strain.
$\epsilon_0$	Axial strain in drawn (necked) part of material specimen.
$\epsilon_u$	Axial strain in unnecked part of material specimen.
$E$	Material constant. Equal to Young's modulus.
$G$	Gibbs free energy.
$2\gamma(\Delta t_{pz})$	Material function which monotonically decreases due to time dependent material degradation, and is equal to the energy required to extend the crack a distance such that one area unit of new crack faces (a crack has two faces) is created. Called "surface energy".
$2\gamma_0$	Value of $2\gamma(\dots)$ when $\Delta t_{pz} = 0$ . Initial and maximum value of $2\gamma(\dots)$ . The value of $2\gamma(\dots)$ for newly drawn material which has not started to degrade.
$\tilde{\gamma}$	Material constant. Called "gamma tilde". The specific energy of drawing. Equal to ratio of areas above and below line $\sigma = \sigma_{dr}$ and within PZ formation stress-strain curve (Figure 2.). (Note: There is no connection between $2\gamma(\dots)$ and $\tilde{\gamma}$ . As a result of the evolution of notation, both names contain "gamma".)

## LIST OF NOMENCLATURE (continued)

$h_a$	Width of active process zone.
$h(x)$	Width of original material strip which is transformed into PZ.
$H$	Half length of plane specimen in direction perpendicular to CLC.
$i$	The (integer) number of the current time step ( $0 \leq i \leq n$ ).
$J_1$	Amount that the system potential energy decreases when the crack extends a distance such that one area unit of new crack faces (a crack has two faces) is created. Called "energy release rate".
$k_1$	Material constant. Called "crack length kinetic coefficient".
$k_2$	Material constant. Called "crack layer length kinetic coefficient".
$K_{dr}$	SIF at $L$ due to influence of $\sigma_{dr}$ .
$K_\infty$	SIF at $L$ due to influence of $\sigma_\infty$ .
$l$	x-coordinate of crack tip on a SEN specimen. Crack length.
$\dot{l}$	Time rate of change of $l$ .
$l_a$	$L - l$ . Equals length of active process zone. (The active process zone is in front of the crack tip. The wake process zone is behind the crack tip.)
$l_0$	Initial crack length. Notch length. $N$ .
$\delta l$	$l - l_0$ .
$L$	Maximum x-coordinate of process zone on a SEN specimen. Crack layer length.
$\dot{L}$	Time rate of change of $L$ .
$L_{eq}$	For a fixed value of $l$ , the value of $L$ which causes $X_L$ to equal zero.

## LIST OF NOMENCLATURE (continued)

$L_0$	Initial crack layer length. Notch length. $l_0$ .
$\lambda$	Material constant. Called "draw ratio". Is found by increasing the load on a tensile specimen until a cross section undergoes necking and is drawn. Is equal to the ratio of the new lengths of originally equal intervals in the drawn and undrawn parts of the specimen.
$n$	Number of time steps taken in order to reach the current time $t$ .
$N$	x-coordinate of notch tip on a SEN specimen. Notch length. $l_0$ .
$R_l$	Resisting part of $X_l$ .
$R_L$	Resisting part of $X_L$ .
$\sigma(x)$	The stress distribution which is applied normal to the crack faces.
$\sigma_{dr}$	Material constant. Called material "drawing stress". Applied normal to CLC on crack imaginary faces between x-coordinates $l$ and $L$ . $\sigma_{dr}$ compresses the crack. For all calculations in this thesis, $\sigma_{dr}$ is a negative quantity.
$\sigma_{\infty}(x)$	Specimen remote loading function. Stress distribution which would be present along location of CLC, if crack layer did not exist. Is applied normal to CLC on crack faces between x-coordinates 0 and $l$ , and on crack imaginary faces between x-coordinates $l$ and $L$ . $\sigma_{\infty}$ can possibly be a function of position along the CLC, i.e., if for instance, the specimen is loaded in bending. $\sigma_{\infty}$ can be tensile and/or zero and/or compressive.
$t$	Elapsed (material) time since the start of a computer simulation. Current time. Current clock reading. Also, $t \equiv t[n]$ .
$t_r$	Rupture time. Elapsed time until a drawn fiber subjected to true stress $\lambda\sigma_{dr}$ , breaks. Maximum possible elapsed time until a PZ fiber breaks.
$\Delta t_0$	Initial time increment. An input parameter specified by the user. The first attempt at executing every time step is performed using $\Delta t = \Delta t_0$ .

## LIST OF NOMENCLATURE (continued)

$\Delta t$	Time increment used during a time step. $t = t[n] = \sum_{i=1}^{i=n} \Delta t_i$ .
$t_f$	Total elapsed (material) time from the start of a computer simulation until the numerical criterion for specimen failure is satisfied.
$\Delta t_{pz}$	Elapsed (material) time since the material at the current location of the crack tip was drawn (since the material became part of the process zone).
$t_{pz}$	Time (clock reading) when the material at the current location of the crack tip was drawn (when the material became part of the process zone).
$U$	Potential energy of an SEN specimen.
$x$	x-axis located along CLC. x-coordinate measured along this x-axis. (For an SEN specimen, the notched edge has x-coordinate zero.)
$x_{COD}$	x-coordinate where COD is desired ( $0 \leq x_{COD} \leq L$ ).
$X_l$	Driving force for crack length extension.
$X_L$	Driving force for crack layer length extension.
$W$	Length of plane specimen in direction parallel to CLC. SEN specimen width.

## SUMMARY

In engineering applications, plastic structural components are often needed to perform for many years under relatively small stresses. These components usually fail suddenly and without warning, when a slowly growing crack originating from a material defect reaches a critical length, and then accelerates, causing almost instantaneous fracture. In order to determine if a certain plastic is adequate for a particular structural application, it would be ideally desirable to make many lifetime tests of the plastic component functioning in the actual mechanism, and then to build a probability distribution of component lifetime. The distribution would provide a measure of the plastic's adequacy. This method is in effect used, when the failures of a commercially released mechanism are tracked. But the knowledge comes with the cost of real world failures. It is seldom if ever possible to conduct failure tests of a mechanism which is being designed. For instance, if a new machine was being designed which required a plastic component, failure testing of the component would require that many of the machines be built and each operated until its component failed. The time to conduct the failure tests would be comparable to the machine's design-lifetime, and so for a long term design-lifetime, completing the tests would be greatly impractical.

The usual alternative to mechanism design-lifetime failure tests, is to perform failure tests on plastic samples using material testing machines. The use of testing machines eliminates the need to use the actual mechanism during the tests. Standard tests are performed in order to provide a way to compare plastics, and also to estimate lifetimes. The standard tests are performed using standard specimen geometries. The actual geometry of the component which is being designed is not accounted for. One or more design parameters (initial crack length, applied stress, temperature) is increased enough above its design value, so that the testing can be completed

## SUMMARY (continued)

within the allotted time. Empirical methods are used to extrapolate from the determined test lifetimes to (much) longer estimated design lifetimes.

The Crack Layer Model (CLM) for slow crack growth in engineering plastics was created by Professor A. Chudnovsky in 1984 [1]. The model provides a mechanical explanation of slow crack growth. A numerical implementation of the equations of the model can be used to predict the time evolutions of a crack and the damage zone which precedes it, in a plastic structural component. Computer modeling of a particular problem requires the specification of certain of the plastic's material properties. The values of these properties are found by performing standard short term tests on material specimens. Also required is the ability to calculate the stress intensity factor (SIF) at the crack tip for the specific component geometry and loading. If the required material properties and SIF calculation are available, then the numerical solution is found by solving a system of two ordinary differential equations thru time. A lifetime for the component is found without resorting to historical data, long term mechanism failure tests, or short term material tests which use empirical manipulations.

This thesis is basically a numerical implementation of the equations of the CLM. Algorithms are presented for the cases of time varying prescribed load and time varying prescribed displacement. Simplified algorithms are also presented, which save much computing energy and under certain conditions give approximately the same answers. All of the algorithms apply to the simple circumstance of a plane single edge notched (SEN) specimen, with a straight crack. A summary of the theory of the CLM is also presented. The output from computer simulations employing the presented algorithms are reported and analyzed. Computed types of crack growth are compared to experimentally observed types. Computed applied stress - lifetime

### **SUMMARY (continued)**

relations are compared to experimentally found relations. Computed applied stress - lifetime relations are compared for different types of loadings. A method is presented for calculating the reliability function (a function of time which gives the probability that failure has not happened) of a plastic structural component. A computer simulation is made of the ASTM method for measuring the fracture toughness of a plastic. It is shown that the measurement found is displacement rate dependent, and because of this the proposal is made that fracture toughness is not a material property.

## INTRODUCTION

This thesis is another in a sequence of investigations by students of Professor A. Chudnovsky into the behavior of the Crack Layer Model (CLM) for engineering plastics. Previous theses include those of W.L. Huang and K. Kadota. The research for this thesis consisted of the numerical implementation of the CLM for various loading types (tension, three point bending, etc.) and histories (fixed load, time-varying load, time-varying displacement). The algorithms which were used to construct a computer program are specified. The output from the computer simulations which were made are described and analyzed. A method is shown for determining the reliability of a plastic structural part for any value of service time. It is demonstrated that the accepted method for calculating material fracture toughness is rate dependent, and therefore ambiguous. A proposal is made that fracture toughness is not a material property, and that one material can be found to be more fracture resistant than another, only by accounting for all of the parameters which comprise a particular usage environment.

An understanding of the slow crack growth (subcritical crack growth) in plastics which leads to long-term brittle fracture is very important to industry. The use of plastics as structural components is always increasing. A crack which causes failure usually grows from a defect which is originally present in the material. The defect (often a void) acts as an initial crack with length equal to the defect's largest dimension. When subjected to stress, the crack slowly grows from this beginning length. For temperatures in the range of room temperature, slow crack growth occurs at relatively low stresses, and is the main cause of failure for plastic parts which are in service for many years. The time period from the beginning of service until failure is called the lifetime (or time to failure) and denoted by  $t_f$ . An understanding of slow crack growth would allow the

development of an accelerated material testing procedure, based on the experimental determination of material parameters and the numerical modeling of the crack growth.

Experimental data of long-term fracture due to both constant and cyclic loading have been reported for many plastics [2-6], and are very detailed for polyethylenes [7-24]. For polyethylenes, a region of damaged material referred to as the process zone (PZ), is always present in front of the crack tip. The PZ forms almost immediately after loading, because the crack tip singularity magnifies the transverse tensile stress in the region so that the material's yield (drawing) stress is reached. In polyethylene and some other plastics (for instance, polymethyl methacrylate) microvoids develop and cause the PZ to consist of disconnected drawn fibers which are perpendicular to the direction of the crack. The behavior of PZ material is usually considered to be similar to that of drawn (necked) material [25,26]. It has been shown that the time dependent properties of the PZ fibers (i.e., disentanglement and creep) greatly influence the crack growth rate and lifetime. Analyzing the PZ from the viewpoint of continuum mechanics is usually based on the Dugdale-Barenblatt (DB) model [27,28]. However, observations have shown that actual PZs have significantly shorter lengths than are predicted by the DB model [29].

Experiments have demonstrated that with respect to time, slow crack growth may be continuous (monotonically increasing) or discontinuous (intermittent). Observations of discontinuous growth in polyethylenes subjected to fatigue loading have existed for a long time [3], but only recently has discontinuous growth been observed for constant loading [19]. According to [19], the growth is discontinuous because the crack is arrested until the long chain molecules of the drawn PZ fiber in front of the crack tip untangle and then the fiber breaks. The rate of disentanglement for a drawn fiber is a material property.

Descriptions of the experimentally observed crack kinetics have been based on the assumption

that the stresses and strains in the neighborhood of the crack tip completely determine the conditions for crack initiation and growth. This means that the rate of crack growth ( $\dot{l}$ ) (which is sometimes approximately measured experimentally by using the rate of the notch tip opening displacement ( $\dot{\delta}(N)$ ) [18,19]) is a function of only such fracture parameters as the stress intensity factor ( $K$ ),  $J$ -integral, etc. Observations [7-22] have allowed the approximate determination of the crack growth rate under constant load as linearly proportional to a power of the stress intensity factor at the crack tip, i.e.,  $\dot{l} = c_1 K^j$ ,  $\dot{\delta}(N) = c_2 K^j$ , where  $c_1$ ,  $c_2$  and  $j$  are material constants. According to [30], for polyethylenes  $j$  varies from 3 to 5. The empirical relations mentioned have been established for the simplest conditions of crack propagation, i.e., the specimen material is homogeneous and the crack path is straight. Study of the case when the specimen contains an inclusion (a region with different material properties) has shown that crack kinetics cannot be completely determined from the crack tip parameters. Additional parameters which account for the effect of the PZ on the crack direction and growth rate must be specified.

With respect to lifetime prediction, the most important experimental result has been the development of relations between lifetime, applied stress and temperature. Data about the lifetimes for internally pressurized high density polyethylene pipes at various load levels and temperatures are reported in [5]. Experiments [16-18] on single-edge notched (SEN) tensile specimens of polyethylenes with various molecular weight distributions and branch densities have allowed the determination of lifetime as a function of stress level, temperature and notch length. For a constant load and a particular material, specimen geometry, load type (tension, three-point bending, etc.) and temperature, lifetime is a function of the stress level  $\sigma$  only, i.e.,  $t_f \propto \sigma^{-\alpha}$ . In

[5]  $\sigma$  is the pipe hoop stress, and in [16-18] it is the applied tensile stress.  $\alpha$  is a material constant which depends little or none on temperature, and varies from approximately 2.5 to 5.5 for different polyethylenes. It has been shown that a particular treatment of the lifetime-stress relation obtained from short-term fracture tests (at high temperatures) can give a reasonable estimate of the lifetime-stress relation for long-term processes at room temperature [16-18,23,24].

There are now three approaches used for modeling slow crack growth in plastics. The first assumes that the kinetics are completely determined by the time-dependent properties of the bulk material which surrounds the crack and PZ. According to the most detailed theory of this kind [31], the crack grows because of viscoelastic deformation of the bulk material. The second approach connects crack growth to the time-dependent processes which take place in the PZ material. For polyethylenes, the time-dependent processes are disentanglement and creep of the PZ fibers. This approach has been studied experimentally in [32-42]. An explanation of notch tip opening displacement as being due to visco-elongation of the PZ fibers is given in [30]. The third approach (which this thesis follows) considers the PZ region to consist of damaged material, and the crack and PZ as the two co-dependent components of a system named the crack layer (CL) [1,43]. CL kinetics are analyzed using irreversible thermodynamics, and a complete solution for the general problem has been found. An approximation of the CLM has permitted numerical modeling of various slow crack growth phenomena, including discontinuous crack growth in polyethylenes [29,44-45], etc. The approximation used, is to assume the CL to be a two parameter system, the crack length ( $l$ ) and the crack layer length ( $L$ ) ( $L$  is equal to the sum of  $l$  and the active PZ length ( $l_a$ )). (The numerical algorithms which are used for this thesis, use the two parameter approximation.)

The approximation of the CLM which was just stated, is plausible because observations of actual process zones in plastics have shown that the process zone length ( $l_a$ ) is always much greater than the process zone width ( $h_a$ ). Therefore, in the equations of the thermodynamic analysis, the terms containing  $h_a$  are relatively very small, and when the approximation is used, are neglected. The bulk material is assumed to be linearly elastic. (Actually, all engineering plastics possess viscoelastic properties, but the criteria for crack and PZ growth are related only to the elastic energy of the material. For the case of prescribed load, viscoelastic deformation does not affect the stress field and so does not affect lifetime. For the case of prescribed displacement, viscoelastic deformation would affect the stress field, and so lifetime would be affected. However, viscoelasticity is outside the boundary of this thesis.) During CL growth, the potential energy of the bulk material is used to break the process zone fibers and extend the crack. As the crack extends, its stress intensity factor increases, which forces the PZ to extend. The time-dependent changes of the PZ region are collectively called material degradation. For prescribed external forces and fixed temperature, the Gibbs free energy ( $G$ ) of the bulk material and PZ is the potential which indicates deviation of the system from equilibrium. From irreversible thermodynamics, the thermodynamic force for crack length extension ( $X_l$ ) is defined as the partial derivative of  $G$  with respect to the crack length ( $l$ ), and the thermodynamic force for crack layer length extension ( $X_L$ ) is defined as the partial derivative of  $G$  with respect to the crack layer length ( $L$ ). A crack layer parameter ( $l, L$ ) grows whenever the value of its thermodynamic force is positive. Numerical solution of the CLM kinetic equations has demonstrated emulation of both types of experimentally observed slow crack growth, continuous and discontinuous. Stability

analysis of the CLM indicates that growth of  $l$  and/or  $L$  occurs whenever the system is in an unstable state. Growth continues until a new stable state is attained. For a discontinuous process, stable states exist, and growth stops whenever one is reached. The time-dependent degradation of the PZ material causes a stable system to become unstable. For a continuous process, there are no possible stable states, so growth is never suspended.

This thesis is about the numerical analysis of the CLM for various types of loads and load histories. The CLM was numerically implemented by developing a Fortran computer program. Chapter 1 contains a brief review of the CLM theory, and a derivation of the kinetic equations which are used to model slow crack growth in engineering plastics. Chapter 2 relates the detailed numerical algorithms which were used to construct the program which solves the equations through time. Algorithms are given for the cases of prescribed fixed load, prescribed time-varying load and prescribed time-varying displacement. Simplified algorithms are also given, which are usually very accurate when modeling discontinuous crack growth. The simplified algorithms are included because their use can greatly reduce the work which the computer must do. Chapter 3 analyzes the output from the fixed load computer simulations which were made. The thermodynamic forces are separated into forcing and resisting parts. The set of simulation input parameters is presented in dimensionless form, and the requirements for simulation similarity are indicated. The factors which determine whether a simulation is continuous or discontinuous are discussed. The output from the simplified algorithm is compared to the output from the complete algorithm. Lifetime-applied load relations are provided for both continuous and discontinuous simulations, and also for various types of loading. Chapter 4 shows a way to calculate the reliability function for a plastic structural component. The method involves performing destructive tests on material specimens in order to build a distribution of the largest defects, and then performing computer

simulations to develop a lifetime-defect size relationship. Chapter 5 uses simulations of prescribed time-varying displacement to imitate the ASTM method for measuring the fracture toughness of a material. It is shown that the results depend on displacement rate, and so can be misleading.

# **1. THE CRACK LAYER MODEL FOR SLOW CRACK GROWTH IN ENGINEERING PLASTICS**

## **1.1 INTRODUCTION**

In this thesis, the modeling of slow crack growth which causes brittle fracture of engineering plastics, is based on the idea that slow crack growth is the evolution of two elements. The first element is the crack, and the second is a region of damaged material preceding the crack tip which is called the process zone (PZ). Following [1], the system consisting of the crack and PZ is called the crack layer (CL). Advance of the CL results from the interactions between the crack and the PZ, and between the PZ and the body surrounding it, which is called the matrix. The equations governing CL growth are derived using the conventional procedure of the thermodynamics of irreversible processes. The temperature and load are considered to be prescribed, so the relevant thermodynamic potential is Gibbs free energy. Gibbs free energy accounts for the potential energy of the matrix and mechanism maintaining the load, the energy required for PZ formation, and the energy accumulation on new crack boundaries. Partial derivatives of Gibbs potential with respect to the crack length and PZ length give the thermodynamic forces for crack and PZ extensions. Kinetic equations are formulated as linear relations between the thermodynamic forces and the rates of crack length extension and PZ length extension. The process becomes unstable when the rates begin to monotonically increase. The time period from load application until CL instability is called the lifetime or time to failure, and written  $t_f$ .

Only the opening mode of crack loading (mode 1) and a straight crack are considered. In this case the PZ of an engineering plastic has the shape of a thin strip ahead of the crack tip and along the crack centerline. Therefore, the CL can be described by just two independent parameters, the

crack and PZ lengths. A system of two kinetic equations is formed. The system is nonlinear because the thermodynamic forces depend nonlinearly on the two parameters, and because constraints on the rates of crack and PZ extension are expressed as inequalities.

## 1.2 ENERGY BALANCE FOR CRACK LAYER GROWTH. THERMODYNAMIC FORCES

It is usually accepted that the PZ material is similar to the material obtained from cold drawing (necking) the original plastic. So, the PZ material is supposed to be formed under the drawing stress ( $\sigma_{dr}$ ), and stretched according to the draw ratio ( $\lambda$ ).  $\sigma_{dr}$  and  $\lambda$  are material properties of a particular plastic.

What  $\lambda$  means will now be explained. If a plastic specimen is loaded in tension along the longitudinal axis, when  $\sigma_{dr}$  is reached a transverse band of necked material will appear at the location of the specimen's weakest cross section. The band thickness will grow from zero. While the load is maintained, the band thickness will increase as its boundaries (the two end cross sections of the band) advance in both longitudinal directions. The boundaries can be thought of as material transformers. As a boundary moves across a strip of unnecked material, the strip is transformed into necked material. The axial strain in the unnecked material will be called  $\epsilon_u$ , and the axial strain in the necked material will be called  $\epsilon_0$ . It is important to note that  $\epsilon_0$  is a constant, and that once necking begins  $\epsilon_u$  becomes constant. (It should also be noted that  $\epsilon_0$  is a constant only until all of the material of the specimen becomes necked. When no unnecked material remains, and if the load is still maintained,  $\epsilon_0$  will begin to grow.) An arbitrary longitudinal interval measured on the unloaded specimen, will have length  $l_1$ . When the specimen is loaded until necking occurs, the interval will have a new length. If the measured interval is

completely outside the band of material which becomes necked,  $l_1$  will become  $l_2$ . If the measured interval is completely inside the band of material which becomes necked,  $l_1$  will become  $l_3$ .  $\lambda$  is defined as the ratio of  $l_3$  to  $l_2$ .

$$\lambda \equiv \frac{l_3}{l_2} \quad (1.1)$$

Therefore,

$$\lambda = \frac{l_1 + \epsilon_0 l_1}{l_1 + \epsilon_u l_1}. \quad (1.2)$$

So,

$$\epsilon_0 = \lambda(1 + \epsilon_u) - 1. \quad (1.3)$$

Since,

$$\epsilon_u \ll 1, \quad (1.4)$$

$$\epsilon_0 \approx \lambda - 1. \quad (1.5)$$

The approximation of equation 1.5 will be used in the remainder of this section, i.e.,

$$\epsilon_0 = \lambda - 1. \quad (1.6)$$

Since, as was stated in section 1.1, the PZ is shaped like a thin strip, the stress-strain state of the matrix due to the presence of the CL can be approximated by a slit (a straight one dimensional

cut in the matrix) with tractions of magnitude  $\sigma_{dr}$  distributed along the location of the PZ (Figure 1).

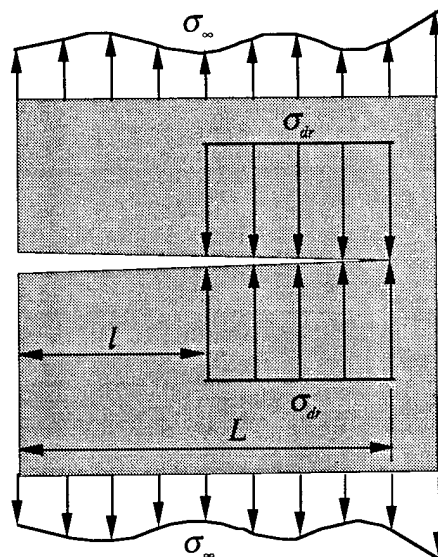


Figure 1. One dimensional approximation of crack layer

The energy balance for PZ formation will be derived. Gibbs potential includes the change in the potential energy of the matrix and mechanism maintaining the prescribed load, and the change in the deformation potential of the material which becomes the PZ. The change in the total potential energy of the matrix and load is

$$\Pi_m = F_m - W_\infty. \quad (1.7)$$

$F_m$  is the change in matrix elastic energy, and  $W_\infty$  is the work done by the applied load moving thru the displacement caused by PZ formation. According to numerous experimental observations, cold drawing (necking) of plastics gives the stress-strain function ( $\sigma(\epsilon)$ ) shown in Figure 2. The function is considered to be a material property for the PZ during its formation. The change in the PZ deformation potential is defined as

$$F_{pz} \equiv \int_{x=l}^{x=L} h(x) \left\{ \int_{\epsilon=0}^{\epsilon=\lambda-1} \sigma(\epsilon) d\epsilon \right\} dx. \quad (1.8)$$

$h(x)$  is the width of the original material strip which is transformed into the PZ. The crack layer opening displacement (CLOD) is defined as

$$\delta_{pz}(x) \equiv \epsilon(x)h(x). \quad (1.9)$$

From equation 1.6,

$$h(x) = \frac{\delta_{pz}(x)}{\lambda - 1}. \quad (1.10)$$

Define

$$\Omega \equiv \int_{\epsilon=0}^{\epsilon=\lambda-1} \sigma(\epsilon) d\epsilon. \quad (1.11)$$

$\Omega$  is the area under  $\sigma = \sigma(\epsilon)$  in Figure 2. Equation 1.8 can be written as

$$F_{pz} = \frac{\Omega}{\lambda - 1} \int_{x=l}^{x=L} \delta_{pz}(x) dx. \quad (1.12)$$

Define

$$\Omega' \equiv \sigma_{dr}(\lambda - 1). \quad (1.13)$$

$\Omega'$  is the area under  $\sigma = \sigma_{dr}$  in Figure 2. If the PZ material was perfectly plastic, then equation 1.12 would become

$$F_{pz}' = \frac{\Omega'}{\lambda - 1} \int_{x=l}^{x=L} \delta_{pz}(x) dx. \quad (1.14)$$

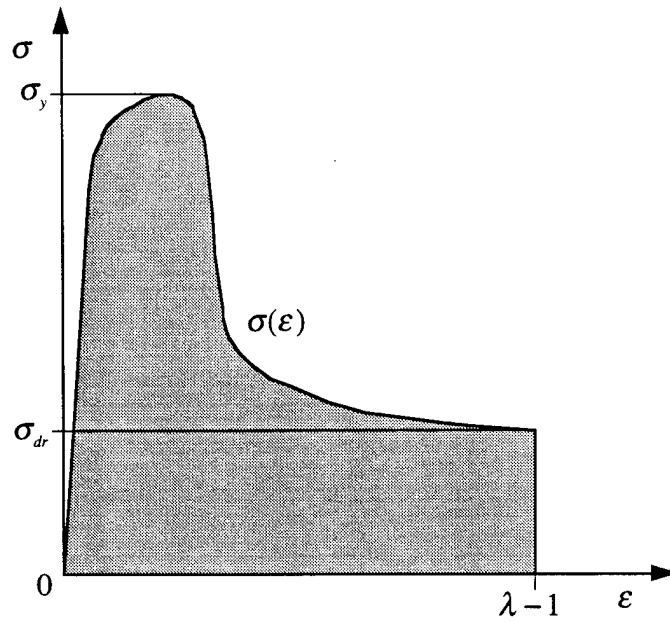


Figure 2. Process zone formation stress-strain diagram

(The definition of  $\Omega'$  implies that Young's modulus is infinite, but the resulting error in  $F_{pz}'$  is very small.) Define

$$\tilde{\gamma} \equiv \frac{\Omega - \Omega'}{\Omega'}, \quad (\geq 0). \quad (1.15)$$

$\tilde{\gamma}$  is the ratio of the overloading energy to the perfectly plastic energy during PZ formation. From equations 1.12-1.15,

$$F_{pz} = (1 + \tilde{\gamma})F_{pz}' . \quad (1.16)$$

Define

$$\Pi_m' \equiv \Pi_m + F_{pz}' . \quad (1.17)$$

The change in Gibbs potential is

$$G = \Pi_m + F_{pz} , \equiv \Pi_m' + F_{pz}'' . \quad (1.18)$$

From applying Clapeyron's theorem (Figure 1),

$$\Pi_m' = \frac{1}{2} \left\{ \int_{x=l}^{x=L} \sigma_{dr} \delta(x) dx - \int_{x=0}^{x=L} \sigma_{\infty}(x) \delta(x) dx \right\} , \quad (1.19)$$

and

$$F_{pz}'' = \tilde{\gamma} F_{pz}' . \quad (1.20)$$

(Within each integral of equation 1.19,  $\delta(x)$  is the displacement of the particular traction.)

The differential of Gibbs potential due to CL growth is

$$-dG = \left( -\frac{\partial \Pi_m'}{\partial l} - \frac{\partial F_{pz}''}{\partial l} - 2\gamma \right) dl + \left( -\frac{\partial \Pi_m'}{\partial L} - \frac{\partial F_{pz}''}{\partial L} \right) dL , \quad (\geq 0) . \quad (1.21)$$

Equation 1.21 is equal to zero when the CL is in equilibrium.  $2\gamma$  is the energy required for the crack to extend into the PZ, i.e., the Griffith fracture energy of the damaged material. (Note that  $\tilde{\gamma}$  and  $2\gamma$  are not related.) Define

$$X_l \equiv -\frac{\partial \Pi_m'}{\partial l} - \frac{\partial F_{pz}''}{\partial l} - 2\gamma , \quad (1.22)$$

and

$$X_L \equiv -\frac{\partial \Pi_m'}{\partial L} - \frac{\partial F_{pz}''}{\partial L}. \quad (1.23)$$

Energy balance 1.21 is written

$$-dG = X_l dl + X_L dL, \quad (\geq 0). \quad (1.24)$$

$X_l$  is called the driving force (thermodynamic force) for crack length extension, and  $X_L$  is called the driving force (thermodynamic force) for crack layer length extension. By using the solution of the elastic problem shown in Figure 1, the partial derivatives in equations 1.22 and 1.23 can be expressed in terms of conventional fracture mechanics parameters.

$$-\frac{\partial \Pi_m'}{\partial l} = -\sigma_{dr}(\delta_\infty + \delta_{dr}) \quad (1.25)$$

$$-\frac{\partial \Pi_m'}{\partial L} = \frac{1}{E}(K_\infty + K_{dr})^2 \quad (1.26)$$

$$-\frac{\partial F_{pz}''}{\partial l} = -\tilde{\gamma}\sigma_{dr}\delta_{dr} \quad (1.27)$$

$$-\frac{\partial F_{pz}''}{\partial L} = \frac{2\tilde{\gamma}K_{dr}}{E}(K_\infty + K_{dr}) \quad (1.28)$$

$E$  is Young's modulus.  $\delta_\infty$  is the crack opening displacement (COD) at the crack tip ( $x = l$ ), due to the influence of  $\sigma_\infty(x)$ .  $\delta_{dr}$  is the COD at  $x = l$ , due to the influence of  $\sigma_{dr}$ .  $K_\infty$  is the stress intensity factor (SIF) at  $x = L$  due to the influence of  $\sigma_\infty(x)$ .  $K_{dr}$  is the SIF at  $x = L$  due to the influence of  $\sigma_{dr}$ . Equations 1.22 and 1.23 are written

$$X_l = -\sigma_{dr}(\delta_\infty + (1 + \tilde{\gamma})\delta_{dr}) - 2\gamma, \quad (1.29)$$

$$X_L = \frac{1}{E}(K_\infty + K_{dr})(K_\infty + (1 + 2\tilde{\gamma})K_{dr}). \quad (1.30)$$

So, the driving forces are expressed in terms of the standard parameters of linear fracture mechanics.

Each of the driving forces can be separated into two parts. The forcing parts of the driving forces are defined as

$$D_I \equiv -\sigma_{dr}(\delta_\infty + \delta_{dr}), \quad (1.31)$$

$$D_L \equiv \frac{1}{E}(K_\infty + K_{dr})^2. \quad (1.32)$$

The resisting parts of the driving forces are defined as

$$R_I \equiv \tilde{\gamma}\sigma_{dr}\delta_{dr} + 2\gamma, \quad (1.33)$$

$$R_L \equiv -\frac{2\tilde{\gamma}K_{dr}}{E}(K_\infty + K_{dr}). \quad (1.34)$$

Each of the quantities  $D_I$ ,  $D_L$ ,  $R_I$ ,  $R_L$  are always positive. Equations 1.29 and 1.30 are written

$$X_I = D_I - R_I, \quad (1.35)$$

$$X_L = D_L - R_L. \quad (1.36)$$

The crack length will increase only when  $X_I$  is positive. The crack layer length will increase only when  $X_L$  is positive.

### 1.3 DEGRADATION OF THE PROCESS ZONE MATERIAL

The two parameter model [38-40] assumes that resistance of the PZ material to crack extension decreases with time. The PZ material is said to degrade with time. PZ formation occurs under the drawing stress ( $\sigma_{dr}$ ) and with stretching subject to the draw ratio ( $\lambda$ ). The PZ material is incompressible, so the true stress acting on the PZ is defined to be  $\lambda\sigma_{dr}$ . The surface energy

$(2\gamma)$  represents a measure of the PZ resistance to crack extension. The PZ consists of many fibers perpendicular to the direction of the crack which are supposed to be drawn.

If a PZ fiber is drawn at time  $t = 0$ , it has an initial axial drawing strain  $(\epsilon_0)$ . As time  $(t)$  increases, and the fiber continues to be subjected to stress  $\lambda\sigma_{dr}$ , the fiber axial strain  $(\epsilon)$  will increase until the critical fiber axial strain  $(\epsilon_c)$  is reached, and the fiber breaks. (The crack advances whenever the fiber at the crack tip breaks.) The critical axial strain  $(\epsilon_c)$  is reached at the critical time of drawing  $(t_r)$ .  $\epsilon_c$  and  $t_r$  are material constants. The axial strain  $(\epsilon)$  grows from  $\epsilon_0$  to  $\epsilon_c$  according to a material function  $\epsilon(t)$ . Define

$$\Delta\epsilon(t) \equiv \epsilon(t) - \epsilon_0, \quad (1.37)$$

$$\Delta\epsilon_c \equiv \epsilon_c - \epsilon_0. \quad (1.38)$$

A PZ fiber strain-time relation is shown in Figure 3.

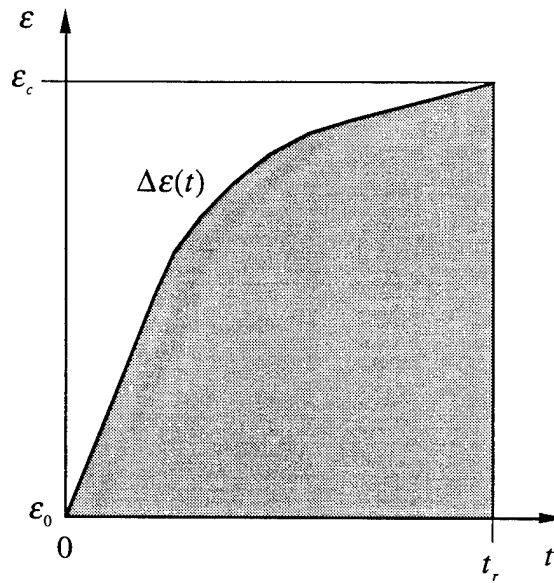


Figure 3. Process zone fiber strain-time relation

At time  $t = 0$  the work done on the PZ fiber is

$$w_0 = \frac{\lambda \sigma_{dr} \epsilon_0}{2}. \quad (1.39)$$

At time  $t$  the work done on the PZ fiber is

$$w(t) = w_0 + \lambda \sigma_{dr} \Delta \epsilon(t). \quad (1.40)$$

At rupture time  $t = t_r$  the amount of work done on the PZ fiber is

$$w_c \equiv w(t_r) = w_0 + \lambda \sigma_{dr} \Delta \epsilon(t_r) = w_0 + \lambda \sigma_{dr} \Delta \epsilon_c. \quad (1.41)$$

The surface energy required for crack length extension ( $2\gamma(t)$ , see equation 1.29) is defined as

$$2\gamma(t) \equiv w_c - w(t). \quad (1.42)$$

$2\gamma(t)$  is the amount of energy required to break the PZ fiber at time  $t$ . The initial and maximum value of the surface energy ( $2\gamma_0$ ) is a material constant and defined as

$$2\gamma_0 \equiv 2\gamma(0) = \lambda \sigma_{dr} \Delta \epsilon_c. \quad (1.43)$$

$2\gamma(t)$  can be written

$$2\gamma(t) = 2\gamma_0 \left( 1 - \frac{\Delta \epsilon(t)}{\Delta \epsilon_c} \right). \quad (1.44)$$

If, for instance the material function  $\Delta \epsilon(t)$  is linear, i.e., if

$$\Delta \epsilon(t) = \alpha t, \quad (1.45)$$

then

$$2\gamma(t) = 2\gamma_0 \left( 1 - \frac{\alpha t}{\Delta \epsilon_c} \right), \quad \left( 0 \leq t \leq \frac{\Delta \epsilon_c}{\alpha} \right). \quad (1.46)$$

If  $\Delta \epsilon(t)$  is exponential, i.e., if

$$\Delta \epsilon(t) = \Delta \epsilon_c (1 - e^{-\beta t}), \quad (1.47)$$

then

$$2\gamma(t) = 2\gamma_0 e^{-\beta t}, \quad (0 \leq t < \infty). \quad (1.48)$$

In equation 1.48,  $t$  represents the elapsed time since a PZ fiber was drawn. A PZ fiber is formed (and drawn), when its material becomes part of the PZ. So later in this thesis,  $2\gamma(\Delta t_{pz})$  will be used instead of  $2\gamma(t)$ .  $\Delta t_{pz}$  signifies the elapsed time since the material at the location of the

crack tip became part of the PZ. (The interest is always with the material at the crack tip, because the state of that material determines whether the crack can grow, i.e., in order for the crack to grow, the PZ fiber directly ahead of the crack tip must be broken.)

Note that another material constant ( $k_0$ ) will be used later in this thesis.  $k_0$  is the reciprocal of the time until rupture ( $t_r$ ) of drawn material, i.e.,

$$k_0 \equiv \frac{1}{t_r}. \quad (1.49)$$

#### 1.4 KINETIC EQUATIONS

The relations between driving forces and instantaneous growth rates are assumed to be linear,

$$\dot{l} = k_1 X_l, \quad (1.50)$$

$$\dot{L} = k_2 X_L. \quad (1.51)$$

$k_1$  and  $k_2$  are material constants which are determined experimentally.  $\dot{l}$  is the instantaneous growth rate for the crack length.  $\dot{L}$  is the instantaneous growth rate for the crack layer length (for the front end of the PZ). If a calculated value of  $\dot{l}$  or  $\dot{L}$  is ever negative, then that value is set equal to zero. Doing this prevents contradictions with physical reality.

Enforced limitations on the values of  $l$  and  $L$  are

$$l \leq L \leq L_{eq}. \quad (1.52)$$

$L_{eq}$  is the equilibrium value for the crack layer length. For a particular value of  $l$ ,  $L_{eq}$  is the value of  $L$  which causes  $X_L$  (equation 1.30) to equal zero. Also, for a particular value of  $l$ ,  $L_{eq}$  is the maximum possible value of  $L$ .

The initial conditions for the system of equations 1.50-1.51 are

$$l(t = 0) = l_0, \quad (1.53)$$

$$L(t = 0) = L_0 \quad ( \leq L_{eq}(l_0) ). \quad (1.54)$$

The two degree of freedom system of equations 1.50-1.51 can be solved numerically through time, yielding the evolutions of  $l$  and  $L$ .

## 1.5 CONCLUSIONS

The driving (thermodynamic) forces for crack extension ( $X_l$ ) and crack length extension ( $X_L$ ) were derived. The opening mode (mode 1) of crack loading and a straight crack were assumed. Therefore it was guaranteed that the length of the PZ would be much larger than its width. Having a narrow PZ allowed the CL to be described one dimensionally, and by just two parameters, the crack length ( $l$ ) and the crack layer length ( $L$ ).

The definition for the material surface energy (or degradation) function was derived. It was assumed that the PZ was composed of fibers which had been drawn. This allowed the strain in the fibers of a newly formed PZ to be calculated using the material's draw ratio ( $\lambda$ ). In the calculation of the area under  $\sigma = \sigma_{dr}$  in Figure 2, the approximation of Young's modulus ( $E$ ) being infinite was used.

The system of two (nonlinear ordinary differential) kinetic equations was presented, along with the initial conditions, and the constraints on the calculated values of the crack length ( $l$ ) and

the crack layer length ( $L$ ). It was assumed that there was a linear relationship between a driving force and the associated instantaneous growth rate.

## 2. NUMERICAL ALGORITHMS FOR SOLUTIONS OF CRACK LAYER MODEL EQUATIONS

### 2.1 INTRODUCTION

This chapter will show numerical procedures for determining the crack length  $l(t, \dots)$ , and crack layer length  $L(t, \dots)$ , in computer simulations of specimen lifetime tests using the equations of the Crack Layer Model (CLM). Algorithms are given for the cases of fixed prescribed load, time-varying prescribed load, and time-varying prescribed displacement. Simplified versions of the algorithms are also included. They are based on the implementation of an assumption which results in the decoupling of equations 2.1. The associated simplified simulations require little computer time relative to simulations using the complete algorithms, and give approximately the same output for the modeling of discontinuous crack growth.

The goal is to be able to solve the system of two nonlinear ordinary differential equations

$$\begin{aligned} \dot{l} &= k_1 \cdot X_l & (a) \\ \dot{L} &= k_2 \cdot X_L & (b) \end{aligned} \tag{2.1}$$

$\dot{l}$  is the instantaneous rate of change of the crack length with respect to time.  $\dot{L}$  is the instantaneous rate of change of the crack layer length with respect to time.  $k_1$ , a material constant, is the crack length kinetic coefficient.  $k_2$ , a material constant, is the crack layer length kinetic coefficient.  $X_l$  is the driving force for crack length extension.  $X_L$  is the driving force for crack layer length extension.

$$\begin{aligned}
 X_l &= J_1 - 2\gamma & (a) \\
 X_L &= \frac{(K_\infty + K_{dr})(K_\infty + (1 + 2\tilde{\gamma})K_{dr})}{E} & (b)
 \end{aligned}
 \tag{2.2}$$

$J_1$  is the rate of system potential energy release for crack length extension.  $2\gamma$ , a material function, is the rate of surface energy required for crack length extension.

$$J_1 = (\delta_\infty + (1 + \tilde{\gamma})\delta_{dr})(-\sigma_{dr}) \tag{2.3}$$

$\delta_\infty$  is the crack tip (at  $x$ -coordinate  $x = l$ ) opening displacement due to the remote (applied) load.  $\tilde{\gamma}$ , a material constant, is the specific energy of drawing.  $\sigma_{dr}$ , a material constant, is the drawing stress.  $\delta_{dr}$  is the crack tip (at  $x$ -coordinate  $x = l$ ) opening displacement due to the process zone stress,  $\sigma_{dr}$ .

$$2\gamma = 2\gamma(\Delta t_{pz}) \tag{2.4}$$

$2\gamma$  is a decreasing material function, of the elapsed time ( $\Delta t_{pz}$ ) since the material at the current location ( $x$ -coordinate) of the crack tip became part of the process zone.  $K_\infty$  is the stress intensity factor at  $L$  (the  $x$ -coordinate of the front of the crack layer) due to the remote load.  $K_{dr}$  is the stress intensity factor at  $L$  due to the process zone stress,  $\sigma_{dr}$ .

## 2.2 ALGORITHM FOR SEN SPECIMEN SUBJECTED TO CREEP LOADING

An SEN (single edge notched) specimen, is a plane specimen with a notch cut in one edge. The notch is cut perpendicular to the specimen's longitudinal axis. "Creep loading", means the loads to which the specimen is subjected are constant.

### 2.2.1 Program arrays

The computer program for the numerical simulation contains arrays<sup>(1)</sup> which record the values of the main variables at the end of each time step. These arrays include

$$\begin{array}{l} t[i] \\ l[i] , \quad i = 0, 1, \dots, n. \\ L[i] \end{array} \quad (2.5)$$

$i$  is the number of the time step, and  $n$  is the total number of time steps which have been completed, in order to reach the current time,  $t[n]$ . The initial conditions are specified as

$$\begin{array}{l} t[0] = 0 \\ l[0] = l_0 , \quad (L_0 = l_0). \\ L[0] = L_0 \end{array} \quad (2.6)$$

### 2.2.2 Determination of the remote load function

The remote load is the external load which is applied to the specimen. The distance from the remote load to the crack layer is assumed to be large enough, such that St. Venant's principle applies with respect to the calculation of remote load stresses in the region of the crack layer. The remote load function,  $\sigma_{\infty}(x)$ , is the normal stress which would be present in the specimen along the crack centerline, if the crack layer (the crack and process zone) did not exist. For instance, for a plane specimen of width  $W$  and thickness  $B$ , and loaded in tension by force  $F$ ,

$$\sigma_{\infty}(x) = \frac{F}{WB}. \quad (2.7)$$

For a plane specimen of width  $W$ , thickness  $B$ , and loaded in the plane by end moments  $M$ ,

---

(1)Note: within this thesis, a symbol immediately followed by parentheses “( )” will indicate a function, and a symbol immediately followed by square braces “[ ]” will indicate an array.

$$\sigma_{\infty}(x) = \frac{(M)\left(\frac{W}{2} - x\right)}{\frac{BW^3}{12}}. \quad (2.8)$$

The origin of the x-axis is at the tension edge (which is also the notch edge) of the specimen.

Note, that this thesis relates only to the states of plane stress, and plane strain, so that  $B$  is always set equal to one, and will usually not be mentioned.

### 2.2.3 Initial time increment

One of the input parameters which the user specifies for a simulation, is the initial time increment ( $\Delta t_0$ ). During the first attempt at executing every time step (sometimes an attempt will fail),  $\Delta t$ , the time increment used during the time step, is set equal to  $\Delta t_0$ .

$$\Delta t = \Delta t_0 \quad (\text{for first attempt of every time step}) \quad (2.9)$$

### 2.2.4 Calculation loop for time evolution of crack and crack layer

This loop is repeated for each time step, until the conditions specified within the computer program which indicate failure of the simulated specimen are satisfied. It is desired to calculate the time evolution of  $l(\dots)$ , the x-coordinate of the crack tip, and of  $L(\dots)$ , the x-coordinate of the front of the crack layer.

#### 2.2.4.1 Increment of time step counter

At the start of each time step, the time step counter ( $n$ ) is incremented,

$$n = n + 1. \quad (2.10)$$

For the first time step,

$$(n = n + 1) \Rightarrow (1 = 0 + 1). \quad (2.11)$$

### 2.2.4.2 Determination of the surface energy

The surface energy ( $2\gamma(\Delta t_{pz})$ ) is calculated for use during the time step. The surface energy (Figure 4) is equal to the amount of energy required to extend the crack a distance such that one area unit of new crack surfaces is generated. (For a specimen with unit thickness ( $B = 1$ ), this distance would equal one half, since as the crack extends two surfaces are generated.) When the crack extends, it does so into process zone material. The fibers of the process zone are subjected to the material drawing stress,  $\sigma_{dr}$ . Subjection to  $\sigma_{dr}$  causes the material of the fibers to degrade and the energy required to extend the crack to decrease, as time passes.  $2\gamma(\dots)$  is a monotonically decreasing material function, with upper limit  $2\gamma_0$ , and lower limit zero.  $2\gamma_0$  is equal to the surface energy of newly drawn and still undegraded material.  $\Delta t_{pz}$  is equal to the elapsed time *since* the material at the current location of the crack tip (at  $l$ ) was drawn, i.e., since that material became part of the process zone.  $t$  is the current time.  $t_{pz}$  is the time *when* the material at the current location of the crack tip was drawn, i.e., when that material became part of the process zone.

$$\Delta t_{pz} = t - t_{pz} \quad (2.12)$$

$t_{pz}$  is equal to the time which makes  $L(t_{pz}, \dots)$  (the x-coordinate of the front of the crack layer at time  $t_{pz}$ ) equal to  $l(t, \dots)$  (the x-coordinate of the crack tip at the current time ( $t$ )).

$$L(t_{pz}, \dots) = l(t, \dots), \quad (\text{with } t_{pz} < t). \quad (2.13)$$

In order to determine  $2\gamma(\Delta t_{pz})$ , it is necessary to find  $\Delta t_{pz}$ . The current time  $t$  is known, so if  $t_{pz}$  can be found, then  $\Delta t_{pz}$  can be calculated. In order to determine  $t_{pz}$ , it is first necessary to find  $j$  such that

$$L[j] \leq l[n-1] \leq L[j+1]. \quad (2.14)$$

(It might seem strange that although this is the  $n$ th time step,  $l(n-1)$  is used in equation 2.14. But it would be impossible to use  $l(n)$ , since it has not been calculated yet.) Finding  $j$  is done by searching the (ordered) array  $L[i]$ , beginning with  $L[0]$ , and comparing the values with  $l[n-1]$ . Once  $j$  has been found, then by linear interpolation,

$$t_{pz} = t[j] + \frac{l[n-1] - L[j]}{L[j+1] - L[j]}(t[j+1] - t[j]). \quad (2.15)$$

After  $t_{pz}$  is found,  $\Delta t_{pz}$  can be calculated using equation 2.12. Then  $\Delta t_{pz}$  can be substituted into the prescribed material function  $2\gamma(\dots)$ .

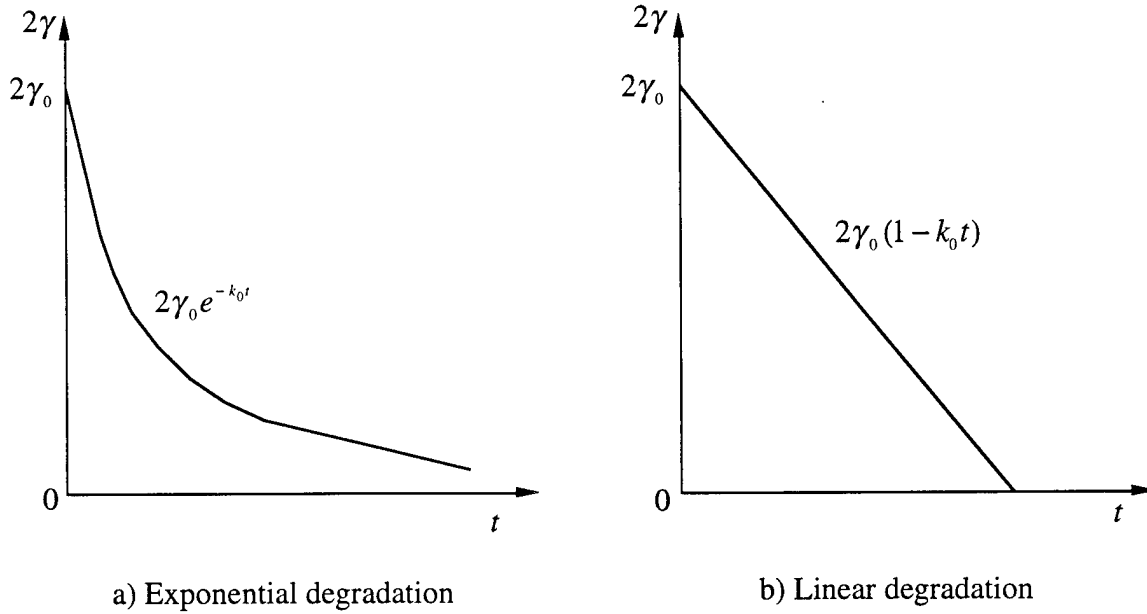


Figure 4. Surface energy as a function of time

#### 2.2.4.3 Calculation of the SIFs and CODs

The appendix gives the algorithms for calculating the stress intensity factors (SIFs) and crack opening displacements (CODs). The parameters for each of the functions will be shown here.

$$\begin{aligned}
K_{\infty} &= K_{\infty}(L, W, \sigma_{\infty}(x)) \\
K_{dr} &= K_{dr}(l, L, W, \sigma_{dr}) \\
\delta_{\infty} &= \delta_{\infty}(l, L, E, W, \sigma_{\infty}(x)) \\
\delta_{dr} &= \delta_{dr}(l, L, E, W, \sigma_{dr})
\end{aligned} \tag{2.16}$$

$E$  is Young's modulus, and  $W$  is the specimen width.

Note, that within this sub-subsection, and in every numerical procedure of this thesis, when  $\sigma_{dr}$  is used, it is a negative quantity. With respect to this sub-subsection,  $\sigma_{dr}$  being negative will result in  $K_{dr}$  and  $\delta_{dr}$  being negative.

$$\sigma_{dr} = -\text{abs}(\sigma_{dr}) \quad (\text{for all calculations in this thesis}) \tag{2.17}$$

#### **2.2.4.4 Calculation of the energy release rate**

Once the CODs have been determined, the energy release rate ( $J_1$ ) is calculated using equation 2.3.  $J_1$  is equal to the amount that the system potential energy decreases when the crack extends a distance such that one area unit of new crack surfaces is generated.

#### **2.2.4.5 Calculation of the driving forces**

The driving forces for crack extension  $X_l$  and crack layer extension  $X_L$  are calculated using equations 2.2. It is mathematically possible for either of them to be negative, which would cause the crack length and/or the crack layer length to decrease. This would be physically impossible, so whenever one of the quantities is calculated and found to be negative, it is set equal to zero.

#### 2.2.4.6 Calculation of the growth increments and new values for the crack and crack layer lengths

The growth rates for the time step are calculated using equation 2.1. Using these rates, and the time increment for the time step ( $\Delta t$ ), the growth increments for the crack ( $\Delta l$ ) and the process zone ( $\Delta L$ ) are calculated by the forward Euler method.

$$\Delta l = \dot{l} \cdot \Delta t \quad (a) \quad (2.18)$$

$$\Delta L = \dot{L} \cdot \Delta t \quad (b)$$

The new values of the crack length ( $l_{\text{new}}$ ) and crack layer length ( $L_{\text{new}}$ ) are

$$\begin{aligned} l_{\text{new}} &= l_{\text{old}} + \Delta l \\ L_{\text{new}} &= L_{\text{old}} + \Delta L \end{aligned} \quad (2.19)$$

#### 2.2.4.7 Update of program arrays

The program arrays are now be updated, and then the calculation loop of subsection 2.2.4 is restarted from the beginning.

$$\begin{aligned} l[n] &= (l_{\text{new}}), = l[n-1] + \Delta l \\ L[n] &= (L_{\text{new}}), = L[n-1] + \Delta L \\ t[n] &= t[n-1] + \Delta t \end{aligned} \quad (2.20)$$

#### 2.2.5 Calculation of equilibrium crack layer length

During each time step, after the candidate new values of the crack length ( $l_{\text{new}}$ ), and the crack layer length ( $L_{\text{new}}$ ) are calculated (sub-subsection 2.2.4.6), some conditions are tested for using those values. If one or more of the conditions are true, it may be necessary to repeat the time step using a smaller time increment. Three of the conditions require the value of the

equilibrium crack layer length ( $L_{eq}$ ). So it is necessary to calculate  $L_{eq}$ . Always, the value of  $L_{eq}$  is the upper limit for the value of  $L$  ( $l < L < L_{eq}$ ) (Figure 5).

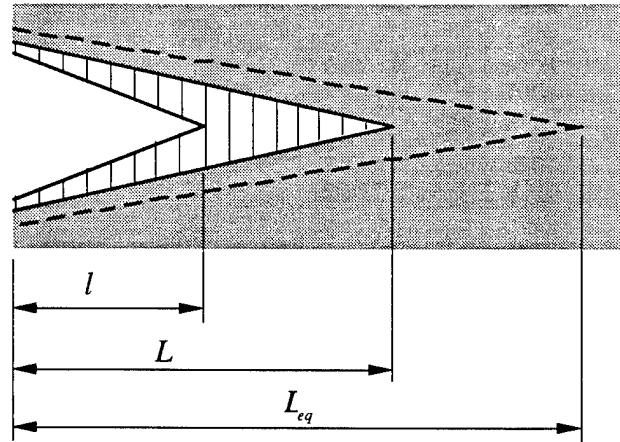


Figure 5. Crack layer configuration

For a fixed value of  $l$ ,  $L_{eq}$  is the value of  $L$  which causes the driving force for crack layer extension ( $X_L$ ) to equal zero. From equation 2.2(b),  $X_L = 0$  can be true in two ways,

$$\begin{aligned} K_{\infty} + K_{dr} &= 0 & (a) \\ K_{\infty} + (1 + 2\tilde{\gamma})K_{dr} &= 0 & (b) \end{aligned} \quad (2.21)$$

In equations 2.21, (b) gives the shorter (and stable) value of  $L_{eq}$  ( $0 \leq \tilde{\gamma} < \infty$ ) (Figure 6). (In equations 2.21, (b)'s value of  $L_{eq}$  is shorter because  $|K_{dr}^{(b)}| \leq |K_{dr}^{(a)}|$  ( $K_{dr} \leq 0$ , always.), and because  $|K_{dr}|$  increases from zero as  $L$  increases from  $l$ .) Therefore, while holding all other parameters fixed,  $L_{eq}$  equals the value of  $L$  which makes

$$K_{\infty} + (1 + 2\tilde{\gamma})K_{dr} = 0. \quad (2.22)$$

Therefore, define

$$f(\tilde{\gamma}, W, \sigma_{dr}, \sigma_{\infty}(x), l, L) \equiv K_{\infty} + (1 + 2\tilde{\gamma})K_{dr}. \quad (2.23)$$

Define

$$g(L) \equiv \text{value of } f(L, \dots), \text{ for fixed values of } \tilde{\gamma}, W, \sigma_{dr}, \sigma_{\infty}(x), l. \quad (2.24)$$

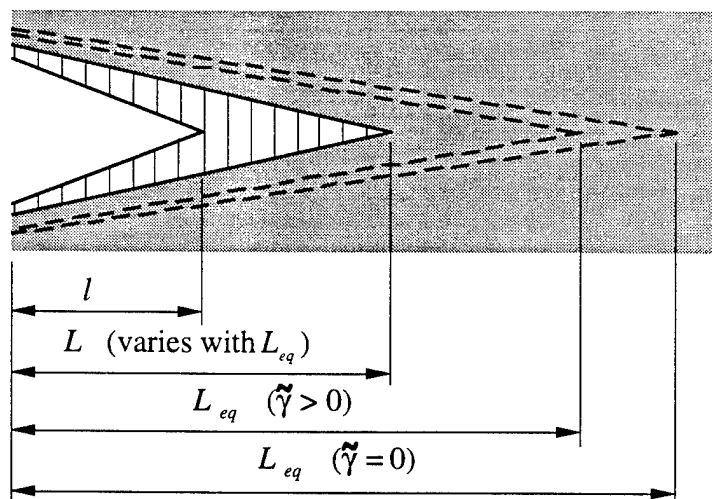
Then,

$$L_{eq}(\tilde{\gamma}, W, \sigma_{dr}, \sigma_{\infty}(x), l) = , \quad L \text{ so that } g(L) = 0. \quad (2.25)$$

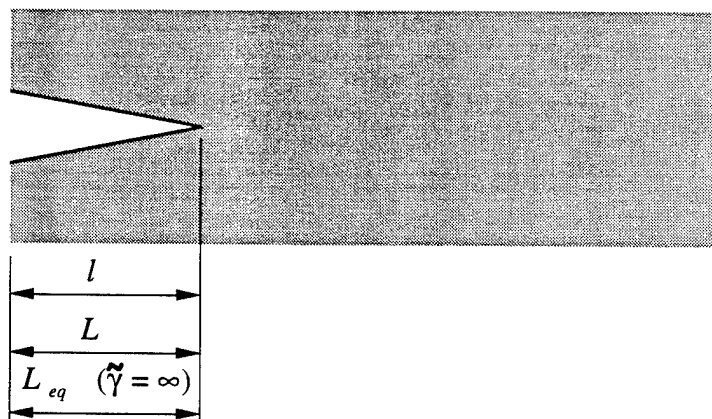
For a particular simulation,  $\tilde{\gamma}$ ,  $W$ , and  $\sigma_{dr}$  are constants; and  $\sigma_{\infty}(x)$  is a prescribed function.

Therefore, for any value of  $l$  (such as the new value of  $l$  calculated during a time step),  $L_{eq}$  can be calculated. The value of  $L$  which makes  $g(L) = 0$ , can be found by any method for

determining the root of a nonlinear function  $(g(L))$ . The root is located within the interval  $l < \text{root} < W$ .



a) Showing maximum possible value



b) Showing lower limit

Figure 6. Equilibrium crack layer lengths

### 2.2.6 Enforcement of constraints on the crack and crack layer lengths

The test conditions referred to in subsection 2.2.5 are

$$\begin{aligned}
 l_{\text{new}} &> L_{\text{new}} & (a) \\
 L_{\text{new}} &> L_{\text{eq}(\text{new})} & (b) \\
 \frac{L_{\text{eq}(\text{old})} - L_{\text{old}}}{L_{\text{eq}(\text{old})}} &< \epsilon & (c) \\
 \frac{L_{\text{new}} - L_{\text{eq}(\text{new})}}{L_{\text{eq}(\text{new})}} &< \epsilon & (d)
 \end{aligned} \tag{2.26}$$

$\epsilon$  is a prescribed small number, ( $\epsilon \ll 1$ ).

If (a) and (b) are both false, then the time step continues (sub-subsection 2.2.4.7).

If (a) is true, then the time step is repeated<sup>(1)</sup>, with an adjusted time increment.

$$\Delta t = (\Delta t) \left( \frac{L_{\text{old}} - l_{\text{old}}}{(l_{\text{new}} - L_{\text{new}}) + (L_{\text{old}} - l_{\text{old}})} \right) \quad (\text{Figure 7}) \tag{2.27}$$

If (b) and (c) are true, then the value of  $L_{\text{new}}$  is adjusted, and then the time step continues (sub-subsection 2.2.4.7).

$$L_{\text{new}} = L_{\text{eq}(\text{new})} \tag{2.28}$$

If (b) and (d) are true, and (c) is false, the value of  $L_{\text{new}}$  is also adjusted according to equation 2.28, and then the time step continues (sub-subsection 2.2.4.7).

If (b) is true, and (c) and (d) are false, then the time step is repeated, with an adjusted time increment.

---

(1) Within section 2.2, whenever a time step is repeated, the repetition begins with sub-subsection 2.2.4.6.

$$\Delta t = (\Delta t) \left( \frac{L_{eq(old)} - L_{old}}{(L_{new} - L_{eq(new)}) + (L_{eq(old)} - L_{old})} \right) \quad (2.29)$$

During the first attempt for all time steps, the time increment ( $\Delta t$ ) is set equal to the prescribed initial time increment ( $\Delta t_0$ ). If the first attempt fails, then  $\Delta t$  will be adjusted, so that during the second attempt  $\Delta t < \Delta t_0$ . There is no limit on the number of attempts that a time step may require, but  $\Delta t = \Delta t_0$  only on the first attempt.

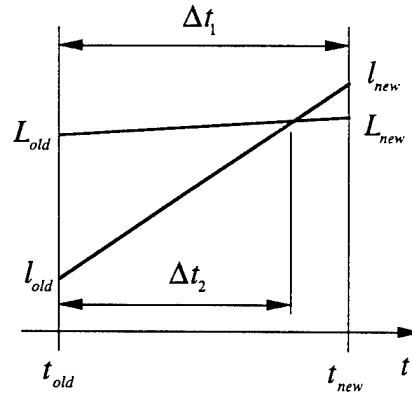


Figure 7. Time increment adjustment

### 2.2.7 Prevention of crack extension into undegraded material

Another program array is introduced in this subsection, for the driving force for crack extension,  $X_l[i]$ .

Define  $\Delta t_{pz(0)}$ , so that

$$2\gamma(\Delta t_{pz(0)}) \approx 0. \quad (2.30)$$

$\Delta t_{pz(0)}$  is the elapsed time for the resistance to crack extension of a material subjected to the drawing stress, to reach zero (or at least to reach a value close to zero). (Equation 2.30 uses “ $\approx$ ”, instead of “ $=$ ”, because some material surface energy functions ( $2\gamma(\dots)$ ) decrease exponentially. For an exponentially decreasing  $2\gamma(\dots)$ , only  $2\gamma(\infty) = 0$ .) The time increment for the current time step is  $\Delta t$ . If

$$\frac{\Delta t}{\Delta t_{pz(0)}} \ll 1, \quad (\text{in practice, is always true (Figure 8.)}) \quad (2.31)$$

then it may be numerically possible for the crack to extend into undegraded material. But, it is normally physically impossible for the crack to extend into undegraded material. The purpose of the procedure within this subsection is to prevent the physically excluded crack extension.

**Procedure:** If at the end of the  $n$ th time step (after the calculation loop of subsection 2.2.4 has been successfully completed),

$$\begin{aligned} X_l[n-1] &> 0 \\ X_l[n] &= 0 \end{aligned}, \quad (\text{if both are true}) \quad (2.32)$$

then, the (ordered) array  $l[\dots]$  is searched backwards from  $l[n]$ , to find  $l[i]$ , so that  $l[i] = l[i-1]$ . What makes it possible to find  $l[i]$ , so that  $l[i] = l[i-1]$ , is that a crack may sometimes not grow for a sequence of time steps. If one or both conditions of equation 2.32 are false, then the  $n$ th time step is accepted as valid. If equations 2.32 are true, and

$$\frac{l[n] - l[n-1]}{l[i] - l[n-1]} > (1 + \epsilon), \quad (\epsilon \text{ is a prescribed small number, } (\epsilon \ll 1).) \quad (2.33)$$

is true, then the time step is repeated with a smaller time increment,

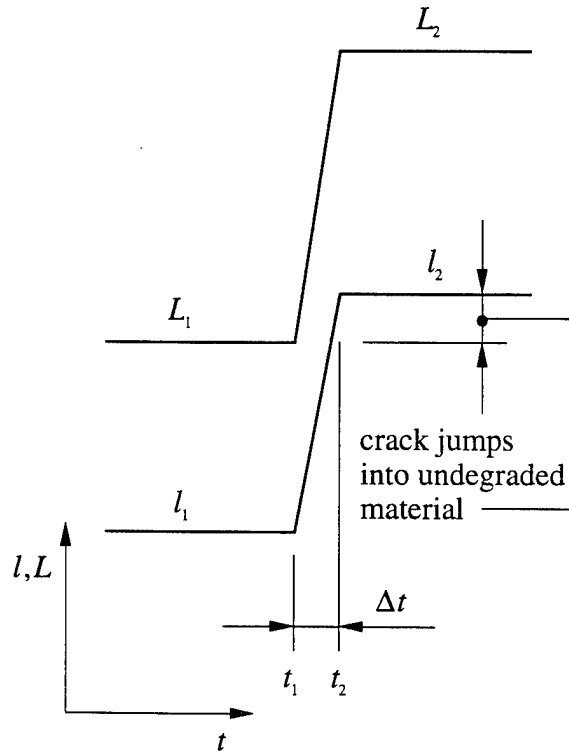


Figure 8. Penetration of crack into undegraded material

$$\Delta t = (\Delta t) \left( \frac{L[i] - l[n-1]}{l[n] - l[n-1]} \right) (1 + \varepsilon). \quad (2.34)$$

Otherwise, the  $n$ th time step is accepted as valid.

### 2.2.8 Time jumps to decrease required computer time

Recall equation 2.1

$$\begin{aligned} \dot{l} &= k_1 \cdot X_l & (a) \\ \dot{L} &= k_2 \cdot X_L & (b) \end{aligned} \quad (2.35)$$

and equation 2.18

$$\begin{aligned}\Delta l &= \dot{l} \cdot \Delta t & (a) \\ \Delta L &= \dot{L} \cdot \Delta t & (b)\end{aligned}\tag{2.36}$$

These equations indicate that if the calculated values of the driving forces for crack length extension ( $X_l$ ) and crack layer length extension ( $X_L$ ) are negative (in which case they will be set equal to zero), or zero, then the crack and crack layer lengths cannot increase. The parameters of  $X_l$  and  $X_L$  are

$$\begin{aligned}X_l &= X_l(l, L, E, \tilde{\gamma}, \sigma_{dr}, W, \sigma_{\infty}(x), \Delta t_{pz}) & (a) \\ X_L &= X_L(l, L, E, \tilde{\gamma}, \sigma_{dr}, W, \sigma_{\infty}(x)) & (b)\end{aligned}\tag{2.37}$$

For fixed values of  $l$  and  $L$ , the only parameter in equations 2.37 which changes with time, is  $\Delta t_{pz}$  (the elapsed time since the material at the current location of the crack tip (at  $l$ ) was drawn, i.e., since that material became part of the process zone).

If the current value of  $X_l$  is zero, and the current value of  $X_L$  is very small (the calculated value of  $X_L$  will always be positive, but it can approach zero), then the system will be effectively frozen until enough time has passed, so that  $\Delta t_{pz}$  has increased and become greater than some critical value ( $\Delta t_{pz(cr)}$ ). Recall that  $X_l = J_1 - 2\gamma(\Delta t_{pz})$ .  $\Delta t_{pz(cr)}$  will make the equality  $J_1 = 2\gamma(\Delta t_{pz(cr)})$  true. The maximum time increment used within a simulation is  $\Delta t_0$  (the user prescribed time increment, which is used during the first attempt at executing every time step). Depending on the particular set of input parameters, it can be possible that during a simulation there will be multiple instances when  $\Delta t_0 \ll \Delta t_{pz(cr)}$  (and,  $X_l = 0$  and  $X_L \ll 1$ ). In these instances, many time steps will be taken during which the only system parameter which changes

significantly is time ( $t$ ). This can result in a simulation which requires a great amount of computer time. The purpose of the procedure within this subsection is to, when possible, instantly increment the time by an amount ( $\Delta t_j$ ), which causes the equality  $\Delta t_{pz} = \Delta t_{pz(cr)}$  to be true (Figure 9.).

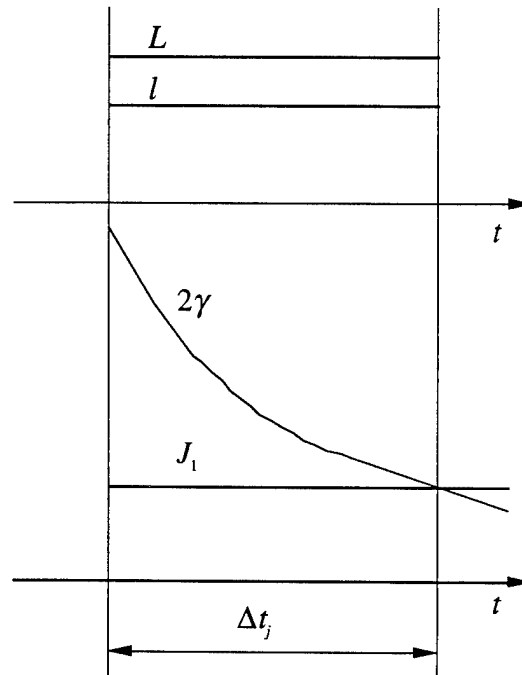


Figure 9. Time jump under constant load

**Procedure:** At the end of the  $n$ th time step (if the procedure of subsection 2.2.7 does not cause the time step to be repeated), the following conditions are tested for

$$\begin{aligned}
 &X_l[n] = 0 \\
 &\frac{L_{eq}[n] - L[n]}{L_{eq}[n]} < \epsilon \quad (\epsilon \text{ is a prescribed small number, } (\epsilon \ll 1).) \quad (2.38)
 \end{aligned}$$

If both of conditions 2.38 are true, then a time jump can be made. (If a time jump cannot be made, then the next time step begins normally.) Define

$$X_I(\Delta t_1) \equiv J_1 - 2\gamma(\Delta t_1). \quad (2.39)$$

The root  $(\Delta t_r)$  of function 2.39, is found by any method for finding the root of a nonlinear equation. The lower limit of the interval which contains  $\Delta t_r$  is the current value of  $\Delta t_{pz}$ . The upper limit is  $\Delta t_{pz(0)}$  (see equation 2.30).

$$\Delta t_{pz} < \Delta t_r < \Delta t_{pz(0)} \quad (2.40)$$

Define

$$\Delta t_j \equiv \Delta t_r - \Delta t_{pz}. \quad (2.41)$$

Now the time step counter is incremented and then the array values are set for this new time step,

$$\begin{aligned} n &= n + 1 \\ l[n] &= l[n - 1] \\ L[n] &= L[n - 1] \\ t[n] &= t[n - 1] + \Delta t_j \end{aligned} \quad (2.42)$$

The calculation loop of subsection 2.2.4 is now restarted from the beginning.

### **2.2.9 Determination of specimen failure**

The criterion for specimen failure, is that  $L$ , the crack layer length, equals (approaches very close to)  $W$ , the specimen width. Equivalently, the specimen fails when all (almost all) of the material ahead of the crack tip (at  $l$ ) is drawn (when the process zone reaches (almost reaches) the far edge of the specimen).

**Procedure:** During each time step, after the candidate new values of the crack length ( $l_{\text{new}}$ ), and the crack layer length ( $L_{\text{new}}$ ) are calculated (sub-subsection 2.2.4.6), and immediately before the procedure of subsection 2.2.6 is performed, the following condition is tested for.

$$L_{\text{new}} \geq W \quad (2.43)$$

If condition 2.43 is false, then the time step continues normally with subsection 2.2.6. If condition 2.43 is true, then the time increment is adjusted, and the time step repeated.

$$\Delta t = \frac{\Delta t}{10} \quad (2.44)$$

If during the  $n$ th time step, condition 2.43 becomes true for the sixth time, the  $n$ th time step is abandoned, the specimen is presumed to have failed, and the simulation is ended. The lifetime (or time to failure) ( $t_f$ ) of the specimen is

$$t_f = t[n - 1]. \quad (2.45)$$

Using this method to determine specimen failure, insures that the final value of the crack layer length ( $L_f$ ) satisfies

$$\frac{W - L_f}{W} \ll 1. \quad (2.46)$$

### 2.3 ALGORITHM FOR SEN SPECIMEN SUBJECTED TO LOAD CONTROL

This section will specify the changes which are made to the algorithm of section 2.2 (constant remote load) when the remote load varies with time, i.e., when the remote load function changes from  $\sigma_{\infty}(x)$  to  $\sigma_{\infty}(x, t)$ .

A new sub-subsection (2.2.4.1(a)) is added, in which the remote load function ( $\sigma_{\infty}(x, t)$ ) is updated at the beginning of each time step for the new time. For instance, at the start of the first time step, the function would be  $\sigma_{\infty}(x, 0)$ .

The energy release rate ( $J_1$ ) is now (explicitly) time dependent. It seems logical that the time jumps of subsection 2.2.8 could be used in this algorithm (load control) by modifying equation 2.39 to become

$$X_I(\Delta t_1) \equiv J_1(t) - 2\gamma(\Delta t_1). \quad (t = t_{pz} + \Delta t_1) \quad (2.47)$$

Doing this would be wrong. The algorithm for load control cannot allow time jumps. For a time varying remote load function, equations 2.37 become

$$\begin{aligned} X_I &= X_I(l, L, E, \tilde{\gamma}, \sigma_{dr}, W, \sigma_{\infty}(x, t), \Delta t_{pz}) & (a) \\ X_L &= X_L(l, L, E, \tilde{\gamma}, \sigma_{dr}, W, \sigma_{\infty}(x, t)) & (b) \end{aligned} \quad (2.48)$$

The driving force for crack layer extension ( $X_L$ ) is now time dependent. This means that if a time jump was made, the crack layer length ( $L$ ) would increase. It would be necessary to be able to calculate the size of the increase in  $L$ , in order to be able to calculate  $J_1$  in equation 2.47. However, calculating the value that  $L$  would have after a time jump was made into the future is impossible. The only way to calculate the value of  $L$  for a time  $t$ , is to perform the calculation loop of subsection 2.2.4 until time  $t$  is reached; i.e., there is no equation which will provide a future value of  $L$ . Therefore, every advance in time must be made using subsection 2.2.4, and the time jump procedure of subsection 2.2.8 cannot in any way be used in this (load control) algorithm.

## 2.4 ASSUMPTION OF SIMPLIFIED CRACK LAYER MODEL FOR DISCONTINUOUS GROWTH

The material surface energy function ( $2\gamma(\Delta t_{pz})$ ) usually has one of two forms,

$$2\gamma(\Delta t_{pz}) = 2\gamma_0 e^{-k_0 \Delta t_{pz}}, \quad (\text{exponential}) \quad (2.49)$$

or

$$\begin{aligned} 2\gamma_0(1 - k_0 \Delta t_{pz}) \geq 0: & \quad 2\gamma(\Delta t_{pz}) = 2\gamma_0(1 - k_0 \Delta t_{pz}) \\ 2\gamma_0(1 - k_0 \Delta t_{pz}) < 0: & \quad 2\gamma(\Delta t_{pz}) = 0 \end{aligned} \quad (\text{linear}) \quad (2.50)$$

$2\gamma_0$ , a material constant, is the surface energy for drawn material with no degradation.  $\Delta t_{pz}$  is the elapsed time since the material at the current location of the crack tip (at  $l$ ) was drawn.  $k_0$ , a material constant, is the degradation coefficient. (The information in this (first) paragraph will be used later in this section.)

In industrial applications, plastics are usually subjected to a remote load function ( $\sigma_\infty(x)$ ), whose average value ( $\sigma_{\infty(\text{avg})}$ ) is small compared to the material drawing stress ( $\sigma_{dr}$ ). Laboratory test specimens subjected to a loading in which  $\sigma_{\infty(\text{avg})}$  is small, have been observed to exhibit discontinuous crack and crack layer growth. By “discontinuous growth” is meant; a long time interval during which the crack is stationary and the crack layer is almost stationary, is followed by a very short time interval during which the crack and crack layer grow. This cycle repeats until the specimen has almost failed, when the growth becomes continuous. During the discontinuous part of the growth, each new stationary location of the crack tip (at  $l$ ) is near the previous (almost) stationary location of the front of the crack layer (at  $L$ ). This type of crack and crack layer growth is referred to as “discontinuous”, “stepwise” or “staircase” growth.

Discontinuous growth similar to what has been experimentally observed, can be numerically simulated if the set of input parameters is adjusted so that two conditions are satisfied. Condition 1 is that the value of the energy release rate at the start of the simulation ( $J_{1(0)}$ ), is less than the material's initial surface energy ( $2\gamma_0$ ). Whenever  $J_1 < 2\gamma(\Delta t_{pz})$ , growth is discontinuous. This is because the driving force for crack extension,  $X_I$ , equals  $J_1 - 2\gamma(\Delta t_{pz})$ . When  $X_I$  is calculated to be negative (in which case it is set equal to zero), or zero, then time passes during which the crack does not grow. During a creep (constant load) simulation (or test),  $J_1$  is an increasing function, so that if and when  $J_1$  becomes greater than  $2\gamma_0$  (the maximum possible value of  $2\gamma(\Delta t_{pz})$ ), the remainder of the test will exhibit continuous growth, i.e., the crack will then always be growing. Satisfaction of condition one guarantees that the growth is discontinuous (at least initially).

The second condition required to simulate experimentally observed discontinuous growth, is that

$$k_1, k_2 \gg k_0. \quad (2.51)$$

$k_1$ , a material constant, is the crack length kinetic coefficient.  $k_2$ , a material constant, is the crack layer length kinetic coefficient.  $k_0$  is the degradation coefficient mentioned in this section's first paragraph. Recall equation 2.1,

$$\begin{aligned} \dot{l} &= k_1 \cdot X_I & (a) \\ \dot{L} &= k_2 \cdot X_L & (b) \end{aligned} \quad (2.52)$$

Satisfaction of restriction 2.51 (condition 2) guarantees that the time intervals between growth are much larger than the time intervals of growth.

During a numerical simulation of discontinuous growth, a cycle is repeated in which: (a) the crack and crack layer simultaneously begin to grow very rapidly; (b) the crack stops growing while the crack layer continues to grow, but very slowly and for a large time interval. Each time the crack stops growing, the crack layer will have almost reached the equilibrium crack layer length ( $L_{eq}$ ). The crack layer length ( $L$ ) will then asymptotically approach the equilibrium crack layer length, until another period of rapid growth begins. ( $L$  approaches  $L_{eq}$  asymptotically, because the driving force for crack layer length extension  $X_L(L, \dots)$  is a decreasing function of  $L$ , having maximum value when  $L = l$ , and minimum value (zero) when  $L = L_{eq}$ .) A natural simplification for modeling discontinuous growth, is to assume that the value of  $L$  is always equal to the value of  $L_{eq}$ .

$$L(t, \dots) = L_{eq}(t, \dots) \quad (\text{simplification for modeling discontinuous growth}) \quad (2.53)$$

When this simplification is made, the parameters (for a creep specimen) of the crack layer length ( $L$ ) become

$$L = L_{eq}(\tilde{\gamma}, W, \sigma_{dr}, \sigma_{\infty}(x), l). \quad (2.54)$$

The only parameter in equation 2.54 which is not constant during a simulation is the crack length ( $l$ ). Therefore, for a particular simulation, the crack layer length is a function of only the crack length ( $L = L_{eq}(l)$ ). So, the crack layer grows when and only when the crack grows. Also, all of the process zone material (in front of the crack tip) will be equally degraded, because the crack layer cannot grow while the crack is stationary. This means that each instance of crack growth consists of an instantaneous jump to the end (at  $L_{eq}$ ) of the process zone. The growth cycle

consists of: (a) time passing until the driving force for crack extension ( $X_I, = J_1 - 2\gamma(\Delta t_{pz})$ ) is positive (until  $J_1 > 2\gamma(\Delta t_{pz})$ ); (b) the crack tip ( $l_{old}$ ) instantaneously jumping to the end of the process zone ( $l_{new} = L_{eq(old)}$ ), while the front of the crack layer instantaneously jumps to the new position  $L_{new} = L_{eq}(l_{new})$ .

Using the simplification of equation 2.53 reduces the complexity of the numerical algorithms for modeling discontinuous growth, and results in simulations which require relatively little computer time. The lifetime (or time to failure) ( $t_f$ ) of a specimen becomes slightly (but not significantly) shorter. So a simulation based on the simplified CLM gives a somewhat more conservative value for  $t_f$  than the same simulation based on the (complete) CLM does (Figure 10.).

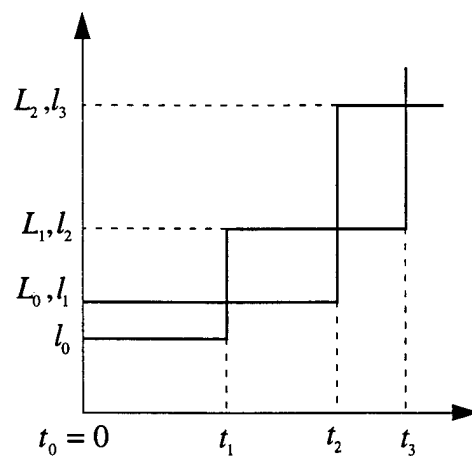


Figure 10. Simplified model of discontinuous crack growth

## 2.5 SIMPLIFIED ALGORITHM FOR SEN SPECIMEN SUBJECTED TO CREEP LOADING

This algorithm uses the simplifying assumption of section 2.4, i.e., that the crack layer length ( $L$ ), is always equal to the equilibrium crack layer length ( $L_{eq}$ ).

### 2.5.1 Determination of remote load function

See subsection 2.2.2.

### 2.5.2 Program Arrays

The initial conditions (of subsection 2.2.1) now become

$$\begin{aligned} t[0] &= 0 \\ l[0] &= l_0 \\ L[0] &= L_{eq}(l_0) \end{aligned} \quad (2.55)$$

Recall from equation 2.25 that

$$L_{eq} = L_{eq}(\tilde{\gamma}, W, \sigma_{dr}, \sigma_{\infty}(x), l). \quad (2.56)$$

With  $l = l_0$ , all parameters of equation 2.56 are known, and  $L[0]$  can be calculated according to the procedure in subsection 2.2.5.

### 2.5.3 Calculation loop for time evolution of crack and crack layer

During odd time steps (1, 3, ...), time ( $t$ ) passes, while the crack length ( $l$ ) and crack layer length ( $L$ ) are stationary. During even time steps (2, 4, ...), the crack length ( $l$ ) and the crack layer length ( $L$ ) both grow, while the time is stationary. ("Time step" is actually a misnomer for the even "time steps", because for them the time increment is zero.)

#### 2.5.3.1 Increment of time step counter

See sub-subsection 2.2.4.1.

### 2.5.3.2 For odd time steps

#### 2.5.3.2.1 Calculation of CODs

The crack opening displacements (CODs),  $\delta_{\infty}$  and  $\delta_{dr}$  are calculated according to sub-subsection 2.2.4.3.

#### 2.5.3.2.2 Calculation of the energy release rate

See sub-subsection 2.2.4.4.

#### 2.5.3.2.3 Calculation of time increment

The procedure in this sub-sub-subsection is similar to the procedure in subsection 2.2.8.

Define

$$f(\Delta t) \equiv J_1 - 2\gamma(\Delta t). \quad (2.57)$$

The time increment is the root ( $\Delta t_r$ ) of function 2.57, which can be found by any method for finding the root of a nonlinear function.

$$0 < \Delta t_r < \Delta t_{pz(0)}. \quad (2.58)$$

$\Delta t_{pz(0)}$  is defined near equation 2.30. According to the assumption ( $L = L_{eq}$ ) of section 2.4, the crack tip ( $l$ ) and the front of the crack layer ( $L$ ) have just jumped to new positions (except for during the first time step, when  $t = 0$ ), and all of the process zone material ahead of the crack tip is now beginning to degrade. That is why the lower limit of interval 2.58 is zero.

As the simulation proceeds, and the crack and crack layer lengths grow, the value of the energy release rate ( $J_1$ ) increases, and the elapsed (degradation) time ( $\Delta t_r$ ) until the crack and crack layer jump to new positions, decreases.

#### 2.5.3.2.4 Update of program array

The time array is now updated, and then the calculation loop of subsection 2.5.3 is restarted from the beginning.

$$t[n] = t[n - 1] + \Delta t, \quad (2.59)$$

#### 2.5.3.3 For even time steps

##### 2.5.3.3.1 Calculation of the new values for the crack and crack layer lengths

The crack tip jumps to the end of the current process zone, and the front of the crack layer jumps to the equilibrium length for the new position of the crack tip.

$$\begin{aligned} l_{\text{new}} &= L_{\text{old}} \\ L_{\text{new}} &= L_{\text{eq}}(l_{\text{new}}) \end{aligned} \quad (2.60)$$

$L_{\text{eq}}(l_{\text{new}})$  is calculated according to the procedure in subsection 2.2.5.

##### 2.5.3.3.2 Update of program arrays

The crack and crack layer length arrays are now updated, and then the calculation loop of subsection 2.5.3 is restarted from the beginning.

$$\begin{aligned} l[n] &= l_{\text{new}} \\ L[n] &= L_{\text{new}} \end{aligned} \quad (2.61)$$

#### 2.5.4 Determination of specimen failure

When  $J_1$  becomes equal to  $2\gamma_0$  (the maximum value for  $2\gamma(\Delta t_{pz})$ ), the growth changes from discontinuous to continuous (i.e., for the remainder of the simulation no time will pass without crack and crack layer growth). For the simplified CLM, increments in crack and crack layer growth are accomplished in zero time. Since, after the onset of continuous growth,

growth must always be occurring, and since all growth must happen instantaneously, once continuous growth begins time cannot increase. Therefore, the onset of continuous growth must be the indicator of specimen failure. So, the criterion for specimen failure is  $J_1 = 2\gamma_0$  (Figure 11).

**Procedure:** After each odd time step is made, the condition  $J_1 \geq 2\gamma_0$  is tested for. If the condition is true, then the simulation is ended, and the lifetime ( $t_f$ ) (or time to failure) for the specimen is

$$t_f = t[n]. \quad (2.62)$$

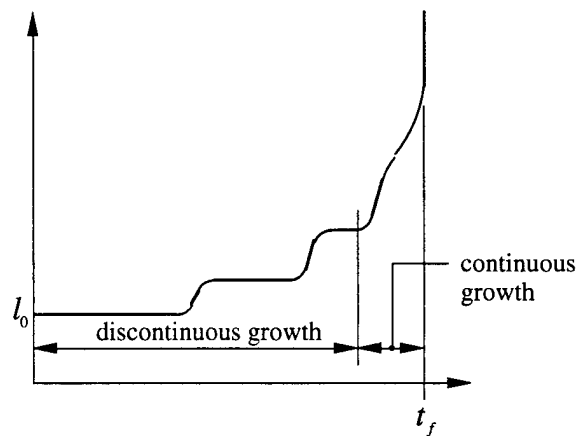


Figure 11. Determination of lifetime

## 2.6 SIMPLIFIED ALGORITHM FOR SEN SPECIMEN SUBJECTED TO LOAD CONTROL

This section will specify the changes which are made to the algorithm of section 2.5 (constant remote load) when the remote load varies with time, i.e., when the remote load function

changes from  $\sigma_{\infty}(x)$  to  $\sigma_{\infty}(x, t)$ . The algorithm uses the simplifying assumption of section 2.4, i.e., that the crack layer length ( $L$ ), is always equal to the equilibrium crack layer length ( $L_{eq}$ ).

A new sub-subsection (2.5.3.1(a)) is added, in which the remote load function ( $\sigma_{\infty}(x, t)$ ) is updated at the beginning of each new time step, whenever the time changes.

### 2.6.1 Program Arrays

This subsection (2.6.1) replaces subsection 2.5.2.

The initial conditions are the same as specified in subsection 2.5.2. The parameters of  $L_{eq}$  (see equation 2.25) become

$$L_{eq} = L_{eq}(\tilde{\gamma}, W, \sigma_{dr}, \sigma_{\infty}(x, t), l). \quad (2.63)$$

With  $l = l_0$  and  $t = 0$ , all parameters of equation 2.63 are known, and  $L[0]$  can be calculated according to the procedure in subsection 2.2.5.

### 2.6.2 Addendum for calculation of time increment

This subsection (2.6.2) modifies sub-sub-subsection 2.5.3.2.3.

Define

$$X_l(t_1) \equiv J_1(t_1) - 2\gamma(\Delta t_{pz}). \quad (\Delta t_{pz} = t_1 - t_{pz}). \quad (2.64)$$

Equation 2.64 replaces equation 2.57.

The root ( $t_r$ ) of function 2.64, is found by any method for finding the root of a nonlinear equation.

The root search interval is

$$t < t_r < t + \Delta t_{pz(0)}. \quad (2.65)$$

Equation 2.65 replaces equation 2.58. Each time function 2.64 is evaluated, the surface energy ( $2\gamma(\Delta t_{pz})$ ) is calculated. The remote load function ( $\sigma_{\infty}(x, t_1)$ ) is updated. The crack layer

length ( $L = L_{eq}(l, \sigma_{\infty}(x, t_1), \dots)$ ) is calculated. The CODs,  $\delta_{\infty} = \delta_{\infty}(l, L, E, W, \sigma_{\infty}(x, t_1))$  and  $\delta_{dr} = \delta_{dr}(l, L, E, W, \sigma_{dr})$  are calculated. The energy release rate ( $J_1 = (\delta_{\infty} + (1 + \tilde{\gamma})\delta_{dr})(-\sigma_{dr})$ ) (equation 2.3) is calculated.

Recall that in section 2.3 (complete algorithm for load control) the size of a time jump could not be calculated, because the value of the crack layer length ( $L$ ) was history dependent. Within this algorithm (section 2.6, simplified algorithm for load control), the size of a time jump (time increment) can be calculated, because the simplifying assumption  $L = L_{eq}$  is used. The value of the equilibrium crack layer length ( $L_{eq}$ ) is not history dependent (Figure 12.).

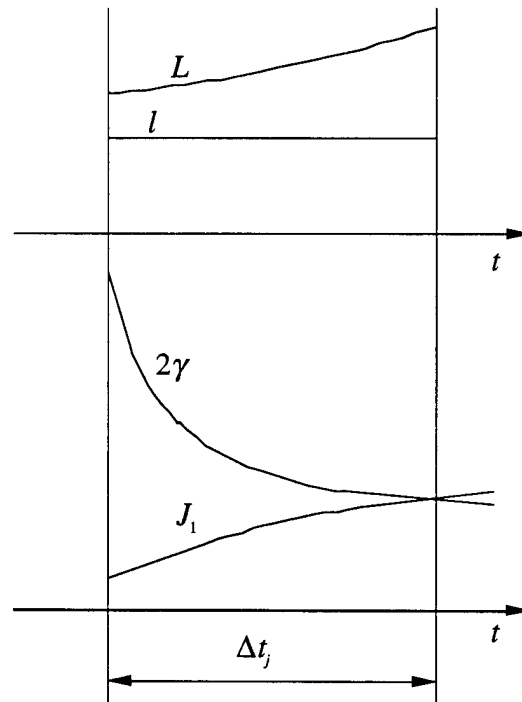


Figure 12. Time jump under increasing load

## 2.7 BASIS FOR SIMPLIFIED ALGORITHM FOR SEN SPECIMEN UNDER DISPLACEMENT CONTROL

When the load is a prescribed function of time (as is true for specimens subjected to creep or load control), the only relevant parameter of specimen geometry is the specimen width ( $W$ ) (the specimen thickness ( $B$ ) is not relevant, (subsection 2.2.2)). When displacement is a prescribed function of time (as is true for specimens subjected to displacement control), an additional parameter of specimen geometry is required, the specimen height ( $2H$ ).  $2H$  is the initial (unstrained) distance between the two grips which hold the specimen.  $H$  is the initial distance from the centerline of the crack to either of the two grips.

For the displacement control mode of loading, the distance ( $2v(x, t)$ ) between the two grips is prescribed as a function of time. The remote load function ( $\sigma_{\infty}(x, t)$ , the traction at either grip) must be calculated. An approximation that will be used in order to make the calculations possible, is that

$$\sigma_{\infty}(x, t) = \sigma_{\infty}(t). \quad (\text{approximation used for displacement control algorithm})(2.66)$$

In other words, at any time  $t$ , the remote load stress will be assumed to be uniform. In order to calculate  $\sigma_{\infty}(t)$ , the displacement which is conjugate to it must be calculated. That displacement is

$$V_p(t) \equiv \frac{1}{W} \int_{x=0}^{x=W} v(x, t) dx. \quad (2.67)$$

$V_p(t)$  is the average value of the prescribed displacement ( $v(x, t)$ ) at the top of the specimen, at time  $t$  (the  $x$ -axis is located at the centerline of the crack). (The average value of the prescribed

displacement at the bottom of the specimen at time  $t$  would be  $-V_p(t)$ .  $v(x, t)$  can be divided into two parts. The first part is due to,  $\sigma_\infty(t)$  applied to the solid (uncracked) body, and is equal to

$$V_s(t) = \frac{H\sigma_\infty(t)}{E}. \quad (2.68)$$

( $E$  is Young's modulus.) The second part of  $v(x, t)$ , which will be called  $V_c(x, t)$ , is due to the tractions  $\sigma_\infty(t)$  and  $\sigma_{dr}$  acting on the top crack face ( $0 \leq \sigma_\infty(t) \leq L$ ,  $l \leq \sigma_{dr} \leq L$ ). The material of the process zone ( $l \leq x \leq L$ ) is imagined to be removed, so that the crack extends from  $x = 0$  to  $x = L$ . The process zone material is then supposed to be replaced by tractions which act to compress the crack, and are equal in magnitude to the process zone stress ( $\sigma_{dr}$ ). Also, when it is

pretended that the process zone material is removed, the specimen becomes linearly elastic.

According to Betti's reciprocal theorem (Figure 13),

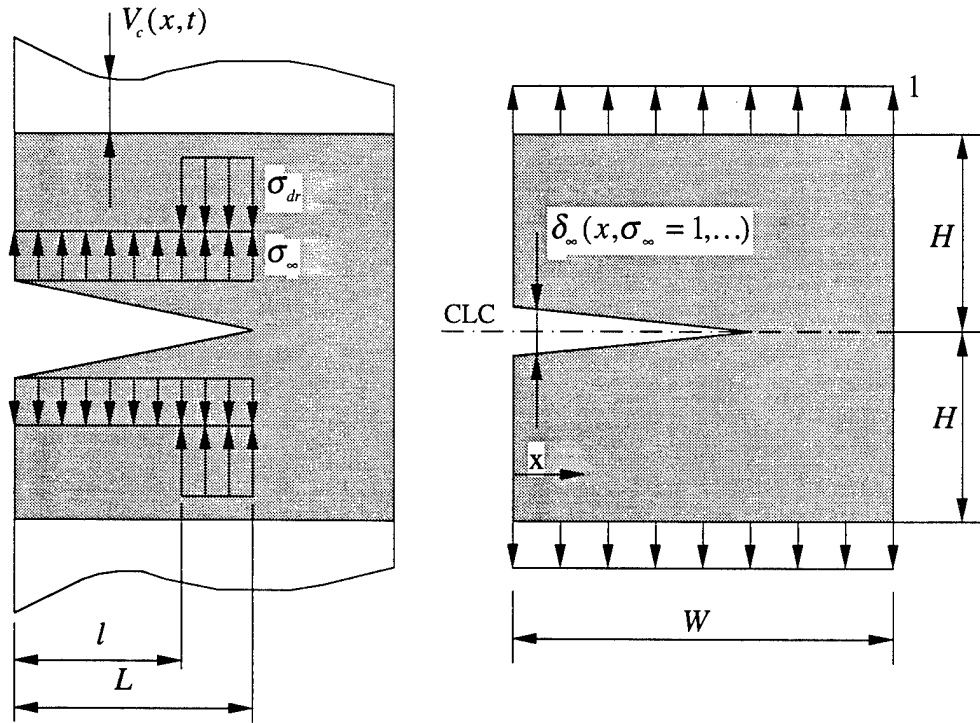


Figure 13. Calculation of edge displacement

$$1 \cdot \int_{x=0}^{x=W} V_c(x, t) dx = \frac{\sigma_{\infty}(t)}{2} \int_{x=0}^{x=L} \delta_{\infty}(x, \sigma_{\infty} = 1, \dots) dx + \frac{\sigma_{dr}}{2} \int_{x=l}^{x=L} \delta_{\infty}(x, \sigma_{\infty} = 1, \dots) dx. \quad (2.69)$$

( $\delta_{\infty}(x, \sigma_{\infty} = 1, \dots)$  is the crack opening displacement at  $x$ -coordinate  $x$ , due to the remote load

function (stress)  $\sigma_{\infty} = 1$ .)  $V_p(t)$  can now be written

$$V_p(t) \equiv \frac{1}{W} \int_{x=0}^{x=W} \{V_s(t) + V_c(x, t)\} dx. \quad (2.70)$$

Therefore,

$$V_p(t) = \frac{H\sigma_\infty(t)}{E} + \frac{\sigma_\infty(t)}{2W} \int_{x=0}^{x=L} \delta_\infty(x, \sigma_\infty = 1, \dots) dx + \frac{\sigma_{dr}}{2W} \int_{x=l}^{x=L} \delta_\infty(x, \sigma_\infty = 1, \dots) dx \quad (2.71)$$

So,

$$\sigma_\infty(t) = \frac{V_p(t) - \frac{\sigma_{dr}}{2W} \int_{x=l}^{x=L} \delta_\infty(x, \sigma_\infty = 1, \dots) dx}{\frac{H}{E} + \frac{1}{2W} \int_{x=0}^{x=L} \delta_\infty(x, \sigma_\infty = 1, \dots) dx}. \quad (2.72)$$

The simplified algorithm for displacement control, is like the simplified algorithm for load control. At the beginning of each time step, time is incremented. Then the prescribed remote displacement function ( $v(x, t)$ ) is updated. From  $v(x, t)$ ,  $V_p(t)$  is calculated. Then using the procedure of subsection 2.2.5, the crack layer length  $L = L_{eq}$  (simplified assumption, section 2.6) is calculated. Then using equation 2.72,  $\sigma_\infty(t)$  can be calculated. After  $\sigma_\infty(t)$  is calculated, the algorithm proceeds like the simplified load control algorithm. But there is a problem regarding the value of  $L$ . The parameters of  $L$  are

$$L = L_{eq}(\tilde{\gamma}, W, \sigma_{dr}, \sigma_\infty(t), l). \quad (2.73)$$

From equation 2.72, the parameters of  $\sigma_\infty(t)$  are,

$$\sigma_\infty(t) = \sigma_\infty(l, L, E, W, H, \sigma_{dr}, v(x, t)). \quad (2.74)$$

So,  $L = L(\sigma_\infty(t), \dots)$ , and  $\sigma_\infty(t) = \sigma_\infty(L, \dots)$ , i.e., each is a function of the other. Therefore,  $L$  and  $\sigma_\infty(t)$  must be computed simultaneously in a cycle during which the value of the first is used to calculate the second, and then the value of the second is used to calculate the first. The cycle continues until the change in  $L$  and  $\sigma_\infty(t)$  between successive cycles is very small.

The computation of  $L$  and  $\sigma_\infty(t)$  is the main difficulty associated with the implementation of the simplified displacement control algorithm. It is also the reason that the complete algorithm ( $L < L_{eq}$ ) for displacement control does not appear in this thesis. A simulation using the complete algorithm would use a relatively great amount of computer time. Also, the primary interest for industry is discontinuous crack and crack layer growth, which the simplified algorithm can model adequately.

## 2.8 SIMPLIFIED ALGORITHM FOR SEN SPECIMEN SUBJECTED TO DISPLACEMENT CONTROL

This algorithm uses the simplifying assumption of section 2.4, i.e., that the crack layer length ( $L$ ), is always equal to the equilibrium crack layer length ( $L_{eq}$ ).

### 2.8.1 Program arrays

The initial conditions are the same as specified in subsection 2.5.2, with one addition specified at the end of this subsection (2.8.1). The parameters of  $L_{eq}$  (see equation 2.25) become

$$L = L_{eq}(\tilde{\gamma}, W, \sigma_{dr}, \sigma_\infty(t), l). \quad (2.75)$$

$l = l_0$  and  $t = 0$ . If the value of the prescribed displacement function  $v(x, t = 0) = 0$ , then  $\sigma_\infty(0) = 0$ , all parameters of equation 2.75 are known, and  $L[0]$  can be calculated according to the procedure in subsection 2.2.5. If  $v(x, t = 0) \neq 0$ , then  $\sigma_\infty(0)$  and  $L[0]$  can be calculated

according to the procedure in sub-subsection 2.8.2.4. Since for displacement control the remote stress ( $\sigma_{\infty}(t)$ ) must be calculated, its values are recorded in an array ( $\sigma_{\infty}[i]$ ). The additional initial condition is

$$\sigma_{\infty}[0] = \sigma_{\infty}(0). \quad (2.76)$$

## **2.8.2 Calculation loop for time evolution of crack and crack layer**

### **2.8.2.1 Increment of time step counter**

See sub-subsection 2.2.4.1.

### **2.8.2.2 Increment of time**

The initial time step increment ( $\Delta t_0$ , see subsection 2.2.3) is used for every time step. The time ( $t$ ) used during a time step, is equal to the previous time ( $t_{\text{old}}$ ) plus  $\Delta t_0$ .

$$t = t_{\text{old}} + \Delta t_0 \quad (2.77)$$

### **2.8.2.3 Update of displacement function**

The prescribed displacement function ( $v(x, t)$ ) is updated for the current value of the time ( $t$ ).

### **2.8.2.4 Simultaneous calculation of the remote load stress and crack layer length**

Note that in this sub-subsection,  $\sigma_{\infty}(t)$  will be called  $\sigma_{\infty}$ , and  $V_p(t)$  will be called  $V_p$ .

The value for the crack layer length ( $L = L_{eq}$ ) must satisfy

$$K_{\infty}(L, W, \sigma_{\infty}) + (1 + 2\tilde{\gamma}) \cdot K_{dr}(l, L, W, \sigma_{dr}) = 0. \quad (\text{see equation 2.22}) \quad (2.78)$$

In order to insure convergence when calculating  $\sigma_\infty$  and  $L$ , it is more convenient to put equation 2.72 in the form,

$$(\sigma_\infty) \left( \frac{H}{E} + \frac{1}{2W} \int_{x=0}^{x=L} \delta_\infty(x, l, L, E, W, \sigma_\infty = 1) dx \right) + \frac{\sigma_{dr}}{2W} \int_{x=l}^{x=L} \delta_\infty(x, l, L, E, W, \sigma_\infty = 1) dx - V_p = 0. \quad (2.79)$$

The value for the remote stress ( $\sigma_\infty$ ) must satisfy equation 2.79. It is more useful to write that the pair ( $\sigma_\infty, L$ ) must satisfy equations 2.78 and 2.79. Therefore, it is desired to solve the system of two nonlinear equations 2.78 and 2.79, for the unknown variables  $\sigma_\infty$  and  $L$  (Figure 14).

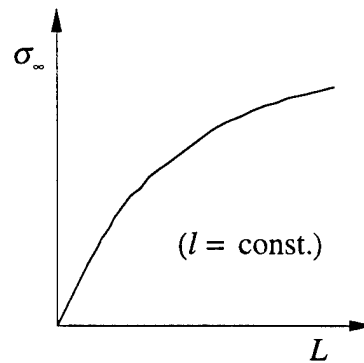


Figure 14. Remote stress - crack layer length relationship

Within the procedure to calculate the remote stress ( $\sigma_\infty$ ) and the crack layer length ( $L$ ), some intermediate values will be used. The intermediate values of  $\sigma_\infty$  will be called  $\sigma_\infty^{\text{old}}$ ,  $\sigma_\infty^{\text{new}}$ ,  $\sigma_\infty^{\text{B}}$ , and  $\sigma_\infty^{\text{D}}$ . The intermediate values of  $L$  will be called  $L^{\text{old}}$ ,  $L^{\text{new}}$ ,  $L^{\text{A}}$  and  $L^{\text{C}}$ .

It is necessary to define some functions which will be used within the procedure to calculate  $\sigma_\infty$  and  $L$ .

$f(\sigma_\infty) \equiv$  function which returns value of  $L$ , by solving equation 2.78 using prescribed value  $\sigma_\infty$

$f(L) \equiv$  function which returns value of  $\sigma_\infty$ , by solving equation 2.78 using prescribed value  $L$

$g(\sigma_\infty) \equiv$  function which returns value of  $L$ , by solving equation 2.79 using prescribed value  $\sigma_\infty$

$g(L) \equiv$  function which returns value of  $\sigma_\infty$ , by solving equation 2.79 using prescribed value  $L$

$\text{mag} \equiv (\sigma_\infty, L)$  function which returns the vector magnitude of the pair  $(\sigma_\infty, L)$

The usual procedure to simultaneously solve equations 2.78 and 2.79, is to repeat a cycle in which equation 2.78 is solved for  $L$  using the value of  $\sigma_\infty$  previously calculated by solving equation 2.79, and then equation 2.79 is solved for  $\sigma_\infty$  using the value of  $L$  previously calculated by solving equation 2.78. But for large values of the prescribed displacement rate ( $v(x, t)$ ), this method diverges. If  $\sigma_\infty$  is represented by the vertical axis, and  $L$  is represented by the horizontal axis, then when equations 2.78 and 2.79 are plotted, they appear in the first quadrant as two intersecting curves. It is desired to find the intersection point  $(L, \sigma_\infty)$ . If the sequence of points

calculated using the procedure just described are connected, they form a rectangular spiral (Figure 15(a)) around the intersection point. For convergence, the spiral grows inward, and for divergence, it grows outward. The procedure which is described below always converges. It works by always remaining on the two upper branches of the intersecting curves, and monotonically moving towards the intersection point (Figure 15(b)).

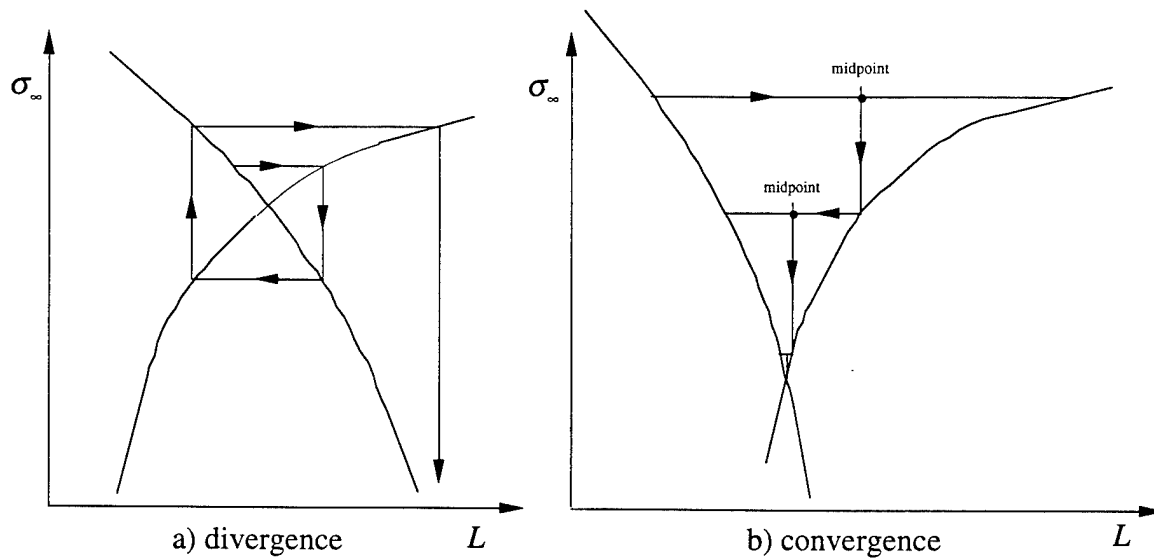


Figure 15. Procedures of solution for two equation system

**Procedure:**

First  $V_p$  is calculated using equation 2.67. Then a numerical procedure is performed which is presented next.

$$\sigma_{\infty}^{\text{old}} = \sigma_{\infty}[n-1] \quad (\sigma_{\infty}[n-1] \text{ equals the value of } \sigma_{\infty} \text{ for the previous time step})$$

$$L^{\text{old}} = L[n-1] \quad (L[n-1] \text{ equals the value of } L \text{ for the previous time step})$$

$$\sigma_{\infty}^{\text{B}} = g(L^{\text{old}})$$

$$L^{\text{A}} = f(\sigma_{\infty}^{\text{B}})$$

$$L^{\text{new}} = \frac{L^{\text{old}} + L^{\text{A}}}{2}$$

*BEGIN LOOP*

$$m^{\text{old}} = \text{mag}(\sigma_{\infty}^{\text{old}}, L^{\text{old}})$$

$$\sigma_{\infty}^{\text{B}} = g(L^{\text{new}})$$

$$\sigma_{\infty}^{\text{D}} = f(L^{\text{new}})$$

IF  $\sigma_{\infty}^{\text{B}} \geq \sigma_{\infty}^{\text{D}}$  THEN

$$\sigma_{\infty} = \sigma_{\infty}^{\text{B}}$$

$$L^{\text{A}} = f(\sigma_{\infty})$$

$$L^{\text{new}} = \frac{L^{\text{new}} + L^{\text{A}}}{2}$$

ELSE

$$\sigma_{\infty} = \sigma_{\infty}^{\text{D}}$$

$$L^{\text{C}} = g(\sigma_{\infty})$$

$$L^{\text{new}} = \frac{L^{\text{new}} + L^{\text{C}}}{2}$$

END IF

$$L = L^{\text{new}}$$

$$m^{\text{new}} = \text{mag}(\sigma_{\infty}, L)$$

IF  $\frac{\text{abs}(m^{\text{new}} - m^{\text{old}})}{m^{\text{old}}} < \varepsilon$  ( $\varepsilon$  is a prescribed small number, ( $\varepsilon \ll 1$ )). THEN EXIT LOOP

$$\sigma_{\infty}^{\text{old}} = \sigma_{\infty}$$

$$L^{\text{old}} = L$$

END LOOP

After the loop is exited, the new values of the remote stress ( $\sigma_{\infty}$ ) and crack layer length ( $L$ ) have been calculated and set.

#### **2.8.2.5 Determination of the surface energy**

The surface energy is  $2\gamma(\Delta t_{pz})$  (see sub-subsection 2.2.4.2). As indicated in equation 2.12,  $\Delta t_{pz} = t - t_{pz}$ . For this algorithm,  $t_{pz}$  is the time of the last crack jump, and (of course)  $t$  is the current time. For the first time step,  $t_{pz} = 0$ .

#### **2.8.2.6 Calculation of CODs**

The crack opening displacements (CODs),  $\delta_{\infty}$  and  $\delta_{dr}$  are calculated according to sub-subsection 2.2.4.3 (actually, according to the appendix).

#### **2.8.2.7 Calculation of the energy release rate**

See sub-subsection 2.2.4.4.

### 2.8.2.8 Calculation of driving force for crack length extension

The driving force for crack length extension ( $X_l$ ) is calculated as specified in sub-subsection 2.2.4.5. What happens next depends on whether  $X_l$  is zero or positive.

### 2.8.2.9 If driving force for crack length extension is zero

#### 2.8.2.9.1 Update of program arrays

The crack and crack layer lengths, and time arrays are now updated, and then the calculation loop of subsection 2.8.2 is restarted from the beginning.

$$\begin{aligned} l[n] &= l[n-1] \\ L[n] &= L \\ \sigma_{\infty}[n] &= \sigma_{\infty} \\ t[n] &= t[n-1] + \Delta t_0 \end{aligned} \tag{2.80}$$

### 2.8.2.10 If driving force for crack length extension is positive

If the driving force for crack length extension ( $X_l$ ) is positive, then the crack tip ( $l$ ) will jump ahead to a new position. It is necessary to calculate the exact time ( $t_j$ ) when  $X_l = 0$ , and the crack jumps.

#### 2.8.2.10.1 Calculation of crack length jump time

Define

$$X_l(t_1) \equiv J_1(t_1) - 2\gamma(\Delta t_{pz}). \quad (\Delta t_{pz} = t_1 - t_{pz}). \tag{2.81}$$

The root ( $t_j$ ) of function 2.81, is found by any method for finding the root of a nonlinear equation.

The root search interval is

$$t_{\text{old}} < t_j < t. \quad (\text{see equation 2.77}) \tag{2.82}$$

In order to determine the value of function 2.81 for a particular value  $t_1$ ,  $t$  (sub-subsection 2.8.2.2) is set equal to  $t_1$ . Then the procedures in sub-subsections 2.8.2.3-2.8.2.8 are performed. After the time ( $t_j$ ) when the crack tip jumps is found, the time ( $t_{pz}$ , see sub-subsection 2.8.2.5) when degradation of the process zone begins is reset,

$$t_{pz} = t_j. \quad (2.83)$$

Now, because the crack length is making a jump, an extra time step must be taken before the calculation loop of subsection 2.8.2 begins again. During the current time step, time jumps from  $t_{old}$  ( $t[n-1]$ ) to  $t_j$ , the crack layer length grows from  $L[n-1]$  to the new calculated value  $L$ , the remote stress grows from  $\sigma_{\infty}[n-1]$  to the new calculated value  $\sigma_{\infty}$ , and the crack length ( $l$ ) remains stationary. During the extra time step (starting with sub-sub-subsection 2.8.2.10.3) the time step counter is incremented ( $n = n + 1$ ), and then the crack length jumps from  $l[n-1]$  to  $L[n-1]$ , while  $L$  and  $\sigma_{\infty}$  jump to new values which are calculated using the new value of the crack length. During the extra "time step", the time ( $t$ ) and therefore the prescribed displacement ( $v(x, t)$ ) remain stationary. For the extra time step, the jump in the remote stress ( $\sigma_{\infty}$ ) is negative, because the displacement remains fixed while the specimen stiffness decreases (because the crack and crack layer lengths have increased).

#### **2.8.2.10.2 Update of program arrays for time jump**

The crack length, crack layer length, remote stress and time arrays are updated.

$$\begin{aligned}
l[n] &= l[n-1] \\
L[n] &= L \\
\sigma_{\infty}[n] &= \sigma_{\infty} \\
t[n] &= t_j
\end{aligned}
\quad (L \text{ and } \sigma_{\infty} \text{ are the values calculated in sub-subsection 2.8.2.4.})(2.84)$$

#### **2.8.2.10.3 Increment of time step counter for extra time step**

See sub-subsection 2.2.4.1.

#### **2.8.2.10.4 Simultaneous calculation of the remote load stress and crack layer length for the extra time step**

The crack length ( $l$ ) is set equal to the current value of the crack layer length ( $L[n-1]$ ), and then new values of the remote stress ( $\sigma_{\infty}$ ) and crack layer length ( $L$ ) are calculated using the procedure of sub-subsection 2.8.2.4.

#### **2.8.2.10.5 Update of program arrays for crack length jump**

The crack length, crack layer length, remote stress and time arrays are updated, and then the calculation loop of subsection 2.8.2 is restarted from the beginning.

$$\begin{aligned}
l[n] &= L[n-1] \\
L[n] &= L \\
\sigma_{\infty}[n] &= \sigma_{\infty} \\
t[n] &= t[n-1]
\end{aligned}
\quad (L \text{ and } \sigma_{\infty} \text{ are the values calculated in sub-subsection 2.8.2.4.})(2.85)$$

### **2.8.3 Determination of specimen failure**

See subsection 2.5.4.

## **2.9 CONCLUSIONS**

This chapter has presented procedures for implementing numerical simulations of standard experimental tests according to the equations of the CLM. After the material properties which appear in the model's equations are determined, the output from numerical simulations can

be compared to experimental results, in order to judge the model's value. Simulations can be used to calculate lifetimes far beyond the possible range of experimental data.

### 3. ANALYSIS OF COMPUTER SIMULATIONS FOR SEN SPECIMENS SUBJECTED TO CONSTANT LOADS

#### 3.1 INTRODUCTION

This chapter presents the results and analysis for numerical simulations of single edge notched (SEN) specimens subjected to constant loads. The driving forces are broken down into sub-quantities, and the behaviors of the sub-quantities are shown. The simulation input parameters are given in dimensionless form, which reduces the number of simulation degrees of freedom, and allows the specification of the criterion for simulation similarity. The factors which determine whether a simulation is discontinuous or continuous are specified. Simulations using the complete Crack Layer Model (CLM) are compared to simulations using the simplified CLM. Lifetime-stress plots are shown and discussed for both discontinuous and continuous simulations. Lifetime-stress plots are compared for discontinuous simulations of tension, eccentric tension and pure bending.

#### 3.2 FORCING AND RESISTING FORCES

From equations 2.2(a) and 2.3, the driving force for crack length extension ( $X_I$ ) can be written

$$X_I = (\delta_\infty + (1 + \tilde{\gamma})\delta_{dr})(-\sigma_{dr}) - 2\gamma. \quad (3.1)$$

Equation 3.1 can also be expressed

$$X_I = D_I - R_I. \quad (3.2)$$

$D_I$  and  $R_I$  are defined as

$$\begin{aligned} D_I &\equiv -\sigma_{dr}(\delta_\infty + \delta_{dr}) \\ R_I &\equiv \sigma_{dr}\tilde{\gamma}\delta_{dr} + 2\gamma \end{aligned} \quad (3.3)$$

$2\gamma$  represents the material function  $2\gamma(\Delta t_{pz})$  (see equations 2.4, 2.49, 2.50). Recall that in this thesis, the drawing stress ( $\sigma_{dr}$ ) is a negative quantity (equation 2.17). Therefore, within this thesis, the COD due to the drawing stress ( $\delta_{dr}$ ) is also a negative quantity.  $D_I$  is called the forcing part of the driving force for crack length extension, and is always positive.  $R_I$  is called the resisting part of the driving force for crack length extension, and is also always positive.

Recall equation 2.2(b),

$$X_L = \frac{(K_\infty + K_{dr})(K_\infty + (1 + 2\tilde{\gamma})K_{dr})}{E}. \quad (3.4)$$

$X_L$  is the driving force for crack layer extension, and can be written

$$X_L = D_L - R_L. \quad (3.5)$$

$D_L$  and  $R_L$  are defined as

$$\begin{aligned} D_L &\equiv \frac{1}{E}(K_\infty + K_{dr})^2 \\ R_L &\equiv -\frac{2\tilde{\gamma}K_{dr}}{E}(K_\infty + K_{dr}) \end{aligned} \quad (3.6)$$

$\tilde{\gamma}$  is the material's specific energy of drawing, with domain  $(0 \leq \tilde{\gamma} < \infty)$ . Because  $\sigma_{dr}$  is negative, within this thesis  $K_{dr}$  is always negative.  $D_L$  is called the forcing part of the driving force for crack layer length extension, and is always positive.  $R_L$  is called the resisting part of the driving force for crack layer length extension, and is also always positive.

Some statements will be written about equations 3.1-3.6, which are always physically true, and can be shown to be always numerically true.

$$\begin{aligned}
\delta_{\infty} &\geq |\delta_{dr}| \\
\delta_{\infty} &\geq (1 + \tilde{\gamma}) |\delta_{dr}| \\
K_{\infty} &\geq |K_{dr}| \\
K_{\infty} &\geq (1 + 2\tilde{\gamma}) |K_{dr}|
\end{aligned} \tag{3.7}$$

If, for instance,  $\tilde{\gamma}$  is very large, then the second of relations 3.7 requires that the magnitude of  $\delta_{dr}$  (the COD at  $x = l$  due to the process zone stress ( $\sigma_{dr}$ ) applied on the crack faces between  $x = l$  and  $x = L$ ) be very small with respect to  $\delta_{\infty}$  (the COD at  $x = l$  due to the remote load stress ( $\sigma_{\infty}(x)$ ) applied on the crack faces between  $x = 0$  and  $x = L$ ). Also if  $\tilde{\gamma}$  is very large, then the fourth of relations 3.7 requires that the magnitude of  $K_{dr}$  (the SIF at  $x = L$  due to the process zone stress ( $\sigma_{dr}$ ) applied on the crack faces between  $x = l$  and  $x = L$ ) be very small with respect to  $K_{\infty}$  (the SIF at  $x = L$  due to the remote load stress ( $\sigma_{\infty}(x)$ ) applied on the crack faces between  $x = 0$  and  $x = L$ ). As Figure 6 shows, as  $\tilde{\gamma}$  increases, the equilibrium crack layer length ( $L_{eq}$ ), which is the upper bound for the crack layer length ( $L$ ), decreases, and  $L - l$  decreases. As  $L - l$  decreases, the ratios  $\delta_{dr}/\delta_{\infty}$  and  $K_{dr}/K_{\infty}$  decrease fast enough so that the second and fourth of relations 3.7 are always true.

In Figure 16, the crack length ( $l^*$ ) and the crack layer length ( $L^*$ ) have values so that the forcing part of the driving force for crack layer length extension ( $D_L$ ) equals zero. From the first of equations 3.6, this implies that

$$K_{\infty}(L^*, \dots) + K_{dr}(l^*, L^*, \dots) = 0. \tag{3.8}$$

In Figure 16, the dimensionless (barred) quantities are normalized by the values of the quantities using  $l^*$  and  $L^*$ , i.e.,

$$\begin{aligned}\overline{D}_l(l, L) &= \frac{D_l(l, L)}{D_l(l^*, L^*)} \\ \overline{D}_L(l, L) &= \frac{D_L(l, L)}{D_L(l^*, L^*)}\end{aligned}\quad (3.9)$$

Figure 16(a) shows the evolution of  $\overline{D}_l$  and  $\overline{D}_L$ , as  $l$  is changed from  $l^*$  to  $L^*$  while  $L$  is held fixed and equal to  $L^*$ . Figure 16(b) shows the evolution of  $\overline{D}_l$  and  $\overline{D}_L$ , as  $L$  is changed from  $l^*$  to  $L^*$  while  $l$  is held fixed and equal to  $l^*$ . Figure 16(b) also shows the evolution of  $\overline{D}_L$  when the crack layer length is close enough to the specimen width ( $W$ ), so that the edge influence is significant. Note as Figure 16 shows, that when  $l = L$  (in Figure 16 when  $l = L^*$  or  $L = l^*$ ),  $\overline{D}_l$  equals zero. When the crack tip and the front of the crack layer have the same location ( $l = L$ ),

then the crack tip opening displacements (CTODS), i.e.,  $\delta_\infty$  and  $\delta_{dr}$  each have value zero. When the CTODS are equal to zero, then the first of equations 3.3 shows that  $D_l$  (or  $\overline{D}_l$ ) equals zero.

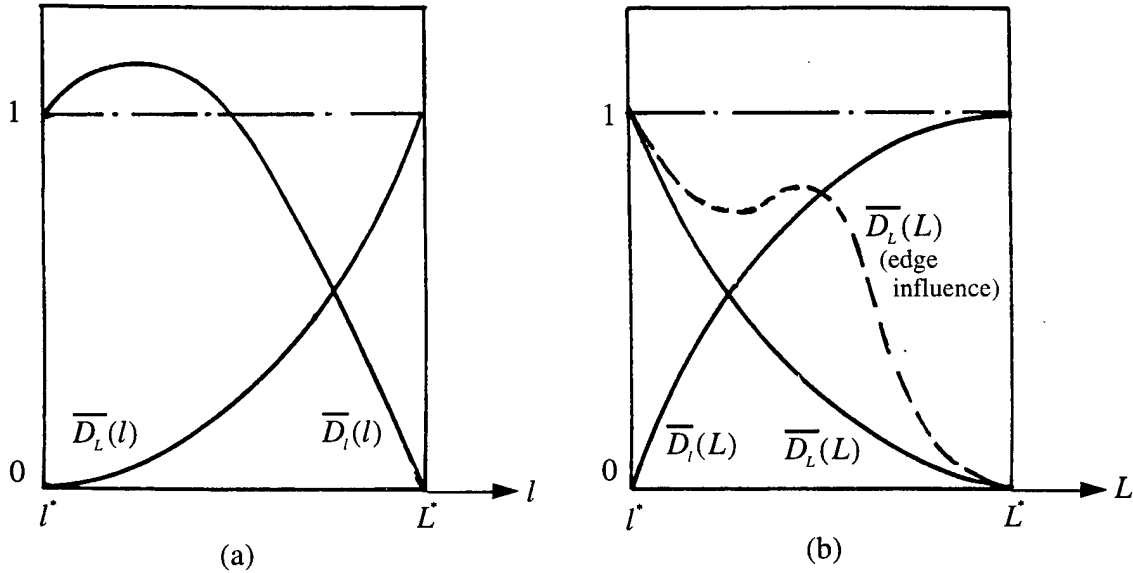


Figure 16. Forcing forces as functions of: (a) crack length; (b) crack layer length

### 3.3 DIMENSIONLESS REPRESENTATION OF SIMULATION INPUT PARAMETERS

The goal of this section is to represent all simulation input parameters in dimensionless form. By doing this, the number of simulation degrees of freedom is reduced, and the criterion for simulation similarity can be specified.

The material constants which are used as normalizing factors, are Young's modulus

$\left(E, \text{ dimensions} = \frac{\text{force}}{(\text{length})^2}\right)$ , the energy per unit crack surface area for drawn but undegraded

material  $\left(2\gamma_0, \text{dimensions} = \frac{\text{force}}{\text{length}}\right)$ , the degradation coefficient  $\left(k_0, \text{dimension} = \frac{1}{\text{time}}\right)$ , and the drawing stress  $\left(\sigma_{dr}, \text{dimensions} = \frac{\text{force}}{(\text{length})^2}\right)$ . The system characteristic length ( $l_*$ ) is defined as

$$l_* \equiv \frac{2\gamma_0 E}{\sigma_{dr}^2}. \quad (3.10)$$

Note that the dimension of  $l_*$  is length. The dimensionless simulation input parameters can now be specified.

The dimensionless specimen width ( $\bar{W}$ ) is

$$\bar{W} = \frac{W}{l_*}, \quad (3.11)$$

( $W$  dimension = length).

The dimensionless crack length kinetic coefficient ( $\bar{k}_1$ ) is

$$\bar{k}_1 = \frac{\sigma_{dr}^2}{k_0 E} k_1, \quad (3.12)$$

$\left(k_1 \text{ dimensions} = \frac{(\text{length})^2}{(\text{force})(\text{time})}\right)$ .

The dimensionless crack layer length kinetic coefficient ( $\bar{k}_2$ ) is

$$\bar{k}_2 = \frac{\sigma_{dr}^2}{k_0 E} k_2, \quad (3.13)$$

$\left(k_2 \text{ dimensions} = \frac{(\text{length})^2}{(\text{force})(\text{time})}\right)$ .

The dimensionless specific energy of drawing ( $\tilde{\gamma}$ ) is

$$\bar{\tilde{\gamma}} = \tilde{\gamma}, \quad (3.14)$$

( $\tilde{\gamma}$  dimension = 1).

The dimensionless initial crack length ( $\bar{l}_0$ ) is

$$\bar{l}_0 = \frac{l_0}{l_*}, \quad (3.15)$$

( $l_0$  dimension = length).

The dimensionless initial crack layer length ( $\bar{L}_0$ ) is

$$\bar{L}_0 = \frac{L_0}{l_*}, \quad (3.16)$$

( $L_0$  dimension = length).

The dimensionless initial time increment ( $\bar{\Delta t}_0$ ) is

$$\bar{\Delta t}_0 = k_0 \Delta t_0, \quad (3.17)$$

( $\Delta t_0$  dimension = time).

The dimensionless remote load stress ( $\overline{\sigma_\infty(x)}$ ) is

$$\overline{\sigma_\infty(x)} = \frac{\sigma_\infty(x)}{\sigma_{dr}}, \quad (3.18)$$

$\left( \sigma_\infty \text{ dimensions} = \frac{\text{force}}{(\text{length})^2} \right).$

A particular dimensionless simulation is defined by specifying the set of dimensionless input parameters  $\{\bar{W}, \bar{k}_1, \bar{k}_2, \bar{\gamma}, \bar{l}_0, \bar{L}_0, \bar{\Delta t}, \bar{\sigma}_\infty(x)\}$ . The set of normalizing parameters  $\{E, 2\gamma_0, k_0, \sigma_{dr}\}$  is eliminated, and these simulation input parameters would each be set equal to 1. For a dimensionless simulation, every calculated quantity is dimensionless, i.e., stress intensity factors (SIFs), crack opening displacements (CODs), values of the energy release rate ( $J_1$ ), etc. Simulation "A" and "B" are similar if their sets of dimensionless input parameters are identical. For similar simulations, outputs can be scaled. For instance, if simulations "A" and "B" are similar, then the total time for simulation "B" ( $t_{f(B)}$ ) can be found from the total time for simulation "A" ( $t_{f(A)}$ ), without having to actually perform simulation "B". If the dimensionless total simulation times are equal, then

$$\bar{t}_{f(A)} = \bar{t}_{f(B)}. \quad (3.19)$$

Therefore,

$$k_{0(A)} t_{f(A)} = k_{0(B)} t_{f(B)}. \quad (3.20)$$

So,

$$t_{f(B)} = \frac{k_{0(A)}}{k_{0(B)}} t_{f(A)}. \quad (3.21)$$

### 3.4 DISCONTINUOUS AND CONTINUOUS GROWTH MODES

Figure 17 shows graphs made from two computer simulations of an SEN specimen subjected to creep loading. Each graph plots the time evolutions of the crack length ( $l$ ), crack layer length ( $L$ ), and equilibrium crack layer length ( $L_{eq}$ ). Figure 17(a) shows a simulation in which the growth rates of the three plotted variables are always positive, so this type of growth is

called continuous. This means that the forcing part of the driving force for crack length extension ( $D_l$ ) is greater than the resisting part of the driving force for crack length extension ( $R_l$ ), during the entire simulation. In Figure 17(b), intervals of positive growth rates alternate with intervals of zero growth rates, so this type of growth is called discontinuous. This means that time intervals in which  $D_l > R_l$  alternate with time intervals in which  $D_l \leq R_l$ . Note that the time scales used in Figures 11(a) and 11(b) are not equal.

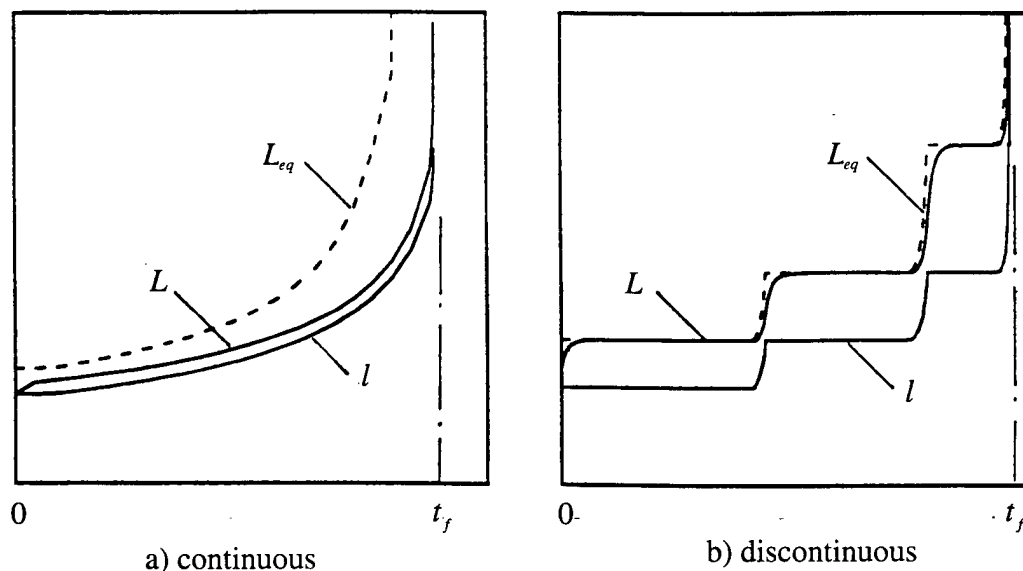


Figure 17. Crack layer growth

Simulation "A" is identical to simulation "B", if for each simulation input parameter "C", the value of "C" for simulation "A" equals the value of "C" for simulation "B". Simulation "A" is comparable to simulation "B", if exactly one simulation input parameter prevents "A" and "B" from being identical. If a particular simulation is discontinuous, then a continuous comparable

simulation can be made by either increasing the input parameter corresponding to the remote load ( $\sigma_{\infty}(x)$ ), or by adjusting the input parameter associated with temperature ( $2\gamma_0$ ) to reflect a temperature increase. The material constant  $2\gamma_0$  is called the initial surface energy, and represents the rate of energy required for extending the crack in undegraded drawn material (i.e., in material which has been drawn for a time interval  $\Delta t = 0$ ).  $2\gamma_0$  is a decreasing function of temperature. So, a comparable discontinuous simulation can be made from a continuous simulation, by either increasing  $\sigma_{\infty}(x)$  or by decreasing  $2\gamma_0$ . If from the start, a simulation is discontinuous, it means  $D_l(t = 0)$  is less than  $R_l(t = 0)$  (equations 3.2, 3.3). If  $\sigma_{\infty}(x)$  is increased, then  $D_l(t = 0)$  and  $R_l(t = 0)$  will both increase, but  $D_l(t = 0)$  will increase more.  $\sigma_{\infty}(x)$  can be increased enough so that,  $D_l(t = 0)$  is greater than  $R_l(t = 0)$ , and the simulation becomes initially continuous. If  $2\gamma_0$  is decreased, then  $R_l(t = 0)$  will decrease, while  $D_l(t = 0)$  will not change.  $2\gamma_0$  can be decreased enough so that the simulation would also become initially continuous.

As a simulation continues, the crack length ( $l$ ) and the crack layer length ( $L$ ) will grow. As  $l$  and  $L$  increase, the quantity  $\delta_{\infty} + \delta_{dr}$  ( $\delta_{dr}$  is negative) will increase. This means that all simulations (if not manually stopped) will end as continuous. Using equations 3.3, when

$$\delta_{\infty} \geq - \left( \frac{2\gamma_0}{\sigma_{dr}} + \delta_{dr}(1 + \tilde{\gamma}) \right) \quad (3.22)$$

becomes true, the remainder of the simulation will be continuous. For a simulation which is entirely continuous, condition 3.22 will be true at time  $t = 0$ .

In Figure 17(a), for every time  $t$ , the crack layer length ( $L$ ) is smaller than the equilibrium crack layer length ( $L_{eq}$ ). In Figure 17(b), for most times  $t$ ,  $L$  is almost equal to  $L_{eq}$  ( $L$  can approach closely to  $L_{eq}$ , but is always prohibited from reaching it). The ratio of the crack layer length kinetic coefficient ( $k_2$ ) to the crack length kinetic coefficient ( $k_1$ ) determines how closely  $L$  can approach to  $L_{eq}$ . The observation of computer simulations has shown that if the ratio ( $k_2/k_1$ ) of these two material constants is at least  $1/10$ , then it is possible for  $L$  to approximate  $L_{eq}$ .

For a continuous simulation, the lifetime ( $t_f$ ) is strongly dependent on  $k_1$  and  $k_2$ . If  $k_1 = k_2$ , then  $t_f$  is approximately inversely proportional to them. For a discontinuous simulation (a simulation in which condition 3.22 becomes true just before the simulation finishes)  $t_f$  is only weakly dependent on  $k_1$  and  $k_2$ .  $k_1$  and  $k_2$  only affect the sizes of the time intervals when growth occurs, and for a discontinuous simulation, these intervals are usually designed to be much smaller than the time intervals without growth. For a discontinuous simulation using a particular value for the remote load  $\sigma_\infty(x)$ ,  $t_f$  depends mostly on the material constants  $2\gamma_0$  and  $k_0$  ( $k_0$  is the degradation coefficient, see equations 2.49, 2.50). These constants determine the sizes of the time intervals without growth.

During the time periods between intervals of discontinuous growth, the values of the driving forces for crack length extension ( $X_l$ ) and crack layer length extension ( $X_L$ ) equal zero (see equation 2.1). During intervals of discontinuous growth,  $X_l$  and  $X_L$  are positive. So for a cycle of

no growth - growth - no growth, the driving force rates ( $\dot{X}_I$  and  $\dot{X}_L$ ) increase from zero, and then decrease back to zero. This type of growth is called stable. When a discontinuous simulation becomes continuous,  $\dot{X}_I$  and  $\dot{X}_L$  monotonically increase. The growth is then said to have become unstable. For a simulation which is continuous from  $t = 0$  (a continuous simulation),  $\dot{X}_I$  and  $\dot{X}_L$  are always monotonically increasing, and all growth is unstable.

Most experimental observations have been of discontinuous growth, and have yielded a linear relationship between the logarithms of the applied stress and lifetime (see Figure 18), i.e.,

$$\log(t_f) = \alpha + \beta \log(\sigma_\infty). \quad (3.23)$$

The experimentally observed interval (range) of coefficient  $\beta$  is approximately  $(-2.5, -5.5)$ . It will be shown in section 3.7 that discontinuous simulations can be used to reproduce this interval, while continuous simulations cannot.

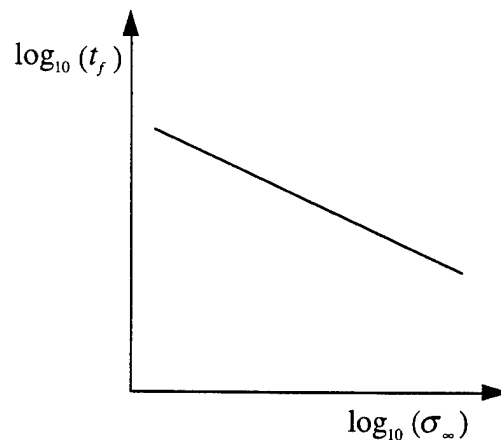


Figure 18. Experimental stress-lifetime relationship

### 3.5 SIMPLIFIED MODEL FOR DISCONTINUOUS GROWTH

The simplification used to implement the simplified CLM for discontinuous growth, is that the crack layer length ( $L$ ) is always equal to the equilibrium crack layer length (see equation 2.53). This simplification results in growth intervals which happen in zero time (see Figure 19). Instantaneous growth intervals could be instituted within numerical simulations of the complete CLM if it was possible to set each of the kinetic coefficients ( $k_1$  and  $k_2$ , see equation 2.1) equal to infinity.

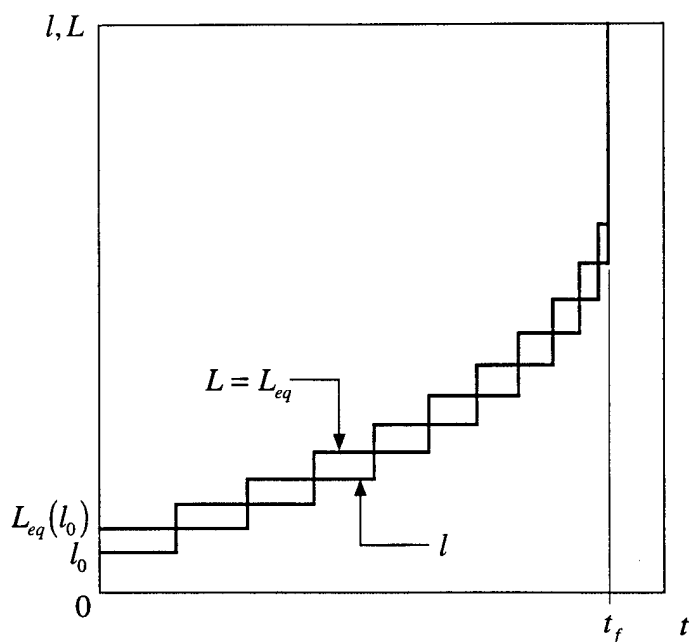


Figure 19. Discontinuous growth using simplified CLM

Figure 20 is a plot of lifetime ( $t_f$ ) versus the kinetic coefficients  $k_1$  and  $k_2$  (for this plot, the degradation coefficient  $k_0$  equals 1, see equation 2.51) made from simulations using the complete

CLM. The horizontal lines are the lifetimes for the same simulations using the simplified CLM. The complete and simplified lifetimes become almost identical when  $k_1$  and  $k_2$  are approximately equal to 10. Experimental observations have shown growth corresponding to large values of  $k_1$  and  $k_2$ . So the simplified model can be used to accurately predict the lifetimes of real specimens. All calculations for plots which appear in the rest of this chapter are made from simulations using the simplified CLM.

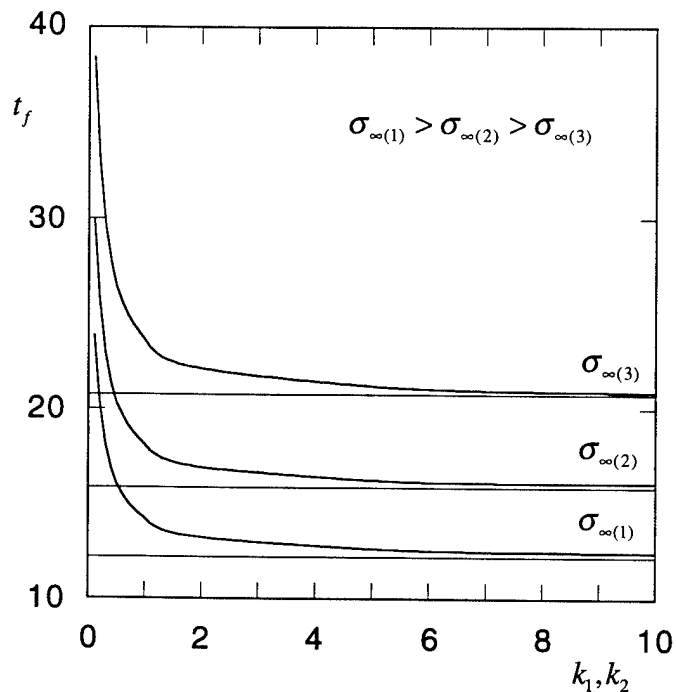


Figure 20. Lifetime versus kinetic coefficients

Figure 21 is a plot made from computer simulations of the dimensionless critical (failure) crack length ( $\bar{l}_c$ ) versus the logarithm of the dimensionless specimen width ( $\bar{W}$ ). ( $\bar{l}_c$ ) and ( $\bar{W}$ )

are normalized by  $l_*$  (see equation 3.10). The values of  $(\bar{l}_c)$  at the right of the plot are almost identical to those for the analytical solutions for a semi-infinite plate.

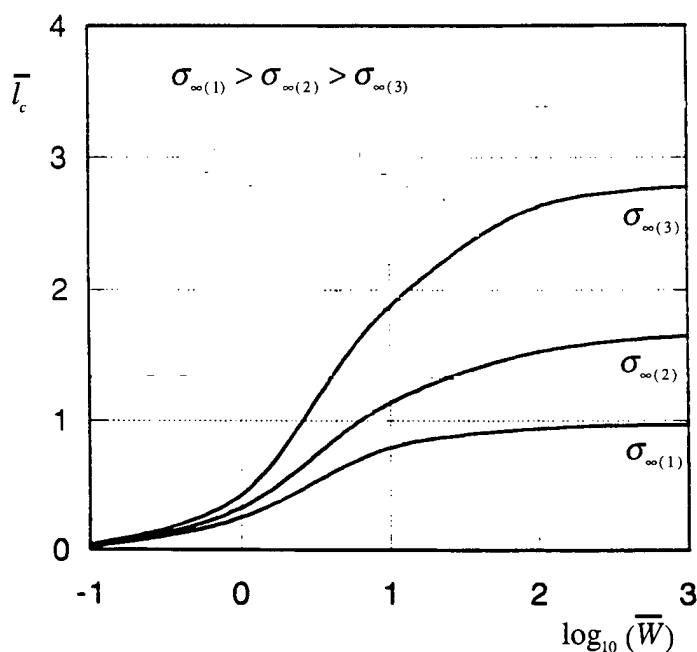


Figure 21. Failure crack length versus specimen width

### 3.6 LIFETIMES FOR TENSION SIMULATIONS

Figures 22(a) and (b) are plots of the logarithm of dimensionless lifetime  $(\bar{t}_f)$  versus the logarithm of applied remote stress, made from simulations of specimens subjected to constant tension loads. Figure 22(a) is made from simulations of discontinuous growth, and Figure 22(b) is made from simulations of continuous growth. Best fit lines are drawn thru the points for each of the values of the dimensionless specimen width  $(\bar{W})$ . The only simulation input parameter which

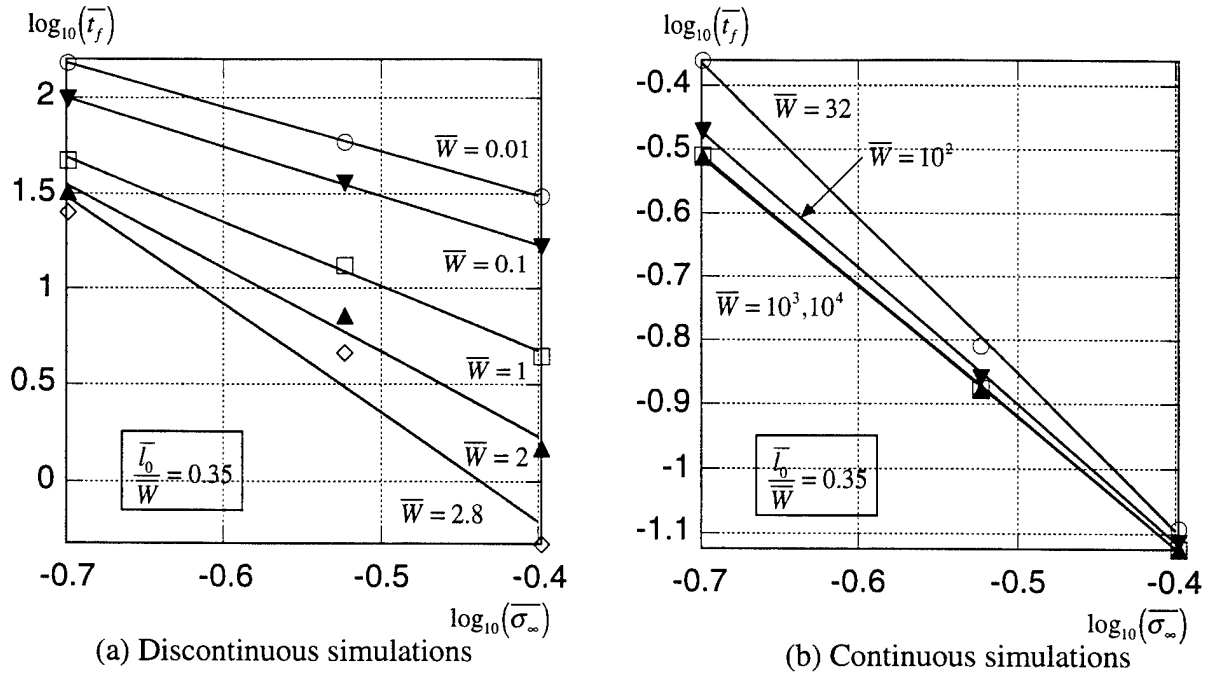


Figure 22. Tension simulations lifetime-stress relations

varies in Figures 22 is  $\bar{W}$ . Since  $\bar{l}_0/\bar{W}$  is constant, as  $\bar{W}$  changes the specimen is geometrically scaled. The formal explanation for why the dimensionless lifetime ( $\bar{t}_f$ ) changes as the specimen changes size is that the similarity referred to in section 3.3 is violated. The physical explanation is that geometrically scaling a specimen also scales the specimen's energy release rate ( $\bar{J}_1$ ). For instance, if the size of a specimen is doubled, then so is  $\bar{J}_1$ . But changing the size of a specimen does not change the properties of the material from which the specimen is made, i.e., the specimen's resistance to crack extension (the material function  $2\bar{\gamma}(\Delta\bar{t}_{pZ})$ ) is constant for geometric scaling. A crack will grow when the driving force for crack length extension

$(\bar{X}_l = \bar{J}_1 - 2\bar{\gamma}(\Delta t_{pz}))$  becomes positive. As  $\bar{W}$  increases,  $\bar{J}_1$  increases, the waiting time until each interval of crack growth decreases, and the lifetime  $(\bar{t}_f)$  decreases.  $\bar{W} = 32$  is used in Figure 22(b), because 32 is very close to being the smallest value of  $\bar{W}$  for which the simulation is initially continuous (remember that within this thesis, a continuous simulation is one which is continuous at time  $t = 0$ , and a discontinuous simulation is one which is discontinuous at time  $t = 0$ ). So  $\bar{W} = 32$  is approximately the lower limit of  $\bar{W}$  for a continuous simulation. Note in Figure 22(b) that as  $\bar{W}$  is increases, the best fit lines appear to converge to a limit.

Figures 23 are plots of the coefficients  $\alpha$  and  $\beta$  (see equation 3.23) of the best fit lines of Figures 22. Note that the discontinuous simulations can reproduce the experimentally observed interval for  $\beta$ ,  $(-2.5, -5.5)$ , while the continuous simulations cannot.

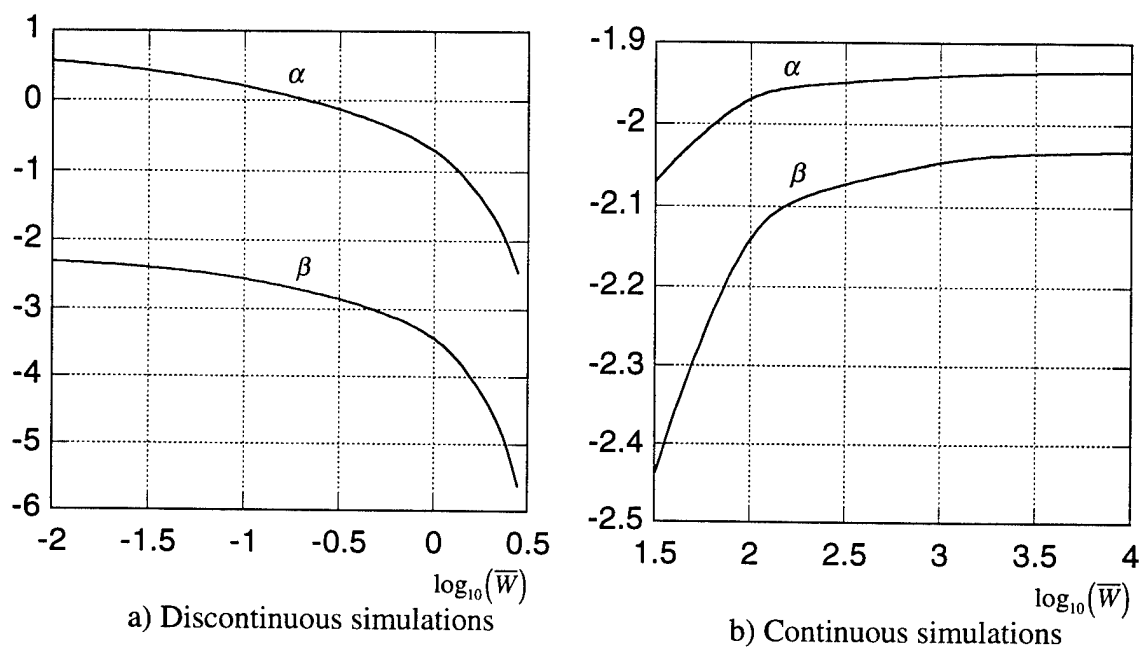


Figure 23. Log(lifetime) - Log(applied stress) best fit line coefficients

### 3.7 LIFETIMES FOR ECCENTRIC TENSION AND PURE BENDING

This section compares lifetimes for discontinuous simulations of tension, eccentric tension and pure bending. The input parameters are adjusted so that each type of loading has the same maximum applied stress (see Figure 24).

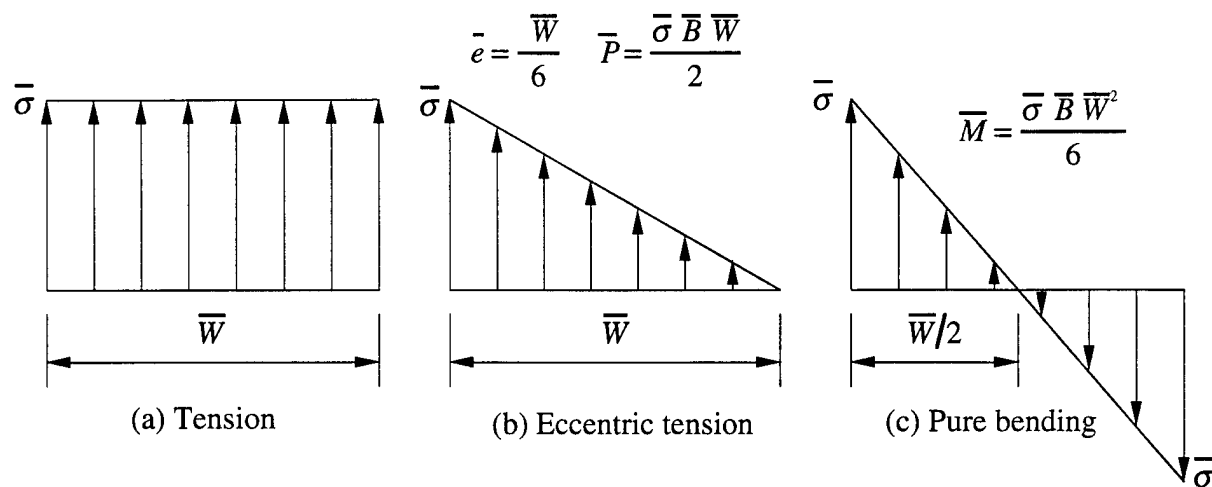


Figure 24. Applied stress distributions

Figures 25 show the calculated lifetime-applied stress relationships. Note that for the small value of  $\bar{W}$  the coefficients  $\beta$  of equation 3.23 are approximately equal, while for the big value of  $\bar{W}$  each value of  $\beta$  is distinct. (Note that the “tension” best fit line of Figure 25(a) and the top best

fit line of Figure 22(a) are the same. Also note that the “tension” best fit line of Figure 25(b) and the bottom best fit line of Figure 22(a) are the same.)

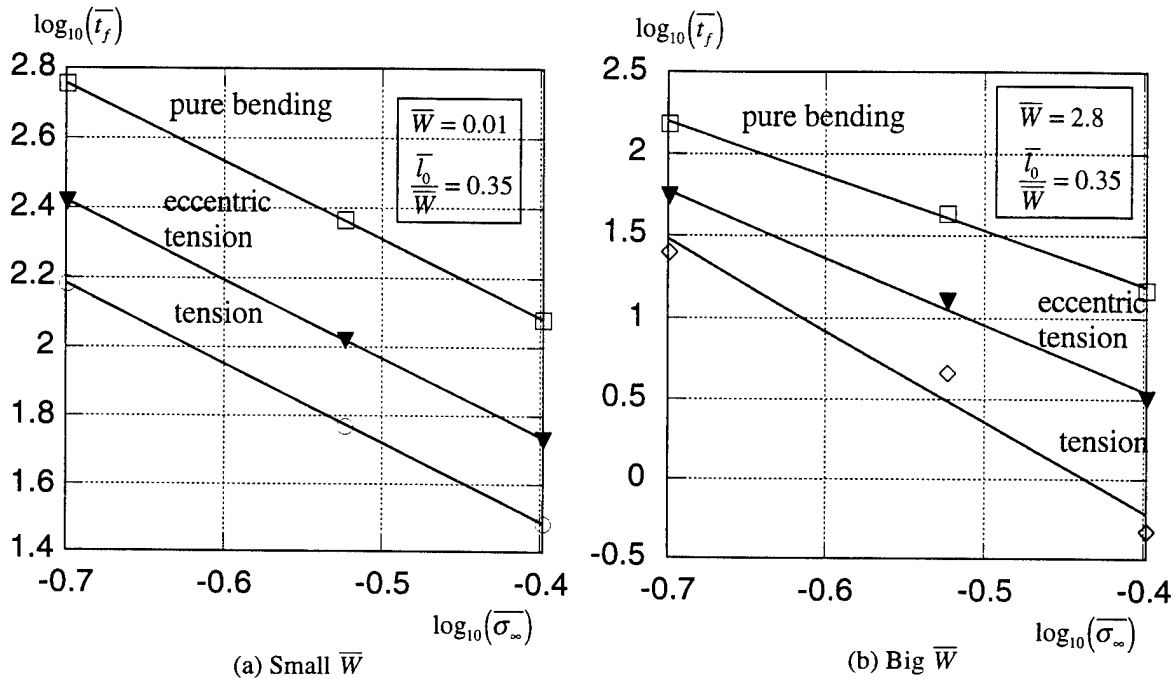


Figure 25. Lifetime-stress relations for tension, eccentric tension and pure bending

### 3.8 CONCLUSIONS

This chapter has analyzed the output from numerical simulations of SEN specimens subjected to constant loads. The behaviors of the driving forces were described. The simulation input parameters were presented in dimensionless form. Discontinuous and continuous simulations were examined and compared. Simulations using the complete CLM were compared to simulations using the simplified CLM. Simulation lifetime-stress relations were shown to have the same form as those obtained experimentally. It was shown that discontinuous simulations can

reproduce the same range of coefficient values in the lifetime-stress relations as have been experimentally determined. It was shown that continuous simulations cannot reproduce this range. Lifetime-stress relations were compared for discontinuous simulations of tension, eccentric tension and pure bending.

## **4. RELIABILITY CALCULATIONS FOR PLASTIC STRUCTURAL COMPONENTS**

### **4.1 INTRODUCTION**

This chapter will show a method for calculating the reliability of statically loaded plastic structural components. For a particular stress ( $\sigma$ ) and time ( $t$ ), the reliability ( $R(t, \sigma)$ ) is the probability that the component is still functioning, i.e., that it has not failed. The use of plastic in engineering structures is always increasing, so with respect to safety and liability it is very important to be able to know the expected lifetime for a plastic part. Classical theories have been developed for elastic, brittle materials which can be used to calculate reductions in ultimate strength when flaws are present. But recent studies of plastic field failures show that a plastic part will develop a crack after being loaded for a long time by a relatively small stress [46,47]. The crack originates from the part's largest defect (assuming homogeneous stress). The defect locally magnifies the stress, a process zone develops, and slow crack growth begins. The defects are introduced into the plastic material during the manufacturing process, and are in the form of voids or dust particles. Tests are performed on sample specimens to determine the probability density function (PDF) of the critical (largest) defect size. The defect is considered to be a crack with length equal to the defect size. For a particular applied stress and structural component geometry, the equations of the crack layer model provide a relation between the initial crack length (defect size) and lifetime. Having both the PDF for initial crack length (defect size) and the equation linking initial crack length and lifetime, allows the calculation of the PDF for lifetime. Once the PDF for lifetime is known, the reliability function for the structural part can be determined.

### **4.2 METHOD ASSUMPTIONS**

- 1) The sizes and locations of the defects are random and cause local stress concentrations.

- 2) The stress concentration induced by a defect results in process zone formation.
- 3) A crack in a structural part originates from the largest defect. Therefore one of the PDFs from the distribution of extremes should be used for the PDF of defect size.
- 4) The crack layer model can adequately predict lifetimes for plastic specimens.

### 4.3 ANALYSIS OF DEFECTS

Destructive tension tests in which the load is increased until failure occurs are performed on many smooth (unnotched) specimens of the given material. The fracture surface of each specimen is examined, and the size of the defect from which the crack originated (which is assumed to be the largest defect in the specimen) is measured. A histogram is constructed from the failure defect sizes, and the parameters of the PDF of the statistics of extremes for a finite interval are fitted to the histogram. The cumulative distribution function (CDF) of the statistics of extremes for a finite interval is [48]

$$F(l_0) = \begin{cases} 0 & : l_0 < l_{\min} \\ \exp\left(-\alpha\left(\frac{l_{\max} - l_0}{l_0 - l_{\min}}\right)^\beta\right) & : (l_{\min} \leq l_0 \leq l_{\max}) \\ 1 & : l_{\max} < l_0 \end{cases} \quad (4.1)$$

The PDF ( $f(l_0)$ ) is obtained by differentiating equation 4.1 with respect to  $l_0$  (the initial crack length or defect size). Figure 26 shows  $f(l_0)$  for an observed set of critical defect sizes,  $l_0$ , made from the histogram of destructive tension tests performed on polycarbonate bars.  $l_{\min}$  and  $l_{\max}$  (equation 4.1) are the minimum and maximum values from the histogram.  $\alpha$  and  $\beta$  are chosen so that the PDF most closely approximates the shape of the histogram. There are various statistical criteria which can be used to judge the best fit.

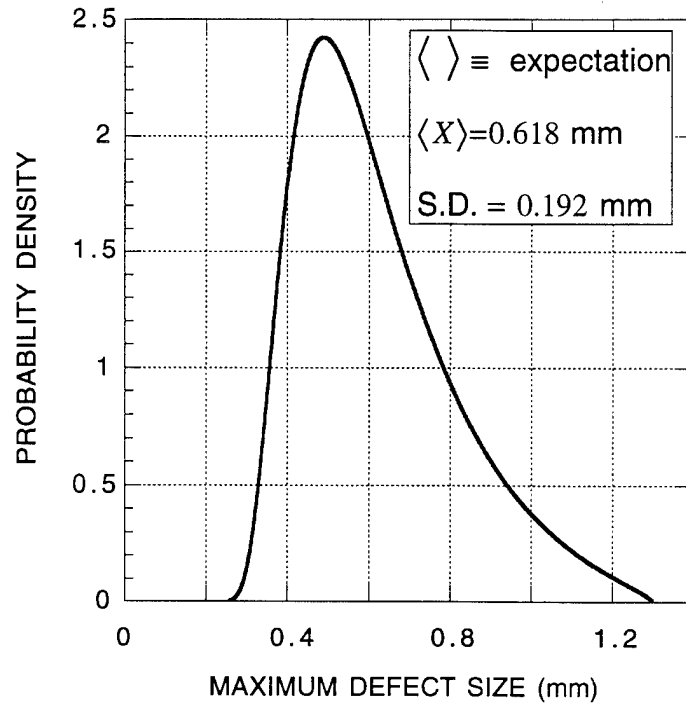


Figure 26. Modeling probability density function for maximum defect size

#### 4.4 KINETICS OF CRACK LAYER EVOLUTION

The driving force for crack extension,  $X_l$ , is the derivative of Gibb's potential,  $G$ , with respect to the crack length,  $l$ . The driving force for crack layer length extension,  $X_L$ , is the derivative of  $G$  with respect to the crack layer length,  $L$  [40]. For slow (quasi-static) crack growth, the rates of growth of the crack and crack layer are assumed to be linearly proportional to the driving forces.

$$\begin{aligned}\dot{l} &= k_1 \cdot X_l \\ \dot{L} &= k_2 \cdot X_L\end{aligned}\tag{4.2}$$

Evaluation of the driving forces requires knowledge of material properties, such as the drawing stress, draw ratio, specific energy of drawing, Young's modulus and the characteristic time of material degradation within the process zone. Also required are conventional fracture mechanics computations of the stress intensity factors and crack opening displacements.

The system of equation 4.2 consists of two strongly bound non-linear ordinary differential equations, and can only be solved numerically. Numerical simulation of the model at moderate

stress levels results in discontinuous crack growth, similar to experimentally observed behavior (Figure 27).

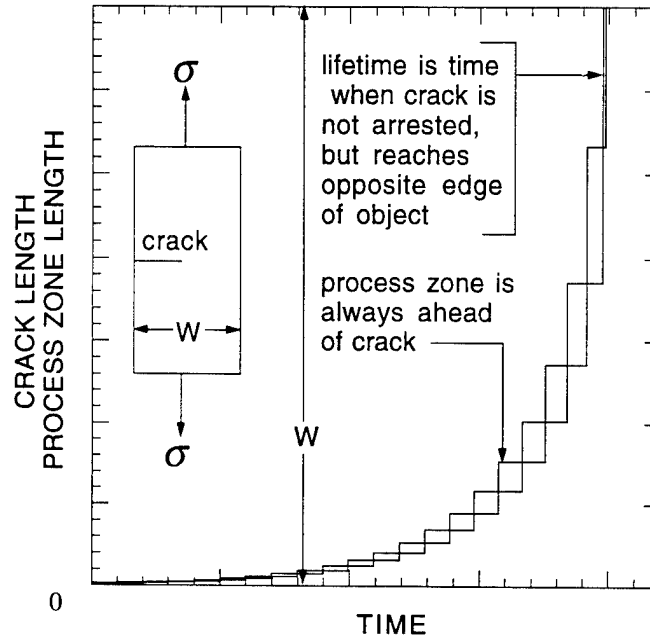


Figure 27. Discontinuous growth of crack and process zone

#### 4.5 LIFETIME - INITIAL DEFECT SIZE RELATIONSHIP

Computations of the total time until part failure,  $t_f$  (lifetime), produce a linear relationship with initial defect size,  $l_0$

$$t_f = \Phi(l_0) = A + B \ln(l_0). \quad (4.3)$$

The coefficients ( $A, B$ ) of equation 4.3 depend on the specimen geometry and type of loading, i.e., uniform tension, three point bending, etc. Figure 28 is a calculated plot at various stress levels

of lifetime as a function of initial defect size for single-edge notched specimens of polyethylene

pipng material. (Note that  $\bar{\sigma} \equiv \frac{\sigma}{\sigma_{dr}}$ .)

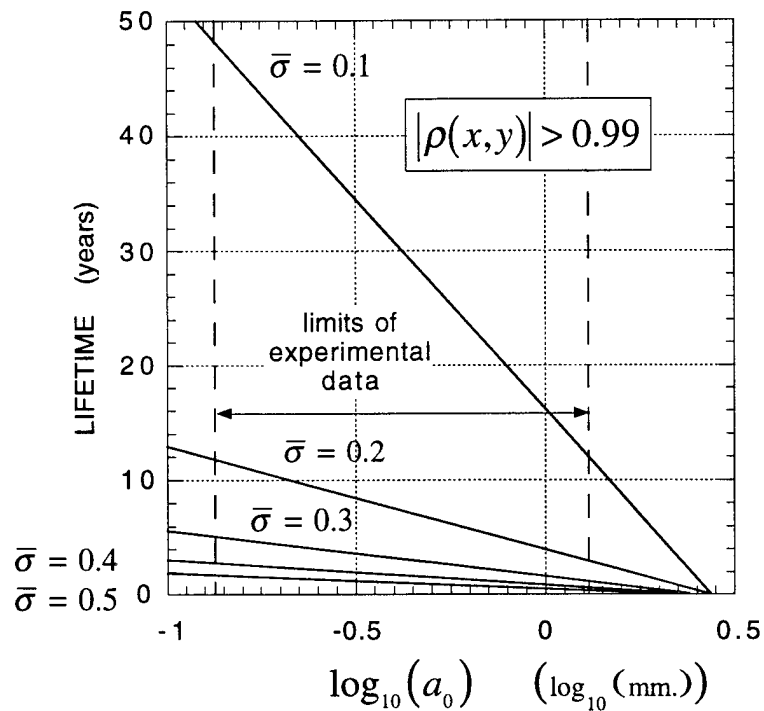


Figure 28. Lifetime versus logarithm of initial crack length for five stress levels

#### 4.6 LIFETIME PROBABILITY DENSITY FUNCTION

Since the lifetime ( $t_f$ ) is a function of the random initial defect size ( $l_0$ ) (equation 4.3), and since the PDF for initial defect size ( $f(l_0)$ ) (derivative of equation 4.1) is known, a standard transformation from probability theory [49] allows the calculation of the PDF for lifetime

$$g(t_f) = f(\Phi^{-1}(t_f)) \left| \frac{d(\Phi^{-1}(t_f))}{d(t_f)} \right|. \quad (4.4)$$

Figure 29 shows the PDF for lifetime for various normalized stress levels. (Figure 29 uses the data from Figures 26 and 28. This means that Figure 29 shows PDFs for a hypothetical material.)

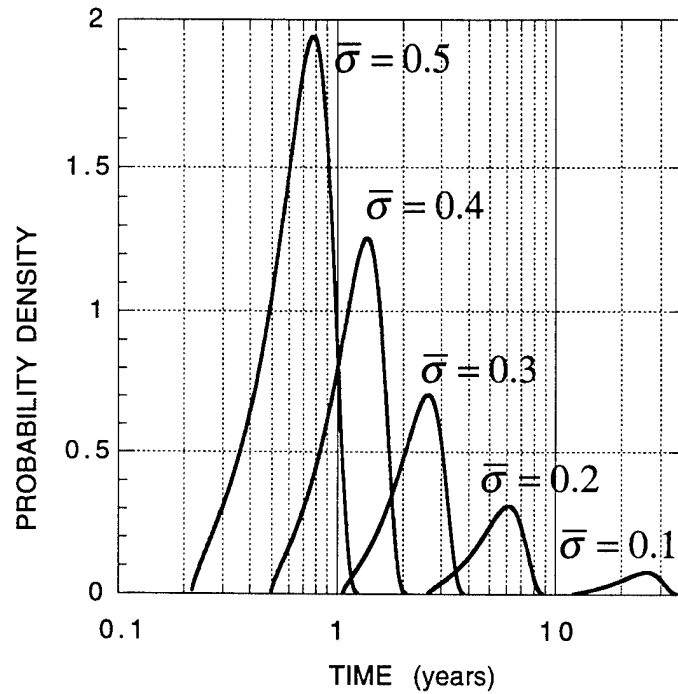


Figure 29. Lifetime probability density functions for five stress levels

#### 4.7 RELIABILITY OF STRUCTURAL COMPONENT

The reliability function, which gives the probability that a part is still functioning at a given time  $t$ , depends on the stress level and is defined as

$$R(t, \sigma) = 1 - \int_{t_f=0}^{t_f=t} g_{\sigma}(t_f) d(t_f). \quad (4.5)$$

Figure 30 is a plot of lifetime versus remote stress for various values of reliability. (Figure 30 uses the data of Figure 29.)

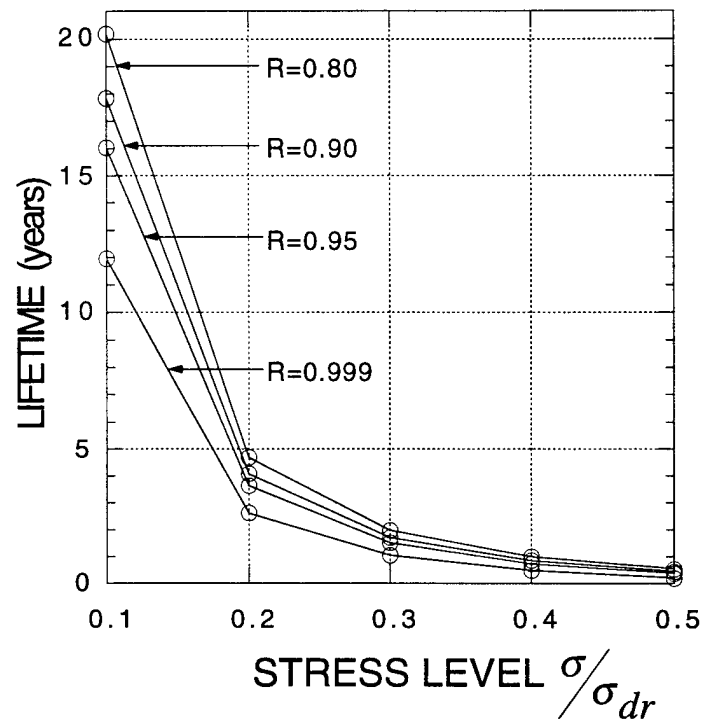


Figure 30. Lifetime versus stress level for four values of reliability

A simpler measure, the mean time to failure,  $\langle t_f \rangle$ , is shown in Figure 31 versus stress level.

(Figure 31 uses the data of Figure 29.)

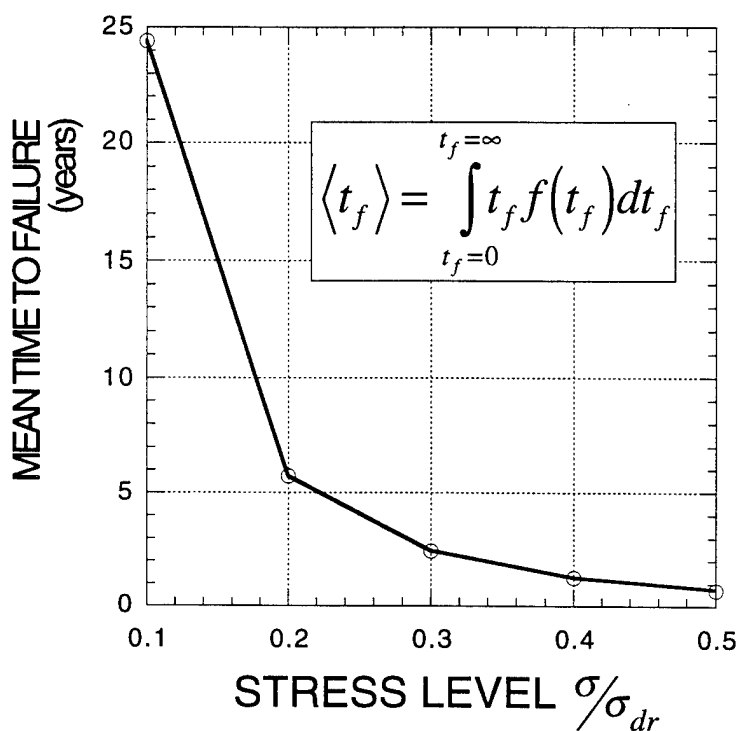


Figure 31. Mean lifetimes for five stress levels

#### 4.8 CONCLUSIONS

A method of reliability determination for plastic structural components has been presented. The method is based on the statistical determination of the probability density function for initial defect size, and on the connection provided by the crack layer model between initial

defect size and lifetime. The method can be used to recommend replacement intervals for structural parts, assist in material selection, and decide on design strategies.

## **5. COMPUTER SIMULATION OF PLASTIC TOUGHNESS TEST**

### **5.1 INTRODUCTION**

Since plastics are increasingly being used instead of metals for industrial applications, there is an interest for obtaining a standard method of quantifying the fracture toughness of a plastic. The first criterions used were simple empirical tests which gave little useful information. More recently, efforts have been made to apply metal testing procedures to plastics. An ASTM subcommittee (D-20) was created to develop methods to rate plastics based on resistance to crack initiation (or fracture toughness) [50], (ASTM Standards E813-89, E1152-89). First, there were attempts to find the linear elastic fracture parameters  $K_{1C}$  and  $G_{1C}$  (which are used as measures of metal fracture toughness). Round-robin tests were performed at several laboratories. Because plastic response is usually nonlinear and inelastic, these parameters were not determinable. Attempts were then made to find the elastic-plastic fracture entities  $J_{1C}$  and the  $J_1$  curve. Round-robin tests were again conducted, and it was found that these measures were not able to be uniquely determined, and so cannot be material properties.

In this chapter, the crack layer model will be used to find  $J_{1C}$  and the  $J_1$  curve as specified in ASTM E813-81. It will be shown that these measures are not unique. Then, the (material) time until failure (or lifetime)  $t_f$ , as found from the solution of the equations of the crack layer model will be proposed as a measure of fracture toughness.

### **5.2 THE CRACK LAYER MODEL**

The crack layer model (CLM) was derived from the observation that for many engineering plastics, the material near the path of a slowly growing crack is permanently altered when the

crack tip passes by [43]. The transformed material is called the process zone (PZ). The change in the PZ material is that it becomes drawn (permanently stretched) in the direction of the applied loading (perpendicular to the crack). The drawing happens because the crack tip magnifies the stress in the material nearby, and the (limiting) drawing stress ( $\sigma_{dr}$ ) is reached within this material. Figure 32 shows using a single edge notched (SEN) specimen, that the crack length is called  $l$ , and the process zone length is called  $l_a$ . The crack and process zone are together called

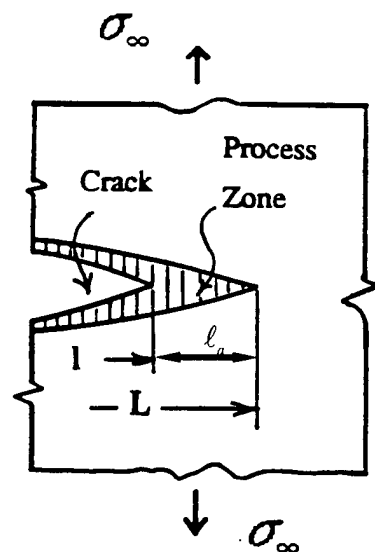


Figure 32. Crack and process zone

the crack layer. The length of the crack layer is named  $L$ . For a material capable of exhibiting a process zone, the process zone will always exist ahead of the crack tip (assuming a nonzero stress

field). As the crack grows,  $l_a$  is not constant. Therefore,  $\dot{l}$  and  $\dot{L}$  are not always equal. Because of this it seems natural to treat  $l$  and  $L$  as independent variables. This is what is done in the CLM. In this model, the two independent variables are  $l(t, L, \dots)$  and  $L(t, l, \dots)$ , and each is a function of the other. The driving forces for crack length extension ( $X_l$ ) and crack layer length extension ( $X_L$ ) are

$$X_l = J_1 - 2\gamma(\Delta t_{pz}) \quad (5.1)$$

(if  $< 0$ , then  $X_l$  is set to 0),

$$X_L = \frac{1}{E}(K_\infty + K_{dr})(K_\infty + (1 + 2\tilde{\gamma})K_{dr}) \quad (5.2)$$

(if  $< 0$ , then  $X_L$  is set to 0).

The instantaneous growth rates for the crack and crack layer are

$$\begin{aligned} \dot{l} &= k_1 X_l \\ \dot{L} &= k_2 X_L \end{aligned} \quad (5.3)$$

Equations 5.3 are a system of two nonlinear ordinary differential equations, which can be solved simultaneously thru time, to provide the chronological evolution of  $l$  and  $L$ . For a computer simulation, the material properties, specimen geometry, initial crack length ( $l_0$ ), test type and loading conditions are specified. The developments of  $l$  and  $L$  are recorded, until  $L$  reaches the specimen width ( $W$ ) indicating specimen failure. It has been shown that the numerical implementation of the CLM can imitate the discontinuous growth which has been observed during experiments on many plastics [45].

### 5.3 SIMULATION OF DISPLACEMENT CONTROL TEST

Figure 33 was generated from the numerical simulation of a displacement control test using the equations of the CLM. It shows a typical plot of remote stress ( $\sigma_\infty$ ) (and the associated plots of  $l$  and  $L$ ) versus displacement ( $\Delta$ ). The specimen stiffness (the slope of the  $\sigma_\infty$  vs.  $\Delta$  curve) is a decreasing function of  $l$ , and so has its maximum value at the start of the simulation, when  $l = l_0$  and  $t = 0$ . The stiffness decreases until it is almost zero when  $L$  reaches the specimen width  $W$ ,  $t = t_f$ , and the simulation ends. The growth of  $l$  is intermittent and discontinuous. The sizes and frequencies of growth jumps in  $l$  are proportional to the current value of the energy release rate ( $J_1$ ). For a displacement control test,  $J_1$  has initial value zero, reaches its maximum value at some intermediate value of  $\Delta$ , and then decreases. At each instant when  $l$  increases, the equations of the CLM require that  $\sigma_\infty$  decreases, resulting in the discontinuities of  $\sigma_\infty$ . The ratio of the decrease of  $\sigma_\infty$  at a crack jump, to the increase of  $\sigma_\infty$

between crack jumps, is an increasing function of  $t$  (or equivalently of  $\Delta$ ).  $\sigma_{\infty}$  attains its maximum value when this ratio equals one.

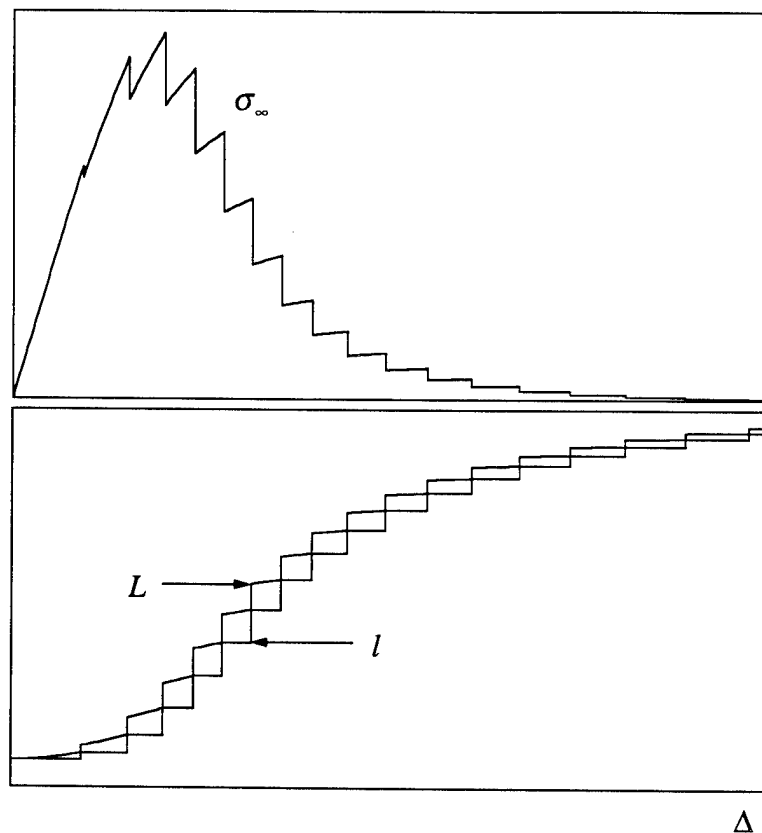


Figure 33. Remote stress, crack length and crack layer length vs. displacement

#### 5.4 ASTM PROCEDURE

According to ASTM E813-81,  $J_1$  can be calculated for any time  $t$  during an experiment from expression

$$J_1(t) = \frac{2U(t)}{B(W-l(t))}. \quad (5.4)$$

In equation 5.4,  $U(t)$  is the potential energy of the specimen, and  $B$  is the specimen thickness.  $U(t)$  is equal to the area under the  $\sigma_\infty$  vs.  $\Delta$  curve at time  $t$ , and  $l(t)$  is the crack length at time  $t$ . The  $J_1$  curve for an experiment is plotted versus crack extension ( $\delta l$ ).  $J_{1C}$  is found as the value of  $J_1$  corresponding to the intersection of the curve with the blunting line. The blunting line is given by  $J_1 = 2\sigma_y \delta l$ . Since for plastics the yield stress ( $\sigma_y$ ) cannot be measured precisely, the drawing stress ( $\sigma_{dr}$ ) can be substituted for it in the blunting line expression.

Figure 34 was generated from numerical simulations of displacement control tests using the equations of the CLM. It shows a partial plot of  $\sigma_\infty$  vs.  $\Delta$  for each of three values of  $\dot{\Delta}$ . For a particular value of  $\Delta$ , increasing  $\dot{\Delta}$ , decreases  $t$ . Decreasing  $t$ , increases the average value of  $2\gamma$ , the resistance to crack extension. Increasing the average value of  $2\gamma$ , decreases  $l$ . Decreasing  $l$ ,

increases the specimen stiffness,  $\sigma_{\infty}/\Delta$ . Increasing  $\sigma_{\infty}/\Delta$ , increases  $\sigma_{\infty}$ . Therefore, for a particular value of  $\Delta$ , increasing  $\dot{\Delta}$ , increases  $\sigma_{\infty}$ .

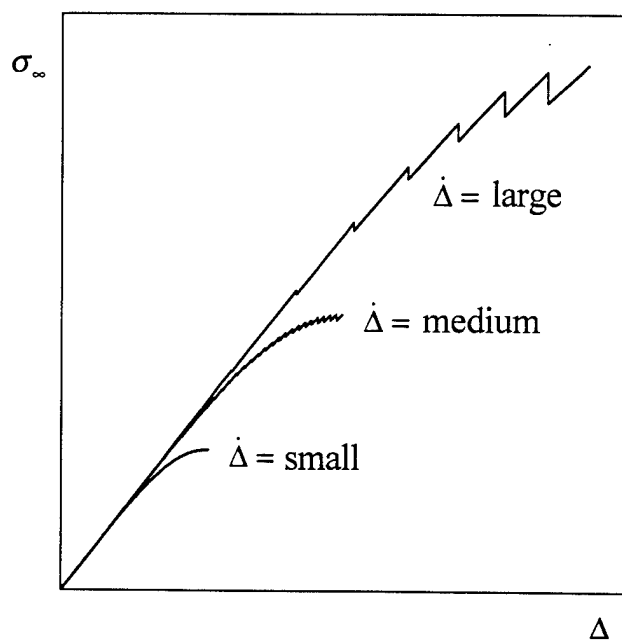


Figure 34. Remote stress vs. displacement for three values of displacement rate

Figure 35 shows the  $J_1$  vs.  $\delta l$  (or J-R) curve, calculated using ASTM E813-81, for each of the  $\sigma_\infty$  vs.  $\Delta$  curves of Figure 33. The blunting line is shown, and each of the three values of  $J_{1C}$  is indicated.

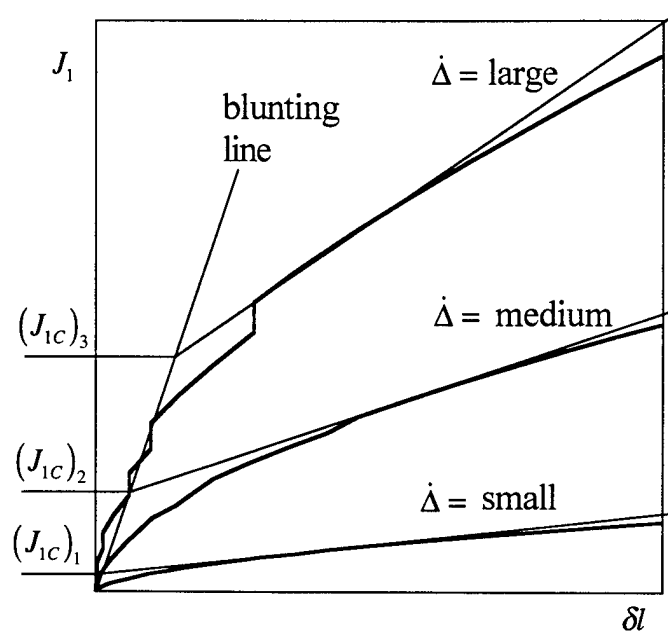


Figure 35. Energy release rates for three values of displacement rate

## 5.5 CONCLUSIONS

The J-R curve and  $J_{1C}$  are rate dependent, and so cannot be material properties. They do not provide a measure of material fracture toughness. No universal measure of material fracture toughness exists. Toughness depends on the material properties, along with the specific conditions of use, i.e., geometry and, type and magnitude of loading. One material can be said to be better

than another only with respect to a particular set of usage conditions. The CLM can be used to simulate the behavior of a plastic specimen for a particular set of usage parameters. Using the CLM, the lifetimes ( $t_f$ ) for two materials subject to identical conditions can be compared, and one material judged superior.

## CONCLUSIONS AND FUTURE RESEARCH

The introduction described the phenomenon of slow crack growth in plastics, and the methods which have been used to model it.

Chapter 1 gave a basic description of the theory of the CLM.

Chapter 2 presented numerical algorithms for modeling slow crack growth in plastics for various loading conditions, using the equations of the CLM. Simplified algorithms were also presented, which give accurate results for discontinuous crack growth processes.

Chapter 3 analyzed the results of computer simulations made using the algorithms of Chapter 2. The driving forces were decomposed and their behaviors were shown. The method for making a dimensionless simulation was given. The characteristics of the two types of crack growth, discontinuous and continuous, were described and compared. The accuracy of simulations using the simplified algorithms was examined. Lifetime-applied stress relationships were presented for both discontinuous and continuous simulations. Lifetime-applied stress relationships were compared for three applied stress functions (three types of loading).

Chapters 4 and 5 presented applications made from computer simulations using the algorithms of Chapter 2. Chapter 4 showed a method for calculating the reliability function for a plastic structural component. Chapter 5 gave a computer imitation of the ASTM experimental method for measuring plastic fracture toughness. It was shown that the computer results were displacement rate dependent. It was suggested that the experimental results would also be rate dependent, and that fracture toughness depends on many usage parameters, and so is not a material property.

The thesis numerically implemented the CLM and presented the results of computer simulations of the implementation. The simulations displayed both kinds of experimentally

observed slow crack growth, discontinuous and continuous. The simulations gave a relationship between lifetime and stress, i.e.,  $\log(t_f) = \alpha + \beta \log(\sigma_\infty)$ , which has been experimentally observed. The simulations were also able to duplicate the experimentally determined range of coefficient  $\beta$ . It is proposed that the thesis has demonstrated that a computer program which models the equations of the CLM, is able to provide realistic predictions of the evolutions of the crack and crack layer, and of long-term lifetime for plastics functioning under small stresses. It is also proposed that the thesis has shown that various load types and histories can be easily accommodated. It is further proposed that the ability to numerically imitate the slow crack growth in plastics has many practical uses, two of which were presented in Chapters 4 and 5.

It was stated in the introduction that viscoelastic deformation does influence lifetime when displacement is prescribed. Future research includes accounting for viscoelastic effects.

## CITED LITERATURE

1. A. Chudnovsky, *Crack Layer Theory*, NASA CR-174634, (1984).
2. E.H. Andrews, *Fracture in Polymers*, Aberdeen University Press (1968).
3. R.W. Herzberg and J. Manson, *Fracture of Engineering Plastics*, Academic Press (1980).
4. A.J. Kinloch and R.J. Young, *Fracture Behavior of Polymers*, Elsevier Applied Science (1983).
5. J.G. Williams, *Fracture Mechanics of Polymers*, Ellis Horwood Ltd. (1984).
6. H.H. Kausch, *Polymer Fracture*, Springer Verlag (1987).
7. M.K. Chan and J.G. Williams, *Polymer* 24 (1983) 234-244.
8. S.K. Bhattacharya and N. Brown, *Journal of Materials Science* 20 (1985) 2767-2775.
9. N. Brown and S.K. Bhattacharya, *Journal of Materials Science* 20 (1985) 4553-4560.
10. X. Lu and N. Brown, *Journal of Materials Science* 21 (1986) 4081-4088.
11. X. Lu and N. Brown, *Polymer* 28 (1987) 1505-.
12. X. Wang and N. Brown, *Polymer* 29 (1988) 463-.
13. X. Lu, X. Wang and N. Brown, *Journal of Materials Science* 23 (1988) 643-.
14. X. Wang and N. Brown, *Polymer* 30 (1989) 1456-.
15. Y.L. Huang and N. Brown, *Journal of Polymer Science: Part B: Polymer Physics* 28 (1990) 2007-2021.
16. X. Lu and N. Brown, *Journal of Materials Science* 25 (1990) 29-34.
17. X. Lu, R. Qian and N. Brown, *Journal of Materials Science* 25 (1990) 411-416.
18. X. Lu and N. Brown, *Journal of Materials Science* 26 (1991) 612-620.
19. X. Lu, R. Qian and N. Brown, *Journal of Materials Science* 26 (1991) 917-924.
20. Y.L. Huang and N. Brown, *Journal of Polymer Science: Part B: Polymer Physics* 29 (1991) 129-137.

21. D. Barry and O. Delatycki, *Journal of Polymer Science: Part B: Polymer Physics* 25 (1987) 883-899.
22. D. Barry and O. Delatycki, *Polymer* 33 (1992) 1261-1265.
23. C.F. Popelar, C.H. Popelar and V.H. Kenner, *Polymer Engineering and Science* 30 (1990) 578-586.
24. C.H. Popelar, V.H. Kenner and J.P. Wooster, *Polymer Engineering and Science* 31 (1991) 1693-1700.
25. L.J. Rose, A.D. Chanell, C.J. Frye and G. Capaccio, *Journal of Applied Polymer Science* 54 (1994) 2119-2124.
26. K. Kadota, *Ph.D. Thesis*, The University of Illinois at Chicago, Chicago (1992).
27. D.S. Dugdale, *Journal of the Mechanics and Physics of Solids* 8 (1960) 100-104.
28. G.I. Barenblatt, *Advances in Applied Mechanics* 7 (1962) 55-129.
29. A. Stojimirovic, K. Kadota and A. Chudnovsky, *Journal of Applied Polymer Science* 46 (1992) 1051-.
30. N. Brown and X. Lu, *International Journal of Fracture* 69 (1995) 371-377.
31. R.A. Schapery, *International Journal of Fracture* 11 (1975) 141-158, 369-387, 549-562.
32. P. Trassaert and R. Schirrer, *Journal of Materials Science* 8 (1983) 3004-3010.
33. R. Schirrer, J. LeMasson, B. Tomatis and R. Lang, *Polymer Engineering and Science* 24 (1984) 820-824.
34. I.M. Ward and M.A. Wilding, *Polymer* 19 (1978) 969-.
35. I.M. Ward and M.A. Wilding, *Journal of Polymer Science: Polymer Physics Ed.* 22 (1984) 561-575.
36. W.L. Huang, *Ph.D. Thesis*, The University of Illinois at Chicago, Chicago (1992).
37. R. Lee, *Ph.D. Thesis*, The University of Illinois at Chicago, Chicago (1994).
38. K. Kadota and A. Chudnovsky, *Recent Advances in Damage Mechanics and Plasticity*, AMD-Vol. 132 / Md-Vol. 30, J.W. Ju (ed.), ASME (1992) 115-130.

39. K. Kadota and A. Chudnovsky, *Proceedings of ASME Winter Annual Meeting* (1991) 101-114.
40. A. Chudnovsky and K. Kadota, *Proceedings of PACAM III* (1993) 419-422.
41. M.J. Cawood, A.D. Channell and G. Capaccio, *Polymer* 34 (1993) 423-.
42. S.H. Beech, A.D. Channell and L.J. Rose, *14th Plastics Fuel Gas Pipe Symposium (1995)* 216-.
43. A. Chudnovsky, V. Dunaevsky and Khandogin, *Archives of Mechanics* 30 (1978) 165-174.
44. A. Stojimirovich and A. Chudnovsky, *International Journal of Fracture* 57 (1992) 281-289.
45. A. Chudnovsky, Y. Shulkin, D. Baron and K.P. Lin, *Journal of Applied Polymer Science* 56 (1995) 1465-1478.
46. K. Sehanobish, A. Moet and P.P. Petro, *Material Science Letters* 4 (1985) 890.
47. S.S. Stivala, S.H. Patel, A. Chudnovsky, A. Kim and Z.W. Zhou, *Society of Plastic Engineers Conference Proceedings* 3 (1994) 3290.
48. B. Kunin, *Ph.D. Thesis*, University of Illinois at Chicago, Chicago (1991).
49. D.G. Kelly, *Introduction to Probability*, Macmillan Publishing Company, New York (1994) 326.
50. M.K. Chan and J.G. Williams, *International Journal of Fracture* (1983) 145.

## APPENDIX

### (algorithms for SIFs and CODs)

#### Introduction

This appendix gives algorithms for calculating the stress intensity factors and crack opening displacements for a single edge notched specimen. (The unit dipole SIF green's function ( $G$ ) is for an SEN specimen with a unit dipole force applied to each crack face and normal to the CLC. <sup>(1)</sup>) (The CODs used in this thesis ( $\delta_{\infty}$  and  $\delta_{dr}$ ) are calculated by using  $x_{COD} = l$  in equations A.9 and A.10.)

#### Abbreviations

CLC	=	crack layer centerline
COD	=	crack opening displacement
SEN	=	single edge notched
SIF	=	stress intensity factor

#### Symbols

$l$	=	crack length, also x-coordinate of crack tip
$L$	=	crack layer length, also maximum x-coordinate of process zone
$W$	=	length of SEN specimen in direction parallel to CLC
$\sigma(x)$	=	the stress distribution which is applied normal to the crack faces
$\sigma_{\infty}(x)$	=	Stress distribution which would be present along location of CLC, if crack layer did not exist. Is applied normal to CLC on crack faces between x-coordinates 0 and $l$ ; and on crack imaginary faces between x-coordinates $l$ and $L$ . ( $\sigma_{\infty}$ could possibly be a function of position along the CLC, i.e., if for instance, the specimen was loaded in bending) ( $\sigma_{\infty}$ can be tensile and/or zero and/or compressive)
$\sigma_{dr}$	=	material drawing stress (applied normal to CLC on crack imaginary faces between x-coordinates $l$ and $L$ ) ( $\sigma_{dr}$ is compressive on crack)
$x$	=	x axis located along CLC, or x-coordinate measured along this x axis (notched edge of SEN specimen has x-coordinate zero)

---

1. Tada, Hiroshi; The Stress Analysis of Cracks Handbook; p. 2-27; St. Louis, Missouri; Del Research Corporation; 1974.

## APPENDIX (continued)

$x_d$  = x-coordinate of dipole forces

$x_{COD}$  = x-coordinate at which COD is desired ( $0 \leq x_{COD} \leq L$ )

$K_\infty$  = SIF at  $L$  due to  $\sigma_\infty$

$K_{dr}$  = SIF at  $L$  due to  $\sigma_{dr}$

$\delta_\infty(x)$  = COD at  $x$  due to  $\sigma_\infty$ . Is measured normal to CLC. For  $x$  between 0 and  $l$ , is equal to the distance between crack faces at location  $x$ . For  $x$  between  $l$  and  $L$ , is equal to the distance between crack imaginary faces at location  $x$ .

$\delta_{dr}(x)$  = COD at  $x$  due to  $\sigma_{dr}$ . Is measured normal to CLC. For  $x$  between 0 and  $l$ , is equal to the distance between crack faces at location  $x$ . For  $x$  between  $l$  and  $L$ , is equal to the distance between crack imaginary faces at location  $x$ .

**Stress intensity factor equations**

$$K_\infty(L, W, \sigma_\infty(x)) = \int_{x=0}^{x=L} F(x, L, W, \sigma_\infty(x)) dx \quad (A.1)$$

$$K_{dr}(l, L, W, \sigma_{dr}) = \int_{x=l}^{x=L} F(x, L, W, \sigma_{dr}) dx \quad (A.2)$$

$$F(x_d, L, W, \sigma) = \sigma G(x_d, L, W) \quad (A.3)$$

$$G(x_d, L, W) = \frac{2}{\sqrt{\pi L}} (T_1 - T_2 + T_3) \quad (A.4)$$

$$T_1 = \frac{3.52(1 - x_d^{(N)})}{(1 - L^{(N)})^{3/2}} \quad (A.5)$$

$$T_2 = \frac{4.35 - 5.28x_d^{(N)}}{\sqrt{1 - L^{(N)}}} \quad (A.6)$$

**APPENDIX (continued)**

$$T_3 = \left( \frac{1.3 - 0.3(x_d^{(N)})^{3/2}}{\sqrt{1 - (x_d^{(N)})^2}} + 0.83 - 1.76x_d^{(N)} \right) (1 - (1 - x_d^{(N)})L^{(N)}) \quad (\text{A.7})$$

$$x_d^{(N)} = \frac{x_d}{L}, \quad L^{(N)} = \frac{L}{W}. \quad (\text{A.8})$$

**Crack opening displacement equations**

$$\delta_\infty(x_{COD}, E, L, W, \sigma_\infty(x)) = \int_{x=0}^{x=L} \sigma_\infty(x) H(x_{COD}, x, E, L, W) dx \quad (\text{A.9})$$

$$\delta_{dr}(x_{COD}, E, l, L, W, \sigma_{dr}) = \sigma_{dr} \int_{x=l}^{x=L} H(x_{COD}, x, E, L, W) dx \quad (\text{A.10})$$

$$H(x_{COD}, x_d, E, L, W) = \frac{2}{E} \int_{x=a}^{x=L} G(x_{COD}, x, W) G(x_d, x, W) dx \quad (\text{A.11})$$

$$a = \max(x_{COD}, x_d) \quad (\text{A.12})$$

## APPENDIX (continued)

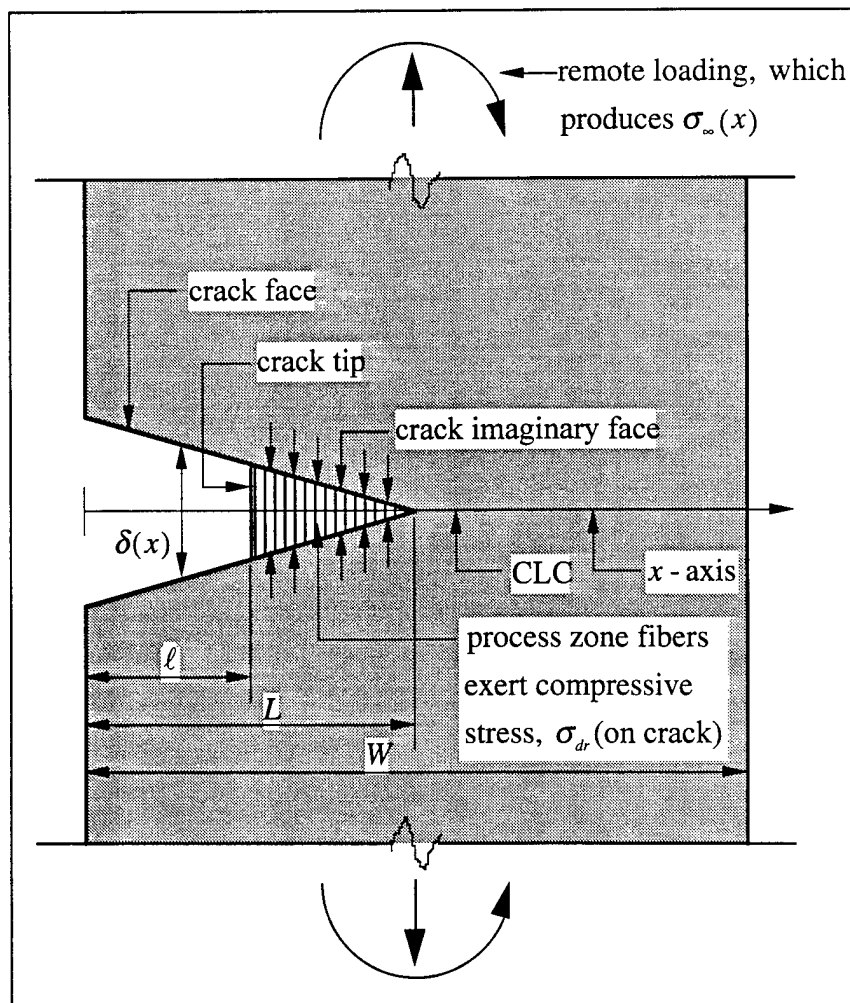


Figure 36. Crack layer diagram